Influence of the trophic environment and metabolism on the dynamics of stable isotopes in the Pacific oyster (*Crassostrea gigas*): modeling and experimental approaches

Antoine Emmery

The research carried out in this thesis was supported by the Conseil Régional de Basse Normandie (Caen, France) and the French Institute for Explotation of the Sea (Ifremer, Plouzané, France)

VRIJE UNIVERSITEIT

Influence of the trophic environment and metabolism on the dynamics of stable isotopes in the Pacific oyster (*Crassostrea gigas*): modeling and experimental approaches

ACADEMISCH PROEFSCHRIFT

ter verkrijging van de graad van Doctor aan
de Vrije Universiteit Amsterdam,
op gezag van de rector magnificus
prof.dr. L.M. Bouter,
in het openbaar te verdedigen
ten overstaan van de promotiecommissie
van de universiteit der Caen Basse Normandie
op donderdag 6 december 2012 om 14:00 uur
in de amfitheater Vauquelin van de universiteit,
Esplanade de la Paix, 1400 Caen

door

Antoine Emmery

geboren te Montauban, Frankrijk

promotoren: prof. dr. S.A.L.M. Kooijman
prof. dr. S. Lefebvre
copromotor: dr. M. Alunno-Bruscia

To my family
and friends

Contents

Chapter 1

Introduction

Ecosystems can be considered as a unit of biological organization made up of all of the organisms in a given area (*i.e.* a community) interacting with their biotic and abiotic environments (adapted from Odum, 1969). Among ecosystems, the notion of trophic (from the greek *trophê*, food) networks can be defined as the set of food chains linked together and from where energy (*i.e.* organic and mineral substrates, food, light) is processed and transfered by living organisms (*e.g.* Lindeman, 1942). The assimilation of trophic resources is a vital need that condition the physiological performances (survival, growth, reproduction) of living organisms.

Characterizing the trophic environment of a given species requires an understanding of its role and an identification of its prey and predator species. The quantification of energy fluxes between organisms and the determination of their origin and fate throughout the food chain, are key steps to assess the ecosystem functioning, state and disturbances (Paine, 1980). The estimation of impacts of anthropic activities on biological compartments, for instance, such as the overfishing in coastal waters (*e.g.* Jackson et al., 2001; Myers et al., 2007), release of contaminants (*e.g.* Fleeger et al., 2003; Piola et al., 2006), impact of invasive species (Troost, 2010), *etc.*, represent an important aspect of characterizing trophic environments. Physical constraints of marine coastal environments make the characterization of trophic environment of aquatic organisms difficult to assess. To overcome this problem, different methods have been developed.

The analysis of gut, stomach and feces contents constitutes one of the most popular methods to obtain information on the taxonomic and size range of ingested prey by a consumer. This method is however frequently biased by the differential digestion efficiency of prey, and only informs about the ingested prey at a given time without knowledge of the assimilated prey over a long time period (Hyslop, 1980). Monitoring over time and space the proxies of primary production (*e.g.* chlorophyll-*a* concentration, phytoplankton concentrations, nutrient concentrations, light availability, *etc.*) give information on the amount of the food available for benthic communities without however

consider its potential composition. To overcome these problems, technological progress allowed the development of indirect methods to determine marine organism diet and and relationships. Biochemical markers, *i.e.* prey DNA, quantification of enzymatic activities in consumers tissues (*e.g.* Fossi, 1994), monitoring of pollutants in both environment and consumers (*e.g.* Monserrat et al., 2007), and organic matter tracers such as natural stable isotopes and fatty acids analysis (Pernet et al., 2012), rapidly replaced traditional methods. Mathematical modelling *e.g.* at individual, population or ecosystem scales, also considerably helped ecologists to assess trophic environments and energy fluxes within ecosystems (Christensen and Pauly, 1992; Cugier et al., 2005). Depending on the type of model (*e.g.* bioenergetic models, ecosystem models) a large variety of data sets and forcing variables can be considered, *i.e.* biomass, productivity, organism's diet, human impacts, environmental variables, *etc.*, offering a general and integrated view of the trophic functioning of ecosystems.

1.1 The isotopic tool: definition, generalities and applications

Natural stable isotopes, discovered by Francis W. Aston in 1919 [1], are forms of the same element that differ only in the number of neutrons in the nucleus. Isotopes with extra neutron(s) are usually qualified of heavy isotopes. These subtle mass differences between isotopes of an element only impart subtle chemical and physical differences at the atomic level (*e.g.* density, melting point, rate of reaction, *etc.*) that do not affect most other properties of an element. (see Fry, 2006). In the case of carbon C which has two different stable isotopes, namely ^{12}C and ^{13}C, the difference of mass between light and heavy isotope is $\approx 1.675 \times 10^{-24}$ g, *i.e.* the mass of 1 neutron.

One of the fundamental properties of stable isotopes is that heavy isotope atoms with extra neutron(s) that compose chemical compounds make bonds that are harder to build as well as to break (from an energetic point of view) and react slower than light isotopes (from a kinetic point of view). Another important property of stable isotopes lies in their natural abundance. This abundance is generally expressed as the ratio of the relative frequency of the heavy isotope over the relative frequency of the light one, *i.e.* the isotopic ratio R. By convention, relative frequency of heavy isotope is on the numerator. The ultimate source of isotopes on Earth originates from Universe formation where the fundamental natural abundances of isotopes have been established, *i.e.* the lightest stable isotope accounting for more than 95 % of all the isotopes. However, R can nevertheless vary in a quantifiable way between the different biological compartments according to physical, chemical and biological processes. For a comparative purpose, isotopic ratios are usually quantified

[1] http://www.nobelprize.org/nobel_prizes/chemistry/laureates/1922/

by using the δ notation which allows comparaison with an international reference. Reference standards were established by the International Atomic Energy Agency (Vienna, Austria [2]); for the carbon, $R_{\text{reference}}$ stands for the V-PDB (*i.e.* Vienna - PeeDee Belemnite) a cretaceous marine fossil, the Belemenite (*Belemnita americana*) from the PeeDee formation (South Carolina, America). For the nitrogen, $R_{\text{reference}}$ stands for the atmospheric nitrogen N_2 (Mariotti, 1983, and references therein). The quantification of stable isotopic ratios in biological materials and fluxes (*i.e.* physical, chemical and biological) thus confers to SIA the powerful role of tracing the origin and fate of organic matter in ecosystems.

1.1.1 Strength and weakness

Stable isotope properties allowed SIA to be used in a myriad of research fields that range from physics and chemistry to biology and ecology, through physiology and paleo-ecology, *etc.* Over the last thirty years, the use of SIA in ecology, *i.e.* terrestrial, freshwater, soil and marine ecology) was very helpful to better understand the trophic functioning of ecosystems. Many different topics benefited of SIA insights such as, *e.g.* the trophic relationships between organisms (Carassou et al., 2008), the fluxes of matter and energy between and within ecosystems, the migration/movement of wild populations (Guelinckx et al., 2008; Hobson, 1999), the seasonal energy and nutrient allocation between tissues (Paulet et al., 2006; Malet et al., 2007; Lorrain, 2002; Hobson et al., 2004), the reconstruction of the food environment of organisms (Kurle and Worthy, 2002; Marín Leal et al., 2008; Decottignies et al., 2007). The technical advantages offered by SIA for ecological investigations, provided successful insights to understand marine coastal ecosystems functioning and specifically to assess the composition of the diet available for benthic fauna such as molluscs (Boecklen et al., 2011).

Paradoxically to their popularity, interpretation of SIA patterns in coastal marine ecology remain nevertheless limited by strong assumptions. This assumptions indirectly point out some weakness in understanding mechanisms that control isotope fluxes between and within living organisms. Different research areas have been therefore identified for further investigations on isotopes fractionation process (see section 1.1.2 for the definition), the dynamics of isotopes incorporation and the mixing of isotopes Gannes et al. (1997); Martínez del Rio et al. (2009); Boecklen et al. (2011).

1.1.2 Incorporation and fractionation of stable isotopes

All the physical, chemical and biological processes that lead to the discrimination of isotopes (*i.e.* variation of the isotopic ratios δ) between two phases, some substrate(s) and some product(s) or a prey and a predator for instance,

[2] http://www.iaea.org/

can be defined as isotopic fractionation. Other terms such as the isotopic effect, the trophic fractionation or the diet to tissues discrimination factor, can be used depending on the scale (*i.e.* atomic, molecular, tissues, organism levels) at which the isotopic fractionation is studied and the type of reaction. At the atomic and molecular levels, a distinction is usually made between the *equilibrium fractionation* and the *kinetic fractionation* (*e.g.* Hayes, 2002; Gannes et al., 1998, and references therein). In the *equilibrium fractionation*, generally associated to reversible exchange reactions at equilibrium, heavy isotopes concentrate in the more "stable" state, *i.e.* in molecules containing the higher number of bonds. In irreversible reactions, the *kinetic fractionation* is characterized by faster reaction of light isotopes (or "light molecule") compared to heavy ones. Although from a physical and chemical point of view isotopic fractionation is a well known phenomenon, the biological processes inducing isotopic fractionation remain complex to assess from a trophic relationship point of view.

Considering a "simple" trophic interaction between a predator and its prey with distinct δ values, the myriad biochemical reactions allowing assimilation of energy (food) to grow, reproduce and maintain the body throughout the life cycle, generally lead to a slight quantifiable enrichment in heavy isotope of the predator compared to the prey, *i.e.* "you are what you eat plus a few per mill" (DeNiro and Epstein, 1978, 1981). This phenomenon is called the trophic fractionation $\Delta = \delta_{\text{organism}} - \delta_{\text{food}}$, and is central for the use of stable isotopes analysis (SIA) in ecology, although the quantification, as well as the factors influencing this enrichment are still poorly understood (Martínez del Rio et al., 2009; Boecklen et al., 2011). Empirical observations (field and experimental) in the early applications of SIA led to the conclusion that, at first approximation, Δ could be considered constant between a predator and its prey, with an average enrichment of $\approx 1\,‰$ for $\Delta^{13}\text{C}$ and $\approx 3.4\,‰$ for $\Delta^{15}\text{N}$ (DeNiro and Epstein, 1978; Minagawa and Wada, 1984).

However, the increasing bulk of results from experimental approaches combined with the development of mathematical models leads to the conclusion that Δ depends on numerous environmental and physiological factors, making the use of an average Δ value more and more controversial (Vanderklift and Ponsard, 2003; McCutchan Jr et al., 2003; Boecklen et al., 2011). For instance, Δ can vary with the amount of food (Emmery et al., 2011; Gaye-Siessegger et al., 2003, 2004b) and starvation duration (Gaye-Siessegger et al., 2007; Hobson et al., 1993; Oelbermann and Scheu, 2002; Castillo and Hatch, 2007), the biochemical composition (in terms of protein, lipid and carbohydrates) of food (Adams and Sterner, 2000; Gaye-Siessegger et al., 2004a; Webb et al., 1998), the diet isotopic ratios (Caut et al., 2009; Dennis et al., 2010), among consumer species (Minagawa and Wada, 1984; Vizzini and Mazzola, 2003), among tissues and organs within organism (Tieszen et al., 1983; Hobson and Clark, 1992; Guelinckx et al., 2007), *etc.* Although a Δ value deals with the individual scale for application at the ecosystem level, the discrimination of stable isotopes occurs at a lower level of metabolic organization, *i.e.* molecular and cellular

levels, complicating thus considerably the understanding and the description of fractionation mechanisms.

Experimental approaches, and specifically fractionation experiments, are still the most suitable to estimate the trophic fractionation value and incorporation rate of isotopes by consumer. During this type of experiment, organisms, which are typically fed on a food source depleted (or enriched) in heavy isotopes, incorporate stable isotopes of the "new" food source. Once isotopic ratios of the consumer become stable, the underlying assumption that organism is in "isotopic equilibrium" with its new food source is done, allowing estimation of Δ values. This assumption remains however questionable since diet isotopic ratios and physiological state of organism can exhibit substantial variations under both natural and controlled conditions. Stable isotope incorporation rate by the organism gives crucial information about the time windows over which the organism's isotopic ratios resemble those of a particular diet. By sampling different types of tissues (or organs) with different incorporation rates, SIA enables to investigate how the organism allocates and uses resources over different temporal scales (Guelinckx et al., 2007; Tieszen et al., 1983) as well as the preferential allocation of particular food items to specific organs. The description of dynamics of stable isotope incorporation remains however rather complex to interpret and to describe from a modeling point of view. Scientists have thus paid increasing interests to the development of models, frequently incorporation models, trying to track and understand changes in the isotopic ratios of a consumer following isotopic diet switch. Amongst the different types of incorporation models, one of the most popular model is a time-dependent model (Hobson and Clark, 1992) where the isotopic ratio of an organism over time $\delta^0_{ij(t)}$ is described by the following expression:

$$\delta^0_{ij(t)} = a + be^{-\lambda t} \tag{1.1}$$

with $a = \delta^0_{ij(\infty)}$, the asymptotic value of $\delta^0_{ij(t)}$, $b = -(\delta^0_{ij(\infty)} - \delta^0_{ij(t_0)})$ the difference between initial and asymptotic values and λ the turnover rate of the isotopic ratio of the organism as a whole. Perhaps because of its simplicity and intuitive interpretation of the parameters, time-dependent models have been widely used over a large variety of species, although some fundamental aspects of animal physiology are not considered. Different authors used the same model framework to account for *e.g.* tissues turnover rate as a function of weight (Fry and Arnold, 1982), contribution of growth and catabolic turnover (Hesslein et al., 1993; Carleton and Del Rio, 2010; Martínez del Rio et al., 2009), excretion and diet isotopic ratios (Olive et al., 2003). The parameters of this type of model are however estimated empirically from experimental measurements; moreover, environmental forcing variables are often considered as constant over time. The model framework (including the underlying assumptions) oversimplifies the organism complexity by considering organism as a single well mixed compartment that reaches isotopic equilibrium. Moreover,

in this type of models are missing: explicit fractionation mechanisms, an explicit quantification (from a mass point of view) of organism metabolism and the environment fluctuations (*i.e.* the variations temperature, food quantity and food isotopic ratios). Martínez del Rio et al. (2009) and Boecklen et al. (2011) recognized that more efforts should be addressed to both the development and the validation of theoretical models to accurately describe isotopes incorporation and fractionation processes and better understand SIA patterns.

1.1.3 Mixing models and diet reconstruction studies

Among the various fields of SIA applications, the reconstruction of organism's diet is a frequent approach to characterize trophic environments. This approach has already been successfully applied in wild diversity of habitats, at varying spatial and temporal scales, and for a large number of species Boecklen et al. (2011). In its simplest form, the diet reconstruction approach attempts to estimate the fractional contribution(s) of one (or several) food source(s) to the diet of a given species (*e.g.* tissue and/or organ samples). The calculation of the fractional contribution(s) is based on the isotopic ratios of both, the food source(s) and the organism's tissues (Phillips, 2001). This approach generally requires the use of isotope mixing models. Briefly, mixing models are linear systems of n equation(s), depending on the number of isotope(s) considered, with $n+1$ unknowns that depend on the number of food source(s). In their simplest formulation, mixing models are written as:

$$\delta^0_{ij} = p\delta^0_{iS1} + (1-p)\delta^0_{iS2} + \Delta \tag{1.2}$$

$$\tag{1.3}$$

with p, the percentage contribution of source 1; δ^0_{ij}, δ^0_{iS1} and δ^0_{iS2} the isotopic ratios of the consumer and of the food sources $S1$ and $S2$ respectively. When the number of equations equals the number of unknown, mixing model are determined (Raikow and Hamilton, 2001; Dawson et al., 2002; Doi et al., 2008). Different versions have been proposed, such as End-members models (Forsberg et al., 1993), Euclidean-distance models (*e.g.* Ben-David et al., 1997). The later type of models are however underdetermined when the number of sources exceeds the number of isotopes by more than one. Generally, they lead to erroneous estimations of food sources contributions. Efforts have therefore been invested in the development of linear mixing models based on mass balance equations. These developments allowed to consider more isotopes and food sources, to accurately consider error estimates about predicted source contributions, to take into account concentrations of elements and to consider all the combinations of food sources that sum to the consumer's isotopic ratios for underdetermined systems (Phillips, 2001; Phillips and Gregg, 2001; Phillips and Koch, 2002; Phillips and Gregg, 2003; Wilson et al., 2009).

Despite the general applicability of these models across a range of systems and trophic levels, these models are based on questionable assumptions. They

assume that the different food sources have the same biochemical composition and the same assimilation efficiency, and that food compounds are disassembled into elements during assimilation (*i.e.* no routing). They also consider that the organism is in "isotopic equilibrium" regardless the variations in both diet isotopic ratios and the incorporation rate of isotopes by consumers. As also noted by Phillips and Koch (2002), "the weakest link in the application of mixing models to a dietary reconstruction studies relates to the estimation of appropriate Δ values". Application of mixing models is also constrained by the fact that food sources must be "isotopically" distinct from each other over time and/or space. In marine coastal ecosystems, for instance, the orders of magnitude in δ_{sources} (*e.g.* phytoplankton, microphytenbenthos, riverine inputs, bacterias) are known. Their values can nevertheless vary significantly (Gearing et al., 1984; Canuel et al., 1995; Savoye et al., 2003) suggesting that temporal and spatial monitoring are necessary to fully characterize trophic environments of organism (Marín Leal et al., 2008; Lefebvre et al., 2009b). From regular growth surveys on oyster stocks, together with temperature measurements and coupling of bioenergetic and mixing models, it is possible to overcome the problem of isotope incorporation rate and to trace the quantitative trophic history of organisms by inverse analysis (Marín Leal et al., 2008).

1.2 Bioenergetic models

Biological performances, *i.e.* growth and reproduction, of bivalves in general, and more specifically of oysters, depend primarily on the quantity and quality of food sources, on temperature and on the metabolism of the organisms themselves. To understand how these factors influence oyster performances, energetic budget models have been extensively used as eco-physiological and management tools. Some of these models are "scope for growth (SFG)" models that describe feeding processes and resource allocation on the basis of empirical relations by using allometric relationships (*e.g.* Barillé et al., 2011). In the last decade, "dynamic energy budget (DEB)" models, from the Dynamic Energy Budget theory (*i.e.* DEB theory Kooijman, 2010; Sousa et al., 2010), have been increasingly developed for various bivalve species in general and especially for *C. gigas* (*e.g.* Van der Veer et al., 2006). With simple mechanistic rules based on physical and chemical assumptions for individual energetics, this type of model describes the uptake (ingestion and assimilation) and use (growth, reproduction and maintenance) of energy and nutrients (substrates, food, light) by organism and the consequences for physiological organisation throughout an organism's life cycle. By considering environmentel fluctuations (*i.e.* temperature and food quantity), this model has already been validated for *C. gigas* both in controlled conditions (Pouvreau et al., 2006) and in contrasted ecosystems throughout the French coasts (Alunno-Bruscia et al., 2011; Bernard et al., 2011). Although the DEB model successfully describes both growth and reproduction of *C. gigas* in varying environmental conditions, some questions

still remain. In particular, *C. gigas* is known to have a broad ecological niche, feeding on a wild variety of food sources such as phytoplankton, microphytobenthos, bacteria, protozoa, macroalgae detritus (*e.g.* Marín Leal et al., 2008; Riera and Richard, 1996; Lefebvre et al., 2009a). However, it is not easy to identify these different food sources and their spatio-temporal variations and to assess their contribution to the growth of bivalves. The recent theoretical developments on dynamic isotope budget (DIB) by Kooijman (2010) and Pecquerie et al. (2010) within the context of DEB theory created a new theoretical framework to assess the dynamics of stable isotopes, recognizing the central role of organism metabolism and mass fluxes in the discrimination of isotopes (Pecquerie et al., 2010).

1.3 The biological model: *Crassostrea gigas*

Native to Japan, the Pacific oyster *Crassostrea gigas* (Thunberg, 1793) is a suspension-feeding bivalve that belongs to the family of ostreidae. After the extinction of the Portuguese oyster *Crassostrea angulata* (Troost, 2010), *C. gigas* has been introduced for aquaculture purposes initially in The Netherlands in 1964 and in France between 1971 and 1973. Reasons of the successful adaptation to European ecosystems lie on both ecological and biological characteristics of *C. gigas* as well as to the human efforts to meet economical requirements of oyster-farming industry. The Pacific oyster presents all the characteristics that are generally attributed to invader species (Troost, 2010, and references therein). The lack of natural enemies, for instance, as well as its ability to respond plastically to spatial variability in food abundance, *i.e.* in terms of survival, growth and reproductive effort (Ernande et al., 2003; Bayne, 2004), the ecosystem engineering (*i.e.* construction of large natural reef structure Lejart and Hily, 2010) and the broad ecological niche of *C. gigas* (*i.e.* eating on a wild variety of food sources) are such characteristics that mainly explain successful adaptation and spread of this species in European coasts. Although the ecological impacts of the introduction of *C. gigas* in European coasts still remain under debate in terms of benefits (*i.e.* promotion of biodiversity) or nuisances (*i.e.* competition with native bivalves), the Pacific oyster became an integral part of the biomass of European coastal ecosystems and became ecologically and economically important.

Considering the problem of characterizing trophic environments in marine coastal ecosystems, suspension feeders and especially the Pacific oyster became a key biological model. Living attached on hard substrates (shell debris, rocks, reefs) at the interface between benthic and pelagic compartments, *C. gigas* is fully dependent on both trophic and abiotic environment fluctuations. At the interface between marine, terrestrial and atmospheric areas, marine coastal ecosystems (*i.e.* littoral areas, estuaries, bays) exhibit a broad and complex diversity in their ecological and trophic functioning. These hinge areas play a key role in structuring life and biodiversity, stepping in the genesis, deteriora-

tion and recycling of the autochthonous and allochthonous particulate organic matter (POM). Composed of both labile living materials, *e.g.* phytoplankton, microphytobenthos, macroalgae, bacteria, *etc.*, and refractory particles, *e.g.* vascular plant detritus and freshwater microalgae, POM constitute the bulk of diet available for primary consumers such as oysters. The complex interplays of hydrological, atmospheric and biological factors forcing the dynamics of marine coastal ecosystems lead, however, to important structural, spatial and seasonal changes in the availability and composition of POM. A benthic organism such as *C. gigas* can be used as an ecological indicator that integrates all changes like a recorder of the ecosystem state (Salas et al., 2006).

1.4 Objectives and thesis outline

The following doctorate work fits into the context of trophic and bioenergetic studies, with the general aim to understand the effect of the trophic environment and the metabolism on the dynamics of stable isotopes δ^{13}C and δ^{15}N in the tissues of the Pacific oyster (*Crassostrea gigas*). To this end, different approaches were considered by combining *in situ* observations, experimental approach and theoretical thinking to better understand how energy is processed by consumers. The originality of this work lies, among others, in the consideration of stable isotopes fluxes of carbon and nitrogen as an integral part of mass budget of oyster, within the framework of DEB model. According to the basic observation that the food quantity is one of the most important factor driving biological performances of organisms, the other originality of this work lies in the investigation of how the amount of food consumed by *C. gigas* affects its isotopic composition. Based on experimental and theoretical approaches, underlying objective of this doctorate is to assess the consequences of the use of DEB model as new tool to better understand isotopic patterns observed in living organism both in field and controlled conditions.

This doctorate work originally begun with an *in situ* survey of oyster growth and isotopic composition (δ^{13}C and δ^{15}N) in two different environments in terms of food quantity and diversity (chapter 2). The trophic resources were considered quantitatively by using chlorophyll-*a* concentration and qualitatively thanks to stable isotopes composition in δ^{13}C and δ^{15}N for the different food sources. Both oyster metabolism as well as spatial and temporal variations of the trophic resource are discussed to interpret and explain the differences in the isotopic patterns of the whole soft tissues and organs of oysters observed between the two ecosystems. Part of these interpretations originate from the theoretical approach carried out before this study (see chapter 3).

In the 3$^{\text{rd}}$ chapter, the dynamics of δ^{13}C and δ^{15}N in oyster tissues are described within the context of DEB theory. Based on published experimental data, the model was used to investigate and to quantify the effect of the feeding level and oyster mass on the value of trophic fractionation Δ. Being the first

application of this type of model in the literature, the study presented in the chapter 3 also allowed *i)* to expose and explain the assumptions in DEB theory required to understand both dynamics and fractionation of stable isotopes in oyster tissues and *ii)* to emphasize the central role of oyster metabolism in understanding isotopes discrimination processes.

To check the consistency of simulations of DEB and DIB models, a fractionation experiment under controlled conditions was carried out using oyster spat as biological model. The experimental results and their interpretations are described in the chapter 4. In this experiment, organisms were first fed at two different feeding levels with a food source depleted in ^{13}C and ^{15}N during 108 d (feeding phase) and then starved for 104 d (starvation phase). Throughout the experiment, the dry flesh mass of oyster tissues (*i.e.* the whole soft body tissues, gills and adductor muscle) and their isotopic ratios were monitored simultaneously. Additionally to the growth and isotopic ratio measurements on organism tissues, the food consumption rate and the isotopic ratios of the food source were also monitored during the feeding phase of the experiment.

The results shown in chapter 4 for the whole soft body tissues (*i.e.* in terms of growth and SIA) are used in the 5^{th} chapter to validate the *C. gigas* DEB and DIB models. Under constant conditions of temperature and considering variations in both the diet isotopic ratios and the amount of food consumed by individuals, the model successfully reproduced the observed trends (in terms of growth and isotope dynamics) in response to the food level. Interpretations based on the model assumptions are suggested to interpret the dynamics of stable isotopes in oyster tissues and the strength and weakness of the model are discussed.

Finally, the results of this doctorate are summarized and discussed in the general conclusion (section 6) and different perspectives are suggested according to the state of development of the different approaches I used.

391 O

Chapter 2

Influence of the trophic resources on the growth of *Crassostrea gigas* as revealed by temporal and spatial variations in δ^{13}C and δ^{15}N stable isotopes

Emmery, A.[a,b,e], Alunno-Bruscia, M.[b], Bataillé, M.-P.[c], Kooijman, S.A.L.M.[d], Lefebvre, S.[e]

Journal of Experimental Marine Biology and Ecology (in revision)

[a] *Université de Caen Basse Normandie, CNRS INEE - FRE*3484 *BioMEA, Esplanade de la paix* 14032 *Caen cedex, France*

[b] *Ifremer UMR* 6539, 11 *Presqu'ile du Vivier,* 29840 *Argenton, France*

[c] *Université de Caen Basse Normandie, UMR INRA Ecophysiologie Végétale et Agronomie, Esplanade de la paix* 14032 *Caen cedex, France*

[d] *Vrije Universiteit, Dept. of Theoretical Biology, de Boelelaan* 1085 1081 *HV Amsterdam, The Netherlands*

[e] *Université de Lille* 1 *Sciences et Technologies, UMR CNRS* 8187 *LOG, Station Marine de Wimereux,* 28 *avenue Foch,* 62930 *Wimereux, France*

Abstract

The influence of the quality and composition of food on the growth of marine bivalves still needs to be clarified. As a corollary, the contribution of different food sources to the diet of bivalves also needs to be examined. We studied the influence of trophic resources (food quantity and quality) on the growth of the soft tissues of suspension feeder *Crassostrea gigas* by using temporal and spatial variations in δ^{13}C and δ^{15}N. Natural spat of oysters originating from

Arcachon Bay were transplanted to two contrasting ecosystems, Baie des Veys (BDV) and Brest Harbour (BH), where they were reared over one year. In each site, the chlorophyll-*a* concentration ([Chl-*a*]) and the δ^{13}C and δ^{15}N of the main food sources, *i.e.* phytoplankton (PHY) and microphytobenthos (MPB) were monitored. In BDV, [Chl-*a*] was 3 times higher than in BH on average, which likely accounts for the large differences in the growth trajectories of oyster tissues between BDV and BH. The temporal variations of *i)* the δ_{PHY} in both BDV and BH and *ii)* the δ_{MPB} in BDV, partly explained the patterns of the isotopic ratios in oysters at each site, *e.g.* the presence of MPB in BDV in autumn coincided with the growth of oysters at the same period. Nevertheless, the gills (Gi), adductor muscle (Mu) and remaining tissues (Re) clearly exhibited different isotopic enrichment levels, with $\delta_{Mu} > \delta_{Gi} > \delta_{Re}$ regardless of the study area and season. This pattern suggests that, due to the maintenance of the organism and the feeding level, the metabolism has a strong influence on the stable isotope dynamics in the oyster organs. The differences in isotope enrichment between organs have implications for the interpretation of animal diets and physiology. Finally, δ^{13}C and δ^{15}N provide information that would be relevant for investigating fluxes of matter within the tissues of organisms.

Keywords: Pacific Oyster; isotopic ratio; metabolism; isotopic discrimination; seasonal variations; phytoplankton

2.1 Introduction

Suspension feeding bivalves are a key ecological component of marine food webs in coastal ecosystems (Gili and Coma, 1998; Jennings and Warr, 2003) as they actively contribute to the transfer and the recycling of suspended matter between the water column and the benthic compartment. They occupy an intermediate trophic niche between primary producers and secondary consumers and are mostly opportunistic, *i.e.* they assimilate a mixture of different food sources according to their bioavailability (Lefebvre et al., 2009b; Saraiva et al., 2011b). A major part of their diet is composed of microalgae, *i.e.* phytoplankton and/or microphytobenthos species (Kang et al., 2006; Yokoyama et al., 2005b), which can differ substantially in their nutritional value (*e.g.* Brown, 2002; González-Araya et al., 2011). Due to their sensitivity to both food quality and quantity, they also act as ecological indicators of the trophic status of the environment (Lefebvre et al., 2009a). However, the availability of food sources for bivalves depends closely on the trophic and hydrological characteristics of coastal ecosystems, which vary on a number of different temporal and spatial scales (Cloern and Jassby, 2008).

Many studies have demonstrated that environmental fluctuations, mainly

temperature and food availability, could directly or indirectly influence individual growth and population dynamics of estuarine benthic species. Laing (2000) and Pilditch and Grant (1999) showed that the growth of the scallops *Pecten maximus* and *Placopecten magellanicus* was closely related to temperature and food supply, respectively. During phytoplanktonic blooms, the high concentrations of chlorophyll-*a* in bottom waters have been shown to induce a decrease and/or halt in the daily shell growth of *P. maximus* (Chauvaud et al., 2001; Lorrain et al., 2000). In *Crassostrea gigas*, Rico-Villa et al. (2009, 2010) pointed out a strong effect of both temperature and food density on the ingestion, growth and settlement of larvae. Water temperature and food density (phytoplankton and/or chlorophyll-a concentration) are the main forcing variables in dynamic energy budget (DEB) models (Kooijman, 2010), built to simulate growth and reproduction of different bivalve species, *e.g.*, *C. gigas*, *Pinctada margaretifera*, *Mytilus edulis* (Alunno-Bruscia et al., 2011; Bernard et al., 2011; Pouvreau et al., 2006; Rosland et al., 2009; Thomas et al., 2011). Meteorological conditions (river inputs, water temperature and light) can also indirectly influence growth and reproduction of bivalves by modifying both the nutrient residence time and light availability required for phytoplankton blooms to occur (Grangeré et al., 2009b).

Temporal and spatial variations of the stable isotopic ratios δ^{13}C and δ^{15}N can offer valuable insights into the relationships among consumers. The isotopic ratio of a consumer closely resembles that of its diet (DeNiro and Epstein, 1978, 1981). Since food items very often have different isotopic compositions, it is possible to estimate the contribution of different food sources to the diet of an organism. Numerous studies have used these properties and mixing models (Phillips and Gregg, 2003) to demonstrate that not only phytoplankton but also microphytobenthos, macroalgal detritus and bacteria can contribute significantly to the diets of benthic suspension-feeders to different extents (*e.g.* Dang et al., 2009; Kang et al., 1999; Marín Leal et al., 2008; Riera et al., 1999). Kang et al. (2006) highlighted the importance of the seasonal development of microphytobenthos as a food source during the critical period of growth and gonad development for suspension- and deposit-feeders *Laternula marilina* and *Moerella rutila*. Sauriau and Kang (2000) showed that around 70 % of the annual production of cockles (*Cerastoderma edule*) in Marennes-Oléron Bay relied on microphytobenthos. Sedimented macroalgal detritus and suspended terrestrial organic matter (supplied by river imputs) can also contribute seasonally to the diet of *C. gigas* (Lefebvre et al., 2009b; Marín Leal et al., 2008). Although both the influence of food density on marine bivalve organ growth and the contribution of different food sources to their diet are widely documented in the literature, the link between the diversity and quality of the food sources and their influence on the growth of organisms has not been yet fully explored.

The temporal and/or spatial dynamics of the isotopic ratios in the organs of an individual and information on its food sources simultaneously provide valuable information on pathways of matter in its tissues. Isotopic ratios in animal organs have already been widely investigated in the literature (*e.g.*, Guelinckx

et al., 2007; Suzuki et al., 2005; Tieszen et al., 1983), but to our knowledge only the studies by Lorrain et al. (2002), Malet et al. (2007) and Paulet et al. (2006) used the seasonal variations of the $\delta^{13}C$ and $\delta^{15}N$ in different organs of bivalves to make a detailed examination of energy allocation processes. Lorrain et al. (2002) showed that for *P. maximus* the seasonal variations in the available suspended particulate organic matter and its $\delta^{13}C$ and $\delta^{15}N$ composition both correlated with the seasonal isotopic variations of the scallop adductor muscle, gonad and digestive gland. These authors also found that the isotopic discrimination and turnover were different between organs and used this property to investigate energy and nutrient flow among them. Malet et al. (2007) used the same approach to explain physiological differences between diploid and triploid oysters (*C. gigas*). Through a diet switching experiment conducted in different seasons, Paulet et al. (2006) measured the isotopic ratios of two suspension feeders, *P. maximus* and *C. gigas* in the gonad, adductor muscle and digestive gland. They showed differences in the isotope incorporation and discrimination between organs, seasons and species that reflected differences in energy allocation strategies.

The objective of this study is to better understand the influence of the trophic resource (food quantity and quality/diversity) on the growth of *Crassostrea gigas* soft tissues by examining both temporal and spatial variations in the isotopic ratios *i.e.*, $\delta^{13}C$ and $\delta^{15}N$. Temporal and spatial variations of these isotopic ratios in different organs were also described to investigate nutrient fluxes through the organism according to its environment.

2.2 Material and methods

2.2.1 Study sites

Two sites (*i.e.* two different ecosystems) were studied, Baie des Veys (Normandy) and Brest Harbour (Brittany) (Fig 2.1), which differ in their morphodynamic and hydrobiological characteristics and in the rearing performances of *C. gigas* (Fleury et al., 2005a,b).

Baie des Veys (BDV), which is located in the southwestern part of the Baie de Seine, is a macrotidal estuarine system with an intertidal area of 37 km^2, a maximum tidal amplitude of $\approx$ 8 m and a mean depth of $\approx$ 5 m. BDV is influenced by four rivers (watershed of 3500 km^2) that are connected to the bay by the Carentan and Isigny channels. In BDV, the culture site of Grandcamp, (49° 23' 124" N, 1° 05' 466" W) is located in the eastern part of the Bay and is characterized by muddy sand bottoms.

Brest Harbour (BH) is a 180 km^2 semi-enclosed marine ecosystem, connected to the Iroise Sea by a deep narrow strait. Half of its surface area is below 5 m in depth (mean depth = 8 m). Five rivers flow into BH but 50 % of the freshwater inputs come from only two of them: the Aulne (watershed of 1842 km^2) and the Elorn (watershed of 402 km^2) rivers. In BH, the study site

at Pointe du château (48° 20' 03" N, 04° 19' 14.5" W) is an area with gravel and rubble bottoms that exclude production of high microphytobenthos biomass.

2.2.2 Environmental data: temperature and Chlorophyll-*a*

The chlorophyll-*a* concentration ([Chl-*a*]) data sets were provided by the IFREMER national REPHY network for phytoplankton monitoring (http://www.ifremer.fr/lerlr/surveillance/rephy.htm) at Géfosse in BDV (49° 23' 47" N, 1° 06' 360" W) and Lanvéoc in BH (48° 18' 33.1" N, 04° 27' 30.1" W). These two environmental monitoring sites are very close to the growth monitoring sites in both ecosystems (Fig. 2.1). In each site, water temperature was measured continuously (high-frequency recording) using a multiparameter probe (Hydrolab DS5-X OTT probe in BH and TPS NKE probe in BDV).

2.2.3 Sample collection and analysis

Oysters

Natural spat of oyster *C. gigas* (mean shell length = 2.72 cm ±0.48 and mean flesh dry mass = 0.02 g ±0.008) originating from Arcachon Bay were split in two groups and transplanted to the two culture sites in March 2009. Oysters were reared from March 2009 to February 2010 at 60 cm above the bottom in plastic culture bags attached to iron tables.

Samples were taken every two months during autumn and winter and monthly during spring and summer. At each sampling date, 30 oysters (in which individual mass was representative of the mean population mass) were collected in the 2 sites. They were cleaned of epibiota and maintained alive overnight in filtered sea water to evacuate their gut contents. Oysters were individually measured (shell length), opened for tissue dissection and carefully cleaned with distilled water to remove any shell debris. After dissection, the tissues were frozen (−20°C), freeze-dried (48 h), weighed (total dry flesh mass W_d), ground to a homogeneous powder and finally stored in safe light and humidity conditions for later isotopic analyses. From March until late June 2009, five individuals out of the 30 sampled were randomly selected for whole body isotopic analyses. From July 2009, the gills (Gi) and adductor muscle (Mu) of the 5 oysters were dissected separately from the remaining tissues (Re), *i.e.*, mantle, gonad, digestive gland and labial palps. As for the whole body tissues, Gi, Mu and Re were frozen at −20°C, freeze-dried (48 h) and weighed (W_{Gi}, W_{Mu} and W_{Re}), prior to being powdered and stored until isotopic analysis. The total dry mass was calculated as follows: $W = W_{Gi} + W_{Mu} + W_{Re}$.

Organic matter sources (OMS)

Two major potential sources of organic matter that are likely to be food sources for oysters were sampled for isotopic analyses (Marín Leal et al., 2008): *i)* phytoplankton (PHY), which is a major fraction of the organic suspended particulate matter in marine waters; and *ii)* microphytobenthos (MPB), which is re-suspended from the sediment by waves and tidal action.

In BDV and BH, PHY was sampled at high tide in the open sea at around 500 m from each oyster culture site. Two replicate tanks of sea water (2 L), collected from 0-50 cm depth, were pre-filtered onto a 200 μm mesh to remove the largest particles, and filtered onto pre-weighed, pre-combusted (450°C, 4 h) Whatmann GF/C (Ø = 47 mm) glass-fibre filters immediately after sampling.

In BDV, MPB was collected by scraping the visible microalgal mats off of the sediment surface adjacent to the culture site during low tide. Immediately after scraping, benthic microalgae and sediment were put into sea water where they were kept until the extraction at the laboratory. Microalgae were extracted from the sediment using Whatmann lens cleaning tissue (dimensions: 100mm × 150mm, thickness: 0.035 mm); sediment was spread in a small tank and covered with two layers of tissue. The tank was kept under natural light/dark conditions until migration of the MPB. The upper layer was taken and put into filtered sea water to resuspend the benthic microalgae. The water samples were then filtered onto pre-weighed, pre-combusted (450°C, 4 h) Whatmann GF/C (Ø = 47 mm) glass-fibre filters. Meiobenthos fauna was removed from the filters under a binocular microscope. No samples of MPH were collected in BH due to the bottom composition of the culture site.

Both PHY and MPB filters were then treated with concentrated HCl fumes (4 h) in order to remove carbonates (Lorrain et al., 2003), frozen (−20°C) and freeze-dried (60°C, 12 h). The filters were then ground to a powder using a mortar and pestle and stored in safe light and humidity conditions until isotopic analyses.

2.2.4 Elemental and stable isotope analyses

The samples of oyster tissues and OMS were analysed using a CHN elemental analyser EA3000 (EuroVector, Milan, Italy) for particulate organic carbon (POC) and particulate nitrogen (PN) in order to calculate their C/N atomic ratios (C_{at}/N_{at}). Analytical precision for the experimental procedure was estimated to be less than 2 % dry mass for POC and 6 % dry mass for PN. The gas resulting from the elemental analyses was introduced online into an isotopic ratio mass spectrometer (IRMS) IsoPrime (Elementar, UK) to determine the $^{13}C/^{12}C$ and $^{15}N/^{14}N$ ratios. Isotopic ratios are expressed as the difference between the samples and the conventional Pee Dee Belemnite (PDB) standard for carbon and air N_2 for nitrogen, according to the following equation:

$$\delta^0_{ij} = \left(\frac{R_{\text{sample}}}{R_{\text{standard}}} - 1 \right) 1000 \tag{2.1}$$

where δ^0_{ij} (‰) is the isotope 0 (13 or 15) of element i (C or N) in a compound j. Subscript j stands for the whole soft tissues W_d, the gills Gi, the adductor muscle Mu, the remaining tissues Re of *C. gigas* or the food sources PHY and MPB. R is the $^{13}C/^{12}C$ or $^{15}N/^{14}N$ ratios. The standard values of R are 0.0036735 for nitrogen and 0.0112372 for carbon. When the organs were sampled, the isotopic ratio and the C/N ratio of the whole soft tissues, *i.e.* $\delta^0_{iW_d}$ and C/N_{W_d} respectively, were calculated as followed:

$$\delta^0_{iW_d} = \frac{\delta^0_{iGi} W_{dGi} + \delta^0_{iMu} W_{dMu} + \delta^0_{iRe} W_{dRe}}{W_{dGi} + W_{dMu} + W_{dRe}} \tag{2.2}$$

$$C/N_{W_d} = \frac{C/N_{Gi} W_{dGi} + C/N_{Mu} W_{dMu} + C/N_{Re} W_{dRe}}{W_{dGi} + W_{dMu} + W_{dRe}} \tag{2.3}$$

The internal standard was the USGS 40 of the International Atomic Energy Agency ($\delta^{13}C = -26.2$; $\delta^{15}N = -4.5$). The typical precision in analyses was $\pm 0.05\,\%$ for C and $\pm 0.19\,\%$ for N. One tin caps per sample was analysed. One tin cap was analysed per sample. The mean value of the isotopic ratio was considered for both animal tissues and OMS.

2.2.5 Statistical analyses

Firstly, comparisons of growth patterns and isotopic composition of whole body tissues between BDV and BH sites were based on the average individual dry flesh mass (W_d), the isotopic signatures $\delta^{13}C$ and $\delta^{15}N$ and the C/N ratio. Differences among W_d, $\delta^{13}C$, $\delta^{15}N$ and C/N were analysed with a two-way ANOVA, with time (*i.e.* sampling date) and site as fixed factors. Secondly, repeated measures ANOVAs were used to test for differences in the individual dry mass, isotopic signatures and C/N ratio among the different organs (gills, adductor muscle and remaining tissues) of *C. gigas*, with site and sampling date as the (inter-individual) sources of variation among oysters, and organs as the (intra-individual) source of variation within oysters. In both cases, all data were square-root transformed to meet the assumptions of normality, and the homogeneity of variance and/or the sphericity assumption checked. In cases where ANOVA results were significant, they were followed by a Tukey HSD post hoc test (Zar, 1996) to detect any significant differences in dry mass, isotopic signatures and C/N ratio for the whole body and for each of the organs between the two sites and/or among the different organs.

2.3 Results

2.3.1 Environmental conditions: chlorophyll-*a* concentration and water temperature at the study sites

From March 2009 to February 2010, [Chl-*a*] was on average 3 times higher in BDV than in BH, with a maximum value of 9.11 μg.L^{-1} in June 2009 in BDV and 4.43 μg.L^{-1} in May 2009 in BH (Fig. 2.2). From March to July 2009, the average [Chl-*a*] were 2.26 μg.L^{-1} in BH and 4.92 μg.L^{-1} in BDV, *i.e.* relatively high compared with the [Chl-*a*] measured from October 2009 to February 2010, which was 0.46 μg.L^{-1} and 1.42 μg.L^{-1} in BH and in BDV, respectively (Fig. 2.2).

Water temperature showed a typical seasonal pattern at both sites, with increasing values between March and August 2009, reaching a maximum value in July or August 2009, followed by a decrease during the autumn (Fig. 2.2). The thermal amplitude was, however, higher in BDV (15.3°C) than in BH (13.7°C). In BDV, the maximum and minimum temperatures were reached in August 2009 (20.8°C) and March 2010 (6.6°C) respectively, while they occurred earlier in BH: in early July 2009 (19.7°C) and early January 2010 (4.4°C), respectively.

2.3.2 Variations in W_d and C/N ratio of *C. gigas*

Significant interaction between site and time occurred for the total dry flesh mass W_d of *C. gigas* (two-way ANOVA, site × time, $F_{7,455} = 40.79$, $P < 0.0001$; Fig. 2.3). From July 2009, W_d was significantly higher in BDV than in BH at each sampling date (Tukey HSD post hoc test, $P < 0.0001$). From March to June 2009 the increase in W_d was relatively slow and similar in BDV and BH (from 0.02 g to 0.36 g in BDV and to 0.39 g in BH), exhibiting no significant differences between sites for any sampling date (Tukey HSD post hoc test, $0.194 \leqslant P \leqslant 0.513$). W_d increased more sharply from July until October 2009 in BDV ($\approx 75\,\%$ increment in W_d) compared with BH (only $\approx 42\,\%$ increment in W_d). A slight decrease in W_d was observed from August 2009 until February 2010 in BH whereas W_d was still increasing slightly in BDV over the same period (Fig. 2.3). At the end of the growth survey (February 2010), the value for W_d in BDV was 1.80 g compared with 0.55 g in BH.

As for W_d, significant interactions between site, time and organs occurred for the dry mass of the different organs, W_{Gi}, W_{Mu}, and W_{Re} (three-way ANOVA, site × time × organs, $F_{8,307} = 8.14$, $P < 0.0001$, Fig. 2.3). In BDV, W_{Re} exhibited an increase of $\approx 30\,\%$ between July and October 2009, whereas it decreased by $\approx 12\,\%$ over the same period in BH (Fig. 2.3 C and 2.3 E). At both sites, W_{Re} was stable from November 2009 until February 2010. Between August 2009 and February 2010, 70 % and 80 % of W_d corresponded to W_{Re} in BH and BDV respectively. From July 2009 to February 2010, W_{Mu} and W_{Re} were significantly different between the two sites at each sampling date (Tukey

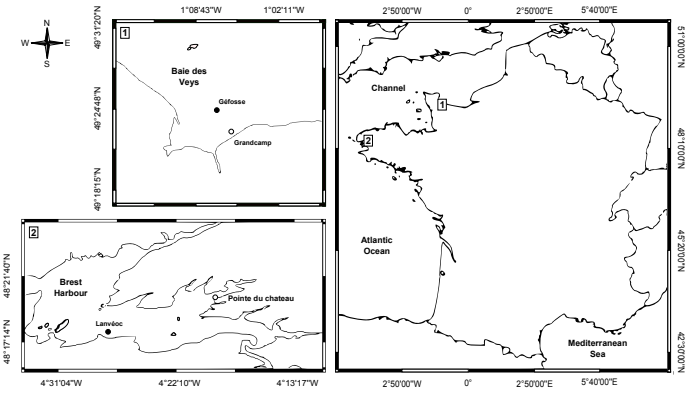

Figure 2.1: Geographic location of the two study ecosystems, Baie des Veys (BDV) and Brest Harbour (BH), along the Channel and Atlantic coasts of France. White circles indicate the oyster culture sites and the black circles indicate the locations where chlorophyll-*a* and temperature were monitored.

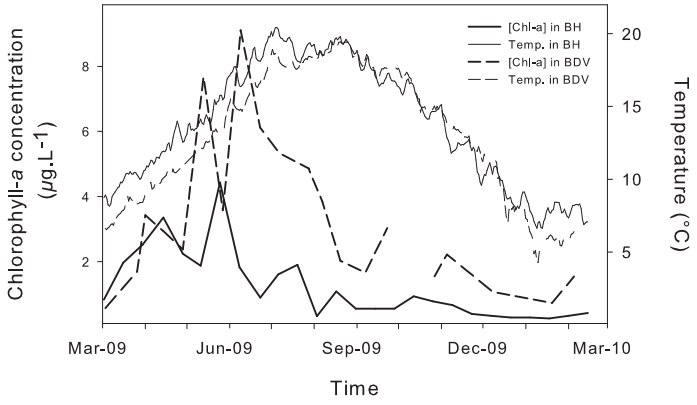

Figure 2.2: Temporal variations in Chlorophyll-*a* concentrations ([Chl-*a*], μg.L^{-1}) and water temperature (°C) in Brest Harbour (BH, solid lines) and Baie des Veys (BDV, dashed lines) from March 2009 to March 2010

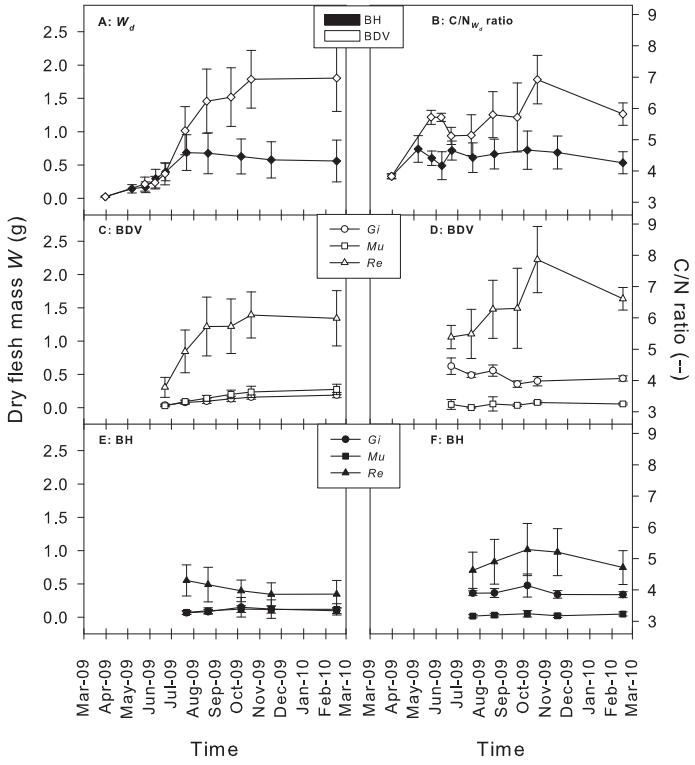

Figure 2.3: Temporal variations in mean individual dry flesh mass W_d (g, left panels) and C/N ratio (–, right panels) of *Crassostrea gigas* tissues from March 2009 to February 2010 at two sites: Baie des Veys in Normandy (BDV, empty symbols) and Brest Harbour in North Brittany (BH, solid symbols). Graphs A and B show the whole body tissues ($\diamond$, $\blacklozenge$) and graphs C, D, E, and F show the organs: gills *Gi* ($\circ$, $\bullet$), adductor muscle *Mu* ($\square$, $\blacksquare$) and remaining tissues *Re* ($\triangle$, $\blacktriangle$), including the mantle, gonad, digestive gland and labial palps. The vertical bars indicate $\pm$SD of the mean for $n = 30$ oysters (W) and $n = 5$ oysters (C/N ratio).

HSD post hoc test, $P \leqslant 0.0346$), while W_{Gi} was not significantly different between BDV and BH at each sampling date from July to October 2009 (Tukey HSD post hoc test, $0.0541 \leqslant P \leqslant 0.1550$). In BDV, W_{Gi} and W_{Mu} were not significantly different in July 2009 (Tukey HSD post hoc test, $P = 0.0682$); in BH, they were also not significant differences in July, August, October 2009 or in February 2010 (Tukey HSD post hoc test, $0.0970 \leqslant P \leqslant 0.9134$, Fig. 2.3 C and 2.3 E).

Interactions between site and time were also significant for the C/N ratio of whole body tissues (C/N_{W_d}, Fig. 2.3 B) which was significantly higher in BDV than in BH at almost all sampling dates (two-way ANOVA, site × time $F_{7,78} = 2.96$, $P = 0.0096$, Fig. 2.3 B). Only in June 2009 did C/N_{W_d} not differ significantly between BDV and BH (Tukey HSD post hoc test, $P = 0.1667$). In BDV, a strong increase of $\approx 87\,\%$ was observed from April to August 2009, when the C/N ratio reached the maximum value of 6.9. In the meantime, the C/N_{W_d} ratio in BH remained rather constant, with a mean value of 4.3 over the whole survey (Fig. 2.3 B). The C/N ratio in BDV fell to the value of 5.8 in February 2010.

Significant interactions between site and time and organs occurred for C/N_{Re}, C/N_{Gi} and C/N_{Mu} (three-way ANOVA, site × time × organs, $F_{8,44} = 4.21$, $P = 0.0008$). C/N_{Re} showed almost the same variations as C/N_{W_d} (Fig. 2.3 B, D and F). The C/N ratios of *Gi*, *Mu*, and *Re* were significantly different from one another in BDV and BH at each sampling date (Tukey HSD post hoc test, $P \leqslant 0.0372$) and the following relative order was: $C/N_{Re} > C/N_{Gi} > C/N_{Mu}$ irrespective of the study site.

2.3.3 δ^{13}C and δ^{15}N signatures in *C. gigas* soft tissues

Interactions between site and time were significant for the δ^{13}C of *C. gigas* whole body ($\delta^{13}C_{W_d}$, two-way ANOVA, site × time, $F_{7,78} = 31.82$, $P < 0.0001$). No significant differences were observed between the two sites in February 2010 (Tukey HSD post hoc test, $P = 0.9568$) conversely to the other sampling dates for which the $\delta^{13}C_{W_d}$ was significantly lower in BDV than in BH, with a mean $\delta^{13}C_{W_d}$ of $-20.65\,‰$ in BDV and $-19.50\,‰$ in BH (Fig. 2.4 A). From March to May 2009, $\delta^{13}C_{W_d}$ in BH decreased from $-19.35\,‰$ to $-20.65\,‰$ and then increased up to $-18.97\,‰$ in July 2009. The highest $\delta^{13}C_{W_d}$ value *i.e.*, $-18.84\,‰$, was reached in August 2009 while a slight general decrease was observed until the end of the survey in BH. A sharp decrease in $\delta^{13}C_{W_d}$ from $-19.35\,‰$ in March 2009 to $-22.13\,‰$ in May 2009 occurred in BDV (Fig. 2.4 A). Between June and July 2009, $\delta^{13}C_{W_d}$ leapt up to the value of $-19.96\,‰$ and remained constant until February 2010. Significant interactions between site and time occurred for the $\delta^{15}N_{W_d}$ (two-way ANOVA, site × time, $F_{7,78} = 11.23$, $P < 0.0001$). From June 2009 to February 2010, $\delta^{15}N_{W_d}$ became significantly higher in BDV than in BH (Tukey HSD post hoc test, $P \leqslant 0.0143$; Fig. 2.4 B) with the exception of June 2009, where no significant differences were observed between BDV and BH (Tukey HSD post hoc test,

$P = 0.8610$). The maximum values for $\delta^{15}N_{W_d}$ was 9.58 ‰ in August 2009 and 10.33 ‰ in September 2009 in BH and BDV, respectively.

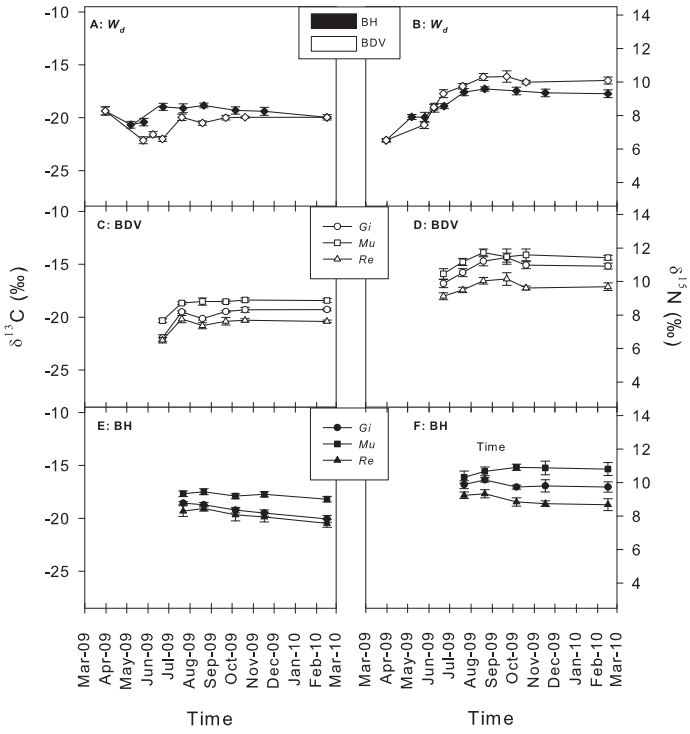

Figure 2.4: Temporal variations from March 2009 to February 2010 of δ^{13}C (‰, left panels) and δ^{15}N (‰, right panels) isotopic signature of *Crassostrea gigas* tissues at the two sites: Baie des Veys in Normandy (BDV, empty symbols) and Brest Harbour in North Britany (BH, solid symbols). Graphs A and B) show results for whole body tissues ($\diamond$, $\blacklozenge$) and graphs C, D, E and F how results for the organs: gills *Gi* ($\circ$, $\bullet$), adductor muscle *Mu* ($\square$, $\blacksquare$) and remaining tissues *Re* ($\triangle$, $\blacktriangle$) including the mantle, gonad, digestive gland and labial palps. The vertical bars indicate $\pm$ SD of the mean for $n = 5$ oysters.

Temporal variations in δ^{13}C and δ^{15}N of the different organs, *i.e.*, δ_{Gi}, δ_{Mu} and δ_{Re} for the gills, adductor muscle and remaining tissues exhibited similar patterns to the whole soft body tissues ($\delta^{13}C_{W_d}$, $\delta^{15}N_{W_d}$) at both sites (Fig. 2.4 C, D, E, F). For both the δ^{13}C and δ^{15}N, interactions between site and time and organs were significant (three-way ANOVA, site $\times$ time $\times$ organs, $F_{8,48} = 8.88$, $P < 0.0001$ for the carbon and $F_{8,48} = 8.88$, $P = 0.0002$ for nitrogen). The $\delta^{15}N_{Mu}$, $\delta^{15}N_{Gi}$ and $\delta^{15}N_{Re}$ were significantly different between the two sites at most dates (Tukey HSD post hoc test, $P \leqslant 0.0064$) except in

July 2009 for $\delta^{15}N_{Re}$ (Tukey HSD post hoc test, $P = 0.1041$). Values were rather constant in BH over the whole survey, while they increased from June to September 2009 in BDV and then decreased slightly and stabilized until February 2010. Patterns of the $\delta^{13}C_{Mu}$, $\delta^{13}C_{Gi}$ and $\delta^{13}C_{Re}$ were less sharp than those observed for nitrogen. From August 2009 to February 2010, the isotopic ratios of oyster organs decreased at BH, while they remained stable in oysters at BDV. No significant differences were observed between BDV and BH in October and November 2009 for the $\delta^{13}C_{Gi}$ (Tukey HSD post hoc test, $P = 0.1037$ and $P = 0.1345$, respectively), in November 2009 and February 2010 for the $\delta^{13}C_{Re}$ (Tukey HSD post hoc test, $P = 0.0729$ and $P = 0.6928$, respectively) and in February 2010 for the $\delta^{13}C_{Mu}$ (Tukey HSD post hoc test, $P = 0.1279$). Except in October 2009, where $\delta^{13}C_{Gi}$ and the $\delta^{13}C_{Mu}$ were not significantly different each other in BDV (Tukey HSD post hoc test, $P = 0.8190$), the $\delta^{13}C$ and $\delta^{15}N$ of *Gi*, *Mu*, and *Re* were significantly different from one another within BDV and BH (Tukey HSD post hoc test, $P \leqslant t0.0371$) at all other sampling dates and the following relative order was observed $\delta_{Mu} > \delta_{Gi} > \delta_{Re}$ (Fig. 2.4 D), irrespective of the study site.

2.3.4 $\delta^{13}C$ and $\delta^{15}N$ signatures of the food sources

From May to September 2009, the $\delta^{13}C$ values of the phytoplankton food source ($\delta^{13}C_{PHY}$) decreased from -18.52 ‰ to -25.44 ‰ in BH (Fig. 2.5 A). From September 2009 to late October 2009, $\delta^{13}C_{PHY}$ varied over a range of 2.4 ‰ and stabilised. In BDV, the temporal pattern of $\delta^{13}C_{PHY}$ differed from BH: a sharp increase in $\delta^{13}C_{PHY}$ occurred in June and July 2009 when the maximum value was reached, *i.e.*, $\delta^{13}C_{PHY} = -18.52$ ‰ followed by a decrease of around 5.23 ‰ over the next three months (Fig. 2.5 A). The values in $\delta^{15}N_{PHY}$ in BH varied between 6.53 ‰ and 8.18 ‰ from May to September 2009, and dropped to 5.56 ‰ in October 2009 (Fig. 2.5 B). Although the values of the $\delta^{15}N_{PHY}$ in BDV showed high variability throughout the survey, the *PHY* food source remained higher in ^{15}N in BDV than in BH, with average $\delta^{15}N_{PHY}$ values over the sampling period of 8.40 ‰ in BDV and of 7.28 ‰ in BH. An increase of $\delta^{15}N_{PHY}$ was observed in BDV during June and July 2009, followed by a decrease until the late September 2009 and then a further increase to a maximum of 10.15‰, reached in late October 2009 (Fig. 2.5 B). In BDV, the *MPB* source was richer in ^{13}C, at $\delta^{13}C = -14.86$ ‰, than the *PHY* source, at *i.e.* $\delta^{13}C = -24.96$ ‰, (Figs. 2.5 A and C). However, this pattern was inverted for the $\delta^{15}N$, with an average value of 5.53 ‰ for $\delta^{15}N_{MPB}$, while $\delta^{15}N_{PHY}$ equalled 8.40 ‰(Fig. 2.5 D).

2.4 Discussion

The trophic environment, as represented by [Chl-*a*] as a quantitative proxy, influences oyster growth (in terms of dry flesh mass: W_d) differently at the

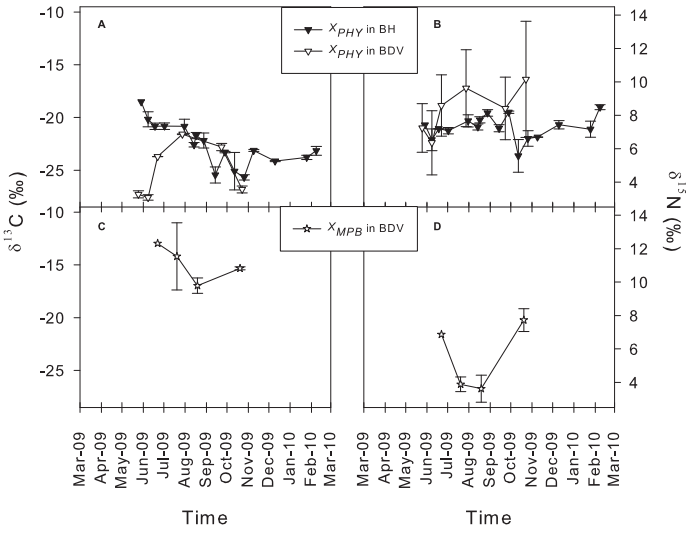

Figure 2.5: Temporal variations of $\delta^{13}C_X$ (‰, left panels) and $\delta^{15}N_X$ (‰, right panels) isotopic ratios of the food sources at two sites: Baie des Veys in Normandy (BDV, empty symbols) and Brest Harbour in North Brittany (BH, solid symbols) from March 2009 to February 2010. Graphs A and B represent the phytoplankton, PHY ($\triangledown$, $\blacktriangledown$) and graphs C and D represent the microphytobenthos, MPB ($\star$). The vertical bars indicate $\pm$ SD of the mean for 2 replicate samples.

sites BDV and BH. The seasonal differences in [Chl-a] between BDV and BH, which are particularly marked in spring and early summer *i.e.*, $[\text{Chl-}a]_{\text{BDV}} \approx 4[\text{Chl-}a]_{\text{BH}}$, likely account for the differences in oyster growth performances observed between the two sites (Figs. 2.2 and 2.3 A). An increase in W_d occurs from March to June 2009 (Fig. 2.3 A) when the Chl-a is likely to be non limiting in both BDV and BH. This suggests that the growth of *C. gigas* (as expressed in W_d) in BDV and in BH mainly relies on the PHY food source. In these two ecosystems, Alunno-Bruscia et al. (2011) and Bernard et al. (2011) have shown that the variability of growth and reproduction in *C. gigas* can be accurately simulated using a dynamic energy budget (DEB) model, with temperature and phytoplankton enumeration data as forcing variables. These authors attributed the spatial variability in growth of *C. gigas* to the local differences in X_{PHY}. The growth patterns of *C. gigas* in BDV, however, differ slightly from the results of Grangeré et al. (2009b) and Marín Leal et al. (2008), who reported a decrease of W_d *i)* in spring due to spawning events and *ii)* in autumn and winter, probably due to the low food conditions. The continuous growth of *C. gigas* observed from March 2009 to February 2010 in our study can be explained by the unusual Chl-a concentrations in BDV in 2009: blooms did not exceed 9.11 μg.L^{-1} and stretched over three months (May - August). Conversely, Grangeré et al. (2009b), Jouenne et al. (2007) and Lefebvre et al. (2009b) reported larger blooms, between 12 μg.L^{-1} and 25 μg.L^{-1}, earlier in the year (March and April).

With respect to the qualitative trophic environment, the temporal variations in both δ_{PHY} and δ_{MPB} in BDV differ from the typical patterns observed in this bay. The PHY source was slightly higher in both ^{13}C and ^{15}N values, ranging from -27.2 ‰ to -21.5 ‰ and from 6.3 ‰ to 10.1 ‰ respectively, compared with previous ranges of values observed ≈ -22 ‰ to ≈ -18 ‰ for ^{13}C and ≈ 3 ‰ to ≈ 6 ‰ for ^{15}N in 2004 and 2005 (Lefebvre et al., 2009b; Marín Leal et al., 2008). The $\delta^{13}C_{MPB}$ values were also higher than usual (overall mean = -14.8 ‰), though the $\delta^{15}N_{MPB}$ were lower (overall mean = 5.53 ‰) than the MPB values found by Marín Leal et al. (2008) in 2004 and 2005 (overall mean = -17.9 ‰ and 7.4 ‰ respectively). Moreover, $\delta^{15}N_{MPB}$ was lower than the $\delta^{15}N_{PHY}$, which is not common since the opposite trend has been usually observed (Kang et al., 2006; Marín Leal et al., 2008; Riera, 2007; Yokoyama et al., 2005b). The suspended particulate organic matter monitored by Lorrain et al. (2002) in BH in 2000 exhibits lower δ^{13}C and δ^{15}N, ranging from -25.6 ‰ to -18.5 ‰ and from 8.4 ‰ to 5.5 ‰ respectively, than in this study (values ranged from -25.6 ‰ to -18.5 ‰ and from 8.4 ‰ to 5.5 ‰ respectively), but stronger temporal variations, probably due to the high sampling frequency.

It is necessary to consider both quantitative ([Chl-a]) and qualitative (δ_X) aspects of temporal variations in the trophic resource to understand the differences in oyster growth among contrasting ecosystems. The decrease of $\delta^{13}C_{W_d}$ in the two sites at the start of the monitoring, *i.e.* during the period when oyster growth is weak, is probably due to the change in diet between the site

of origin (Arcachon Bay) and the culture sites (BDV and BH). The increase of $\delta^{13}C_W$ during the summer in BDV likely results from the increase in $\delta^{13}C_{PHY}$ observed from June to July 2009. However, while both $\delta^{13}C_{PHY}$ and [Chl-*a*] decreased from August to October 2009 in BDV, $\delta^{13}C_W$ remained more constant and the oysters continued to grow until the end of the survey (Fig. 2.4 A). Three explanations, which are not mutually exclusive, could account for this paradox. Firstly, although the phytoplankton biomass (estimated by [Chl-*a*]) strongly decreased in BDV from August to October 2009, the oysters continued to gain mass, suggesting that another food source - such as MPB - could have been supporting *C. gigas* growth (Lefebvre et al., 2009a). This idea is corroborated by the relatively high values of $\delta^{13}C_{MPB}$ observed in late summer and autumn (Fig. 2.5 C and 2.4 A, respectively). The slight decrease of $\delta^{15}N_W$ in September and October 2009 (Fig. 2.4 B) could also be explained by the consumption of MPB by the oysters. Secondly, the high mass of the oyster whole soft body tissues at the end of the survey in BDV implies that they had a large amount of structural protein that would require maintainance (Fig. 2.3 A). As stated by Emmery et al. (2011) and Pecquerie et al. (2010), isotopic discrimination during maintenance metabolism selects for light isotopes. Consequently, the larger the individual, the larger the amount of structure to be maintained and the heavier the organism in ^{13}C and ^{15}N. Thirdly, Emmery et al. (2011) and Gaye-Siessegger et al. (2004b) showed that the increase in feeding level led to a decrease of $\delta^{13}C_W$ and $\delta^{15}N_W$ of the individuals. The decrease in [Chl-*a*] observed from late summer until winter in BDV and BH could therefore explain the enrichment of *C. gigas* in ^{13}C and ^{15}N over the same period. This can also explain the spatial variability in $\delta^{13}C_W$ observed between BDV and BH since [Chl-*a*] is significantly higher in BDV than in BH over the whole experimental period (Fig. 2.2). This explanation, however, does not account for the $\delta^{15}N_W$ values of *C. gigas*. Although $\delta^{15}N_{PHY}$ is higher in BDV than in BH, its values should be interpreted with caution since the water samples may have been collected too close to the shore and oyster tables, which could have caused them to contain not only phytoplankton but also detrital matter. The high variability in the data set (Fig. 2.5 B) supports the idea that the nitrogen signature could be due to a mixture of food sources rather than pure PHY.

The temporal variations in the isotopic ratio of the different organs (*i.e.* gills, adductor muscle and remaining tissues) could also be partly related to the variations in δ_{PHY}. In BDV, the δ isotopic ratios of organs and PHY source increase simultaneously in spring and summer (Fig. 2.4 C and D and Fig. 2.5 A and B, respectively). The general decrease of $\delta^{13}C_{PHY}$ throughout the survey (Fig. 2.5 A) may also account for the slight decrease in the δ_{Mu}, δ_{Gi} and δ_{Re} (Fig. 2.4 E). Nevertheless, for both BDV and BH, the δ_{Gi}, δ_{Mu} and δ_{Re} clearly exhibit different isotopic enrichment over time with respect to one another (Fig. 2.4) that cannot be explained by the variations in δ_{PHY}. The relative order $\delta_{Mu} > \delta_{Gi} > \delta_{Re}$ is observed in the enrichment patterns between organs, irrespective of the study site, suggesting that the metabolism has a strong influence on stable isotope dynamics in oyster tissues. This pattern is

consistent with results of previous studies: Malet et al. (2007) found that δ^{13}C and δ^{15}N were higher in the adductor muscle than in the mantle, digestive gland and gonad of diploid and triploid *C. gigas*. Paulet et al. (2006) also showed that the adductor muscle had higher δ values than the gills and gonad of oysters at the start of an experimental shift in the δ^{13}C of the diet. In the same way, Yokoyama et al. (2005b) pointed out that $\delta^{15}N_{Mu}$ in *C. gigas* was heavier (in terms of isotopic ratio) than $\delta^{15}N_{Gi}$ after equilibrium with the food source. Several interpretations of our results can be proposed based on the Lorrain et al. (2002) study. The δ_{Re} and δ_{Gi} are *i)* similar in terms of temporal variations and *ii)* vary faster than the δ_{Mu} (Fig. 2.4). These results suggest that food uptake is preferentially routed to the storage organs, (*e.g.*, digestive gland and mantle) and/or reproductive tissues (*e.g.* gonad) during active growth periods, *i.e.*, in spring and early summer. The narrow range of variation in δ_{Mu} over the survey might be due to the low turnover rate of this organ. In *P. maximus*, $\delta^{13}C_{Mu}$ and $\delta^{15}N_{Mu}$ exhibit similar low variations compared with the digestive gland and gonad (Lorrain et al., 2002). The carbon incorporation index calculated by Paulet et al. (2006) in the muscle of both *C. gigas* and *P. maximus* showed the lowest value among the studied organs in all seasons.

The differences in isotopic discrimination between organs that have been reported in the literature (*e.g.*, Guelinckx et al., 2007; Suzuki et al., 2005; Tieszen et al., 1983) can be mainly explained by differences in the biochemical composition of different organs. Organs containing a high proportion of lipids have a lower δ^{13}C value than organs with a lower lipid content (or a higher protein content), since lipids are relatively low in ^{13}C (Gannes et al., 1997; Martínez del Rio et al., 2009). The low level in the remaining tissues is thus consistent with their physiological role, *i.e.*, energy storage and reproduction, since the gametogenesis in spring and summer is characterised by an increase in lipids (Berthelin et al., 2000; Soudant et al., 1999). The relatively high values of $\delta^{13}C_{Mu}$ and $\delta^{15}N_{Mu}$, combined with a high protein concentration in the adductor muscle, supports the idea that the adductor muscle is not a storage compartment that supplies the energetic needs of reproduction (Berthelin et al., 2000). These interpretations are supported by the different W_d and C/N ratio dynamics observed among organs. *C. gigas* stores energy (mainly lipids and glycogen) in the digestive gland, gonad and mantle during spring and summer (*e.g.*, Berthelin et al., 2000; Costil et al., 2005; Ren et al., 2003; Whyte et al., 1990), which could explain the high contribution of the W_{Re} to the total dry mass of oysters: 70 % and 80 % in BDV and BH, respectively. The simultaneous increases of W_{Re} and C/N_{Re} from February to October 2009 in BDV confirm that most of the energy assimilated during spring and summer is directed to the reserve tissues (Fig. 2.3 C and D). The same pattern has been previously shown by Marín Leal et al. (2008) for *C. gigas* and by Smaal and Vonk (1997) for *Mytilus edulis*. The decrease in W_{Re} observed in BH from July 2009 to March 2010 may result from the low food quantity ([Chl-*a*] = 0.62 μg.L^{-1} observed from July 2009 to February 2010). The C/N ratio of the gills and adductor muscle tend to remain constant over time, suggesting that these two organs

make very little contribution to reserve storage.

The isotopic ratios of oyster tissues range from −22.1 ‰ to −17.8 ‰ for δ^{13}C and from 8.6 ‰ to 11.7 ‰ for δ^{15}N, irrespective of the study site. Our results on the trophic enrichment (*i.e.* trophic fractionation Δ) between oysters (whole soft tissues and/or organs) and their food source(s) strongly differ compared with the previous values of 1 ‰ and 3.5 ‰ reported in the literature (DeNiro and Epstein, 1978, 1981; Lorrain et al., 2002). Marín Leal et al. (2008) used different scenarios (S) to investigate the effect of different (but constant) Δ values on the contribution of organic matter sources, *i.e.*, S1: δ^{13}C = 1.85 ‰ and δ^{15}N = 3.79 ‰ from Dubois et al. (2007a); S2: δ^{13}C = 0.4 ‰ and δ^{15}N = 2.2 ‰ from McCutchan Jr et al. (2003). The results of the scenarios show strong differences in the contribution of the MPB source in BDV: from 6% to 26.1% between $S1$ and $S2$. These authors showed that the use of a constant Δ without considering either the isotopic comparison of organs or their temporal variations could lead to inaccurate interpretations in dietary reconstruction studies.

To conclude, the results of our transplantation experiment show that the effect of *C. gigas* metabolism on the isotopic discrimination likely has a major influence on the isotopic ratio of the different oyster organs (gills, adductor muscle and remaining tissues). Moreover, neither the contribution of food sources other than phytoplankton nor the amount of trophic resources can be excluded as factors explaining the spatial variability in the isotopic patterns. Consequently, the influence of these factors obviously leads to temporal variations in Δ^{13}C and Δ^{15}N that may lead to wrong interpretations in dietary reconstruction studies. Experiments conducted under controlled conditions are essential to investigate and quantify the factors that influence isotopic differences, such as the effect of ration size (*e.g.*, Barnes et al., 2007; Gaye-Siessegger et al., 2004b). However, the effect of the physiological functions, *i.e.*, assimilation, growth, maintenance and reproduction, on isotopic discrimination processes, as well as the quantification of the factors that influence these functions, need to be clarified to improve our understanding of isotope dynamics in living organisms. In this context, DEB models (Kooijman, 2010), which describe uptakes and use of mass and energy flows in biological systems, can provide a powerful framework for investigating the effect of metabolism on stable isotopes (*e.g.* Emmery et al., 2011; Pecquerie et al., 2010). DEB theory differs from traditional energy budget analyses in that food is first converted to reserves, and these reserves are subsequently used for metabolism (Lika and Kooijman, 2011). Our interpretation of the isotope signal thus supports the way DEB theory handles assimilates.

Acknowledgments

A. Emmery was supported by funding from Région Basse-Normandie and Ifremer. This PhD project was part of the Observatoire Conchylicole network (http://wwz.ifremer.fr/observatoire_conchylicole_eng/Presentation). We would like to thank F. Maheux, S. Parrad, M. Ropert and A. Gangnery from the Environment & Resources Ifremer laboratory in Port-en-Bessin, as well as P. Le Souchu and S. Pouvreau from the Ifremer laboratory at Argenton for their technical help. We also thank J. Le Poittevin from the Physiology and Ecophysiology of Marine Mollusc laboratory for her technical assistance with the isotopic samples. We are also very grateful to A. Sedon for her help with the sample preparation.

Chapter 3

Understanding the dynamics of δ^{13}C and δ^{15}N in soft tissues of the bivalve *Crassostrea gigas* facing environmental fluctuations in the context of Dynamic Energy Budgets (DEB)

Emmery, A.[a,b,c], Lefebvre, S.[c], Alunno-Bruscia, M.[a], Kooijman, S.A.L.M.[d], 2011.

Journal of Sea Research, 66, 361–371

[a] *Ifremer Dept. PFOM-PI,* 11 *Presqu'île du Vivier,* 29840 *Argenton, France*

[b] *Université de Caen Basse Normandie, CNRS INEE - FRE*3484 *BioMEA, Esplanade de la paix* 14032 *Caen cedex, France*

[c] *Université de Lille* 1 *Sciences et Technologies, UMR CNRS* 8187 *LOG, Station Marine de Wimereux,* 28 *avenue Foch,* 62930 *Wimereux, France*

[d] *Vrije Universiteit, Dept. of Theoretical Biology, de Boelelaan* 10851081 *HV Amsterdam, The Netherlands*

Abstract

We studied the dynamics of stable isotopes δ^{13}C and δ^{15}N of an opportunistic suspension feeder the Pacific oyster (*Crassostrea gigas*) to better understand the factors that influence the trophic enrichment (trophic-shift, Δ) between primary producers and consumers. Most of the previous studies on this topic do not quantify mass fluxes or isotopic discrimination phenomena in the organism, which are two pillars in isotope ecology. We used a dynamic energy budget

(DEB) approach (Kooijman, 2010) to quantify *i)* the fluxes of elements and isotopes in *C. gigas* soft tissues and *ii)* the impact of the scaled feeding level, the organism mass and the isotopic ratio of food on the "trophic-shift" Δ, and isotope turnover in tissues. Calibration and parametrization modeling were based on data from the literature. We showed that a five-fold increase in scaled feeding level leads to a decrease of the trophic-shift value of 35 % for carbon and 43 % for nitrogen. This can be explained by the molecule selection for the anabolic and/or catabolic way. When f increases due to the reserve dynamic formulation in the standard DEB model, the half-life of the isotopic ratio $t_\delta^{1/2}$ in tissues also decreases from 13.1 to 7.9 d for δ^{13}C and from 22.1 to 10.3 d for δ^{15}N. Organism mass also affects the trophic-shift value: an increase of the individual initial mass from 0.025 g to 0.6 g leads to an enrichment of 22 % for δ^{13}C and 21 % for δ^{15}N. For a large individual, these patterns show that a high structural volume has to be maintained. Another consequence of the mass effect is an increase of the half-life for δ^{13}C from 6.6 to 12.0 d, and an increase of the half life for δ^{15}N from 8.3 to 19.4 d. In a dynamic environment, the difference in the isotopic ratios between the individual tissues and the food ($\delta^{13}C_W - \delta^{13}C_X$) exhibits a range of variation of 2.02 ‰ for carbon and 3.03 ‰ for nitrogen. These results highlight the potential errors in estimating the contributions of the food sources without considering the selective incorporation of isotopes. We conclude that the dynamic energy budget model is a powerful tool to investigate the fate of isotopes in organisms.

Keywords: oyster; isotopic ratio; discrimination; trophic-shift; diet; DEB theory

3.1 Introduction

In recent years, understanding the ecological role of natural and cultivated suspension - feeding bivalves has gained increasing interest among marine ecologists (*e.g.* Dame, 1996; Newell, 2004). Bivalve populations exclusively inhabit the benthic-pelagic interface and are a key link in the matter fluxes of coastal ecosystems. This is because they transfer organic and mineral suspended matter from the water column to sediments *e.g.* considering their ability to filter a huge amount of pelagic matter (Doering and Oviatt, 1986), benthic suspension-feeders can exert a top-down control on phytoplankton communities in coastal ecosystems (Guarini et al., 2004; Cloern, 1982; Officer et al., 1982). Bivalves are mostly opportunistic and occupy an intermediate trophic niche between primary and secondary consumers. Consequently, they act as ecological indicators of the trophic state of the environment since they are sensitive to both the quality and quantity of the suspended organic matter that serves as their

food source (Jennings and Warr, 2003; Lefebvre et al., 2009a). Many bivalves can feed on a mixture of microalgae (phytoplankton and microphytobenthos) and detritus of marine (macroalgae) and terrestrial origin (Decottignies et al., 2007; Marín Leal et al., 2008).

Knowledge of the trophic role of bivalves in marine ecosystems has been improved by the use of stable isotope analysis (SIA) for tracing pathways of organic matter in food webs and for determining the contributions of different food sources to the organisms' diets (Marín Leal et al., 2008; Riera and Richard, 1996; Riera et al., 2002). Several laboratory studies have shown that the isotopic ratio of an organism, δ^{13}C and δ^{15}N, closely resembles that of the diet at steady state, though with a slight enrichment of heavier isotopes, *i.e.* ^{13}C, ^{15}N (DeNiro and Epstein, 1978, 1981). This enrichment, which is classically named the trophic-shift $\Delta = \delta_{consumer} - \delta_{diet}$, was often considered to be constant across species and trophic levels with an average value of 1 ‰ for δ^{13}C and 3.5 ‰ for δ^{15}N (DeNiro and Epstein, 1978, 1981). This assumption has been widely applied in the literature to better understand the contribution of the different food sources to the diet of bivalves in coastal ecosystems (*e.g.* Riera et al., 1999; Dubois et al., 2007b).

Based on experimental and field data, studies by Vander Zanden and Rasmussen (2001) and McCutchan Jr et al. (2003), have shown that the Δ value has significant variation due to different factors. For instance, Deudero et al. (2009), Suzuki et al. (2005) and Tieszen et al. (1983) pointed out different Δ values for carbon and nitrogen among organs whereas studies by Adams and Sterner (2000), Gaye-Siessegger et al. (2004a) and Mirón et al. (2006) focused on the effects of the quality and nitrogen content of the diet on the trophic-shift. Barnes et al. (2007) and Focken (2001) concluded that the difference in the isotopic ratio between diet and consumer increased when feeding level increased (see Martínez del Rio et al. (2009) for a complete review). In the case of the bivalve *Crassostrea gigas*, the published Δ values are 0.9 ‰ for carbon and 5.4 ‰ for nitrogen (Yokoyama et al., 2008). However, those calculated by Dubois et al. (2007a) are 1.85 ‰ for δ^{13}C and 3.79 ‰ for δ^{15}N (Table 3.1). Determining and quantifying the factors that influence the trophic-shift is essential for trophic network studies. The Δ value makes it possible to correct isotopic signatures of consumers prior to incorporating them into mixing models (*i.e.* linear systems of mass balance equations that calculate contributions of different sources to a mixture). Therefore, the weak point in applying these models for food reconstruction is related to the estimation of appropriate Δ values (Phillips and Koch, 2002; Phillips, 2001; Phillips and Gregg, 2003). Another critical assumption is the steady-state equilibrium between the consumer and its diet which possibly does not occur under natural conditions. Several authors have used bio-energetic modeling approaches to circumvent this problem and to estimate the incorporation rate over time (Marín Leal et al., 2008; Olive et al., 2003).

The isotope approach has some weaknesses due to the lack of ecological tools to quantify mass fluxes (elements) and isotopic discrimination phenom-

ena during assimilation, growth, and maintenance of organisms. The present study therefore aims *i)* to describe and quantify the fluxes of elements and isotopes of an opportunistic suspension feeder, *i.e.* the Pacific oyster *C. gigas*, by using a dynamic energy budget (DEB) approach (Kooijman, 2010) and *ii)* to quantify the impact of factors influencing the "trophic-shift" Δ and isotope tissue turnover which is useful for trophic network studies and diet reconstruction. We based our methods on the study by Pecquerie et al. (2010) which is, to our knowledge, the first theoretical investigation of the impact of metabolism on stable isotope in the context of DEB theory. Here we describe the first study with an application to *C. gigas*.

Table 3.1: Trophic-shift values (Δ, ‰) and half-life of the isotopic ratio ($t_\delta^{1/2}$, d) estimated for bivalve species and derived from literature during diet switching experiments. The Δ values refer to the enrichment of the whole body mass (non-defatted tissues). All individuals were fed *ad libitum* ($f = 1$). Temperature during the experiments was 15.9°C in Dubois et al. (2007a), between 15 and 17°C in Yokoyama et al. (2008), and 22°C in Yokoyama et al. (2005a).

		Carbon δ^{13}C		*Nitrogen* δ^{15}N	
Study	Species	Δ	$t_\delta^{1/2}$	Δ	$t_\delta^{1/2}$
Dubois et al. (2007a)	*Crassostrea gigas*	1.85 (±0.194)	7.7	3.79 (±0.194)	15.1
	Mytilus edulis	2.17 (±0.324)	8.9	3.78 (±0.292)	14.1
Yokoyama et al. (2008)	*Crassostrea gigas*	0.9	1.05	5.4	1.19
Yokoyama et al. (2005a)	*Ruditapes philippinarum*	0.6	––	3.4	––
	Mactra veneriformis	0.9	––	3.6	––

3.2 Material and methods

3.2.1 Standard Dynamic Energy Budget model (DEB)

The standard DEB model describes the rate at which an organism assimilates and utilizes energy for maintenance, growth,, and reproduction as a function of its state and its environment (Nisbet et al., 2000; Kooijman, 2010). Each metabolic transformation defines a chemical transformation in which five organic generalized compounds (food X, reserve E, reproduction buffer E_R, structure V, and feces P) and four mineral compounds (carbon dioxide O, water H, dioxygen O, and nitrogenous waste N) can be involved according to the transformation type (Table 3.2). Water and dioxygen substrates are assumed to be non-limiting. Each compound is composed of the four most abundant elements in organic matter, namely carbon C, hydrogen H, oxygen O, and nitrogen N. The mass of each compound is expressed in C-moles, *i.e.* the amount of each element relative to the amount of carbon per compound. The formula

for generalized compounds can be written as $CH_{n_{Hj}}O_{n_{Oj}}N_{n_{Nj}}$ where n_{ij} is the proportion of atoms in an element i (i = H, O, N) relative to carbon in a compound j ($j = X$, E, V, P). In the DEB model, the biochemical composition of reserve, structure, and the reproduction buffer of *C. gigas* is constant over time (Table 3.2).

Table 3.2: Elemental composition of the organic and mineral compounds used in this study for *Crassostrea gigas*. Values are estimated from the data of Whyte et al. (1990) and the procedures of Kooijman (2010).

	Organic comp.				*Minerals comp.*			
	X	V	E and E_R	P	C	H	O	N
Carbon C	1	1	1	1	1	0	0	0
Hydrogen H	1.8	1.78	1.79	1.8	0	2	0	3
Oxygen O	0.5	0.48	0.53	0.5	2	1	2	0
Nitrogen N	0.2	0.15	0.14	0.15	0	0	0	1

X: food
V: structure
E: reserve
E_R: reproduction buffer
P: feces
C: carbon dioxide
H: water
O: dioxygen
N: nitrogenous waste

The total biomass of the individual (in C-moles) has contributions from reserve, structure, and the reproduction buffer and can be written as: $M_W = M_E + M_V + M_{E_R}$ where M_E, M_V, and M_{E_R} are the mass of the reserve, structure and reproduction buffer respectively. The standard DEB model defines a set of three transformations in living organisms, *i.e.* assimilation (conversion of food to reserve and products), growth (conversion of reserve to structure and products) and dissipation (conversion of reserve to products) where generalized compounds are metabolized (Kooijman, 2010; Pecquerie et al., 2010). Changes in the mass of reserve, structure, maturity, and reproduction buffer can be written as:

$$\frac{d}{dt}M_E = \dot{J}_{EA} + \dot{J}_{EC} \tag{3.1}$$

$$\frac{d}{dt}M_V = (\kappa \dot{J}_{EC} - \dot{J}_{EM})y_{VE} = \dot{J}_{VG} \tag{3.2}$$

$$\frac{d}{dt}M_H = (1-\kappa)\dot{J}_{EC} - \dot{J}_{EJ} = \dot{J}_{ER} \quad \text{if} \quad M_H < M_H^p, \quad \text{else} \quad \frac{d}{dt}M_H = 0 \tag{3.3}$$

$$\frac{d}{dt}M_{E_R} = \kappa_R \dot{J}_{ER} \quad \text{if} \quad M_H = M_H^p, \quad \text{else} \quad \frac{d}{dt}M_{E_R} = 0 \tag{3.4}$$

where $\dot{J}_{EA} = f\{\dot{J}_{EAm}\}L^2$ the assimilation flux ($f = 0$ if $M_H < M_H^b$) and $\dot{J}_{EC} = \{\dot{J}_{EAm}\}L^2\frac{ge}{g+e}(1 + \frac{L}{gL_m})$ the catabolic flux. $e = \frac{\dot{v}[M_E]}{\{\dot{J}_{EAm}\}}$ represents the scaled reserve density and $g = \frac{\dot{v}[M_V]}{\kappa\{\dot{J}_{EAm}\}y_{VE}}$ represents the energy investment ratio. Maintenance fluxes are described by $\dot{J}_{EM} = [\dot{J}_{EM}]L^3$ for the somatic compartment and $\dot{J}_{EJ} = \dot{k}_J M_H$ for the maturity and reproduction compartment. The allocation to maturity and reproduction flux $\dot{J}_{ER}$ is described by

the following expression $\dot{J}_{ER} = (1-\kappa)\dot{J}_{EC} - \dot{J}_{EJ}$. Initiation of allocation to reproduction occurs when individual reaches the threshold of maturity at puberty, *i.e.* $M_H = M_H^p$. The energy allocated to M_{E_R} is then converted into gametes (ovocyte or spermatozoa) with some efficiency denoted κ_R, and the remainder $1-\kappa_R$ is dissipated as overhead. Once enough energy has been accumulated in the reproduction buffer, *i.e.* when a certain gonado-somatic index (GSI, %) has been reached, and if the external temperature is above 20 °C, the buffer is completely emptied and further accumulation is possible (Pouvreau et al., 2006).

To determine the total biomass of the individual in grams (W, g of dry weight), we first calculated the molar weight of the compounds E, V, and E_R (w_E, w_V, and w_{ER} respectively) as: $w_j = \sum n_{ij} w_i$, where w_i is the molar weight of an element (g.mol^{-1}, Table 3.3). Therefore, W can be obtained from the following formula: $W = M_E w_E + M_V w_V + M_{E_R} w_{ER}$.

3.2.2 Dynamic Isotope Budget model (DIB)

The assumptions and equations of the DIB models used for this study are extensively detailed in Kooijman (2010) and Pecquerie et al. (2010). The DIB model describes the changes in the isotope frequency γ_{ij}^0 of reserve, structure, and reproduction buffer where 0 the isotope of an element i in a compound j, *e.g.* γ_{CE}^{13} is the frequency of ^{13}C in reserve.

The chemical reactions of compounds can be synthesized by a set of three macrochemical equations with a constant stoichiometry. In the simplest form, the assimilation macrochemical equation can be written as $X + O \rightarrow E + P + H + N + C$, growth leads to the production of structure from reserve, $E + O \rightarrow V + C + H + N$, and dissipation encompasses the transformation of reserve into mineral products through the following reaction $E + O \rightarrow C + H + N$. Nevertheless these macrochemical reactions do not provide any information on the fate of atoms or on the discrimination of isotopes.

Isotopic discrimination in a macrochemical reaction is a three-step process. Compounds are first mobilized from a pool. Then, compounds are selected for the anabolic or catabolic fluxes according to their isotopic composition. Indeed, all three chemical transformations have an anabolic and catabolic aspect meaning that substrates have a dual function: they serve as a source for energy and building blocks. The catabolic route of any transformation uses substrates to produce energy. The anabolic route uses this energy and substrates as a source of building blocks to produce a given compound. Due to the difference in fate of substrate molecules, selection of molecules with particular isotopes can occur at the partitioning of anabolic and catabolic fluxes (Pecquerie et al., 2010; Kooijman, 2010). The number of molecules with one rare isotope in the anabolic route of a transformation is obtained from the mean of a Fisher's noncentral hypergeometric distribution. This selection depends on the odds ratio parameter value β which is defined as the ratio of probabilities of two isotopes (*i.e.* ^{13}C and ^{12}C) being selected for a particular route (Kooijman, 2010). This

parameter allows the relative frequency of an isotope 0 of an element i in a compound j to be calculated for a given transformation k, n_{ij}^{0k}. $\beta = 1$ means that there is no selection between isotopes whereas $\beta > 1$ implies a discrimination against light isotopes. Finally, atom reshuffling occurs which describes the fraction of atoms in a chemical compound in a substrate which ends up in a product from a given transformation.

To fully describe the isotopic composition of an organism, the structure turnover is taken into account. This process is described by two coupled macrochemical reactions: the production of renewed structure from reserve, L_1: $E + O + V \rightarrow V + C + H + N$, and the degradation of structure, L_2: $V + O \rightarrow V + C + H + N$. Structure turnover, which is part of the volume-specific somatic maintenance, states that the incoming flux of renewed structure is compensated by the outgoing flux of degraded structure and a part of the degraded structure is recycled to form renewed structure. Compound selections and atom reshuffling occur *i)* between reserve and structure *ii)* and between degraded structure and renewed structure. These three fluxes therefore have different isotopic compositions.

The isotopic ratios of reserve, structure and reproduction buffer are described by the following state equations:

$$\frac{d}{dt}\gamma_{iE}^{0} = \left(\frac{n_{iE}^{0A}}{n_{iE}} - \gamma_{iE}^{0}\right)\frac{\dot{J}_{EA}}{M_E}; \tag{3.5}$$

$$\frac{d}{dt}\gamma_{iV}^{0} = \left(\frac{n_{iV}^{0G}}{n_{iV}} - \gamma_{iV}^{0}\right)\frac{\dot{J}_{VG}}{M_V} - \left(\frac{n_{iV}^{0L}}{n_{iV}} - \gamma_{iV}^{0}\right)\frac{\dot{J}_{VL_1}}{M_V}; \tag{3.6}$$

$$\frac{d}{dt}\gamma_{iE_R}^{0} = \left(\frac{n_{iE_R}^{0R}}{n_{iE_R}} - \gamma_{iE_R}^{0}\right)\frac{\dot{J}_{ER}}{M_{E_R}}; \tag{3.7}$$

where, n_{iE}, n_{iV} and n_{iE_R} represent the frequency of an element i relative to that of carbon in compound of reserve, structure and/or reproduction buffer and n_{iE}^{0A}, n_{iV}^{0G}, and $n_{iE_R}^{0R}$ represent the relative frequency of an isotope 0 of element i (*i.e.* ^{13}C, ^{15}N) in a compound of reserve, structure and/or reproduction buffer during assimilation, growth and reproduction. $J_{VL_1} = -y_{VE}^{L}\dot{J}_{EL}$ represents the renewed structure flux with $\dot{J}_{EL} = \kappa_L \dot{J}_{EM}$. The γ notation is converted to δ notation (classically used in SIA) as $\delta_i = 1000((R_i - R_{ref})/R_{ref})$ where $R = \gamma_{ij}^{0}/(1 - \gamma_{ij}^{0})$. The change of isotopic ratio of the whole body, γ_{iW}^{0}, is given by the weighted sum of each of the state variables:

$$\gamma_{iW}^{0} = \frac{\gamma_{iE}^{0} M_E + \gamma_{iV}^{0} M_V + \gamma_{iE_R}^{0} M_{E_R}}{M_E + M_V + M_{E_R}} \tag{3.8}$$

The framework, assumptions and equations of the standard DEB and DIB models used for this study have been extensively detailed in Kooijman et al. (2008); Kooijman (2010) and Pecquerie et al. (2010). Parameter estimation

is performed following the procedure described by Lika et al. (2011a). The zero-variate data used for the procedure are presented in Table 3.4 and the set of DEB and DIB parameters obtained for *C. gigas* are presented in Table 3.3. The model calibration was made on data from Dubois et al. (2007a) to obtain odds ratio values β for carbon and nitrogen isotopic discrimination (Fig. 3.1).

Table 3.3: Estimated parameters for the *Crassostrea gigas* species. The parameter values come from the present study except for the parameters y_{VE}^{L}, κ_L and κ_{Lr} where values come from the study by Pecquerie et al. (2010).

Symbols	Values	Units	Interpretations
T_1	293	K	Reference temperature
T_A	5722	K	Arrhenius temperature
T_L	277	K	Lower boundary tolerance range
T_H	318	K	Upper boundary tolerance range
T_{AL}	20000	K	Arrhenius temperature for lower boundary
T_{AH}	190000	K	Arrhenius temperature for upper boundary
$\{\dot{J}_{EAm}\}$	5.14^{-4}	mol d^{-1} cm^{-2}	Maximum surface-area-specific assimilation rate
$\dot{v}$	0.04932	cm d^{-1}	Energy conductance
$[M_V]$	4.25^{-3}	mol cm^{-3}	Number of C-atoms per unit of structural body volume
$[J_{EM}]$	6.36^{-5}	mol d^{-1} cm^{-3}	Volume-specific maintenance rate
κ	0.69	–	Fraction of reserve allocated to growth and maintenance
M_H^b	1.08^{-10}	mol	Maturation at birth
M_V^p	1.92^{-5}	mol	Mass of structure at puberty
M_H^p	5.46^{-5}	mol	Maturation at puberty
$\dot{k}_J$	0.002	d^{-1}	Maturity maintenance rate coefficient
κ_R	0.95	–	Reproduction efficiency
y_{EX}	0.88	mol mol^{-1}	Yield of reserve from food in assimilation
y_{VE}	0.776	mol mol^{-1}	Yield of structure from reserve in growth
y_{VE}^{L}	0.63	mol mol^{-1}	Yield of structure from reserve in turn-over of structure
κ_L	0.8	–	Fraction of volume-specific somatic maintenance
κ_{Lr}	0.47	–	Fraction of structure turnover that is recycled
β_{CW}^{13}	1.008	–	Odds ratio of the whole body for ^{13}C
β_{NW}^{15}	1.0125	–	Odds ratio of the whole body for ^{15}N
w_{C}	12	g.mol^{-1}	Molar weight of C
w_{H}	1	g.mol^{-1}	Molar weight of H
w_{O}	16	g.mol^{-1}	Molar weight of O
w_{N}	14	g.mol^{-1}	Molar weight of N

3.2.3 Trophic-shift and half-life of the isotopic ratio

The trophic-shift, *i.e.* Δ^{13}C and Δ^{15}N was calculated as the difference between the isotopic ratio of the consumer and the isotopic ratio of the food source, $\Delta = \delta_W - \delta_X$ in a constant environment. Considering that the structure turnover leads to the enrichment of structure, we estimated the derivative of the difference between δ_W and δ_X. We assumed that equilibrium between the individual and its food source is reached when derivative variations are lower

than the threshold of 2 %, *i.e.* $\Delta_{threshold} = 2\,\%$. We also calculated the half-life of the isotopic ratio for δ^{13}C and δ^{15}N, from $t^{1/2}_{\delta^{13}\mathrm{C}}$ and $t^{1/2}_{\delta^{15}\mathrm{N}}$, respectively. The term $t^{1/2}_{\delta}$ corresponds to the time required to reach the half value of the isotopic ratio in the whole body δ_W at the equilibrium state.

3.2.4 Simulations

The dynamics of carbon and nitrogen stable isotopes, *i.e.* $\delta^{13}C$ and $\delta^{15}N$, are simulated in soft tissues of an individual of *C. gigas* under four different scenarios to test for several effects:

Scenario 1 (S 1) Effect of scaled feeding level f: scaled feeding level is described by the scaled functional response f with $0 < f < 1$ (see Kooijman, 2010). Different scaled feeding levels are tested: $f = 0.2, 0.4, 0.6, 0.8, 1$ while temperature T and isotopic ratio of food source for carbon and nitrogen are constant.

Scenario 2 (S 2) Effect of the organism mass W: initial total dry mass of tissues (expressed in grams) at the start of simulations are $W_0 = 0.025, 0.05, 0.1$, and $0.6\,g$ of dry weight. Temperature T and scaled feeding level are constant.

Scenario 3 (S 3) Effect of the isotopic ratio of food source: a varying signal of isotope food source for carbon and nitrogen, namely $\delta^{13}C_X$ and $\delta^{15}N_X$, are used. Temperature T and scaled feeding level are constant.

Scenario 4 (S 4) Effect of a varying environment: scaled feeding level, temperature T and food isotopic ratio are varying over time.

For all scenarios, only one type of food, *i.e.* a mono-specific culture of microalgae is considered. Conditions for each scenario are summarized in Table 3.5.

3.3 Results

3.3.1 DIB model calibration

The calibration of the DIB model based on a fractionation experiment carried out on *C. gigas* by Dubois et al. (2007a) allowed us to estimate the odds ratio values under controlled conditions of temperature ($T = 15.9°C$) and scaled feeding level ($f = 1$) over 90 days (Fig. 3.1). We assumed that the isotope selection, which depends on the odds ratio value, is equal in each metabolic function (assimilation, growth and dissipation, including structure turnover) for a given element. The estimated odds-ratio values are $\beta^{13}_{CW} = 1.008$ for the carbon and $\beta^{15}_{NW} = 1.0125$ for nitrogen. The carbon isotopic ratio of food, $\delta^{13}C_X$, shows an increase of $\approx 3\,‰$ during the experiment that leads to a slight increase of the $\delta^{13}C_W$ on the last sampling date whereas $\delta^{15}N_X$ shows higher variations of $\approx 20\,‰$ but shorter in time than those observed for $\delta^{13}C_X$. The model slightly underestimates nitrogen isotopic ratio at sampling times 8 and 15, but generally the simulations match the observations well.

Table 3.4: Zero-variate data used in the parameter estimation procedure (Lika et al., 2011a) for the *Crassostrea gigas* species.

Symbols	Values	Units	Interpretations	References
a_b	5.5	d	Age at birth	Rico-Villa et al. (2010)
a_p	93	d	Age at puberty	pers. com.
L_b	0.008	cm	Length at birth	Rico-Villa et al. (2009)
L_p	2.4	cm	Length at puberty	pers. com.
L_i	45	cm	Maximum length observed	Van der Veer et al. (2006)
W_{DW}^b	5^{-9}	g	Dry weight at birth	Rico-Villa et al. (2010)
W_W^p	0.2	g	Wet weight at puberty	pers. com.
W_W^i	1430.6	g	Ultimate wet weight	pers. com.
R_i	2.7e6	eggs/d	maximum reproduction rate	pers. com.
a_m	4745	d	Life span	from Van der Veer et al. (2006)
r_B	0.002	d^{-1}	von Bertalanffy growth rate	Van der Veer et al. (2006)

Table 3.5: Conditions of simulations for each scenario. f relates to the scaled feeding level (–), T relates to the temperature (°C), W_0 relates to the initial mass of the organism (g of dry weight), and δ notation relates to isotopic ratio (‰).

Scenario ↓; Conditions →	T	f	W_0	$\delta^{13}C_X$	$\delta^{15}N_X$	$\delta^{13}C_W$	$\delta^{15}N_W$
$S1$, "scaled feeding level" effect	16	varying	0.05	−23.04	−4.93	−19.06	8.11
$S2$, "Organism mass" effect	16	1	varying	−23.04	−4.93	−19.06	8.11
$S3$, "isotopic ratio of food" effect	16	1	0.05	varying	varying	−19.06	8.11
$S4$, "Varying environment" effect	varying	varying	0.05	varying	varying	−20.98	−1.30

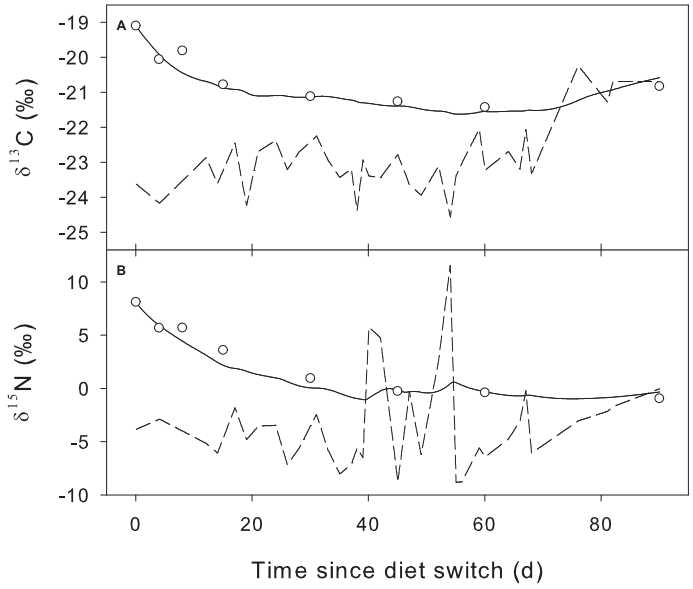

Figure 3.1: Simulated (solid lines) *versus* observed (dots) isotopic ratios of the oyster *Crassostrea gigas* tissues over time for carbon (upper panel) and nitrogen (lower panel) isotopes. The oyster diet switches from natural conditions (day 0) to a mono-specific algal diet of *Skeletonema costatum* with varying isotopic ratios (dashed lines). Data from Dubois et al. (2007a): scale functional response $f = 1$, temperature $T = 15.9°\mathrm{C}$, initial mass $W_0 = 0.05\,\mathrm{g}$, initial signature of oyster tissues $\delta^{13}\mathrm{C}_{W_0} = -19.06\,‰$ for carbon and $\delta^{15}\mathrm{N}_{W_0} = 8.11\,‰$ for nitrogen. For each sampling, oysters were kept alive overnight in filtered sea water to evacuate their gut contents.

3.3.2 S 1: effect of scaled feeding level

A higher scaled feeding level results in a lower half-life of the isotopic ratio and a lower trophic-shift factor at the end of the experiment (Figs. 3.2 A and 3.2 B). As a corollary, an increase in f from 0.2 to 1 results in decreasing trophic-shift values from 3.01 ‰ to 1.93 ‰ for Δ^{13}C (Fig. 3.2 C) and from 5.46 ‰ to 3.06 ‰ for Δ^{15}N (Fig. 3.2 D). The estimated values for the half-life of the isotopic ratio exhibit the same pattern as that observed for the Δ values. For both δ^{13}C and δ^{15}N, there is a decrease of the half-life when f increases: $t^{1/2}_{\delta^{13}\mathrm{C}} = 13.1\,\mathrm{d}$, 12 d, 10.3 d, 8.9 d, 7.9 d, and $t^{1/2}_{\delta^{15}\mathrm{N}} = 22.1\,\mathrm{d}$, 17.4 d, 14.2 d, 12 d and 10.3 d, respectively for $f = 0.2$, 0.4, 0.6, 0.8 and 1.

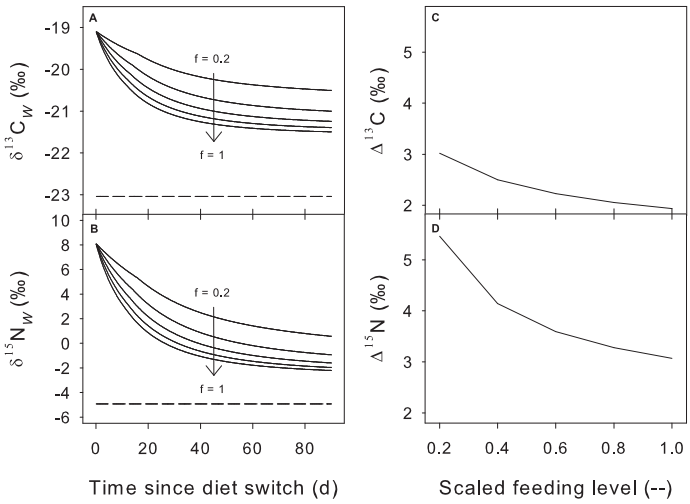

Figure 3.2: *Scenario S*1. *Left panels*: isotopic ratios of the oyster *Crassostrea gigas* tissues (solid lines) and of the food source (dashed lines) for different scaled feeding levels $f = 0.2$, 0.4, 0.6, 0.8, and 1 during a diet-switching simulation. *Right panels*: trophic-shift Δ values as a function of f. Graphs (A, C) and (B, D) relate to carbon and nitrogen stable isotopes respectively. Scenario conditions are described in Table 3.5. Final mass are $W_f = 0.08$, 0.18, 0.29, 0.43, and 0.59 g of dry weight for each scaled feeding level tested.

3.3.3 S 2: effect of organism mass

A larger initial organism mass results in slower rate of change in δ_W during the experiment and higher trophic-shift factors at the end of the experiment (Figs. 3.3 A and 3.3 B). For $W_0 = 0.025\,\mathrm{g}$, 0.05 g, 0.1 g, and 0.6 g, the corresponding trophic-shift values are respectively 1.85 ‰, 1.93 ‰, 2.03 ‰ and 2.37 ‰ for carbon, and 2.94 ‰, 3.06 ‰, 3.22 ‰ and 3.73 ‰ for nitrogen

(Figs. 3.3 C and 3.3 D). For both δ^{13}C and δ^{15}N, the half-life values increase with increasing animal tissue mass: $t^{1/2}_{\delta^{13}\mathrm{C}} = 6.6\,\mathrm{d}$, $7.9\,\mathrm{d}$ $9.1\,\mathrm{d}$ and $12.0\,\mathrm{d}$ and $t^{1/2}_{\delta^{15}\mathrm{N}} = 8.3\,\mathrm{d}$, $10.3\,\mathrm{d}$, $12.2\,\mathrm{d}$ and $19.4\,\mathrm{d}$, respectively for $W_0 = 0.025\,\mathrm{g}$, $0.05\,\mathrm{g}$, $0.1\,\mathrm{g}$, and $0.6\,\mathrm{g}$.

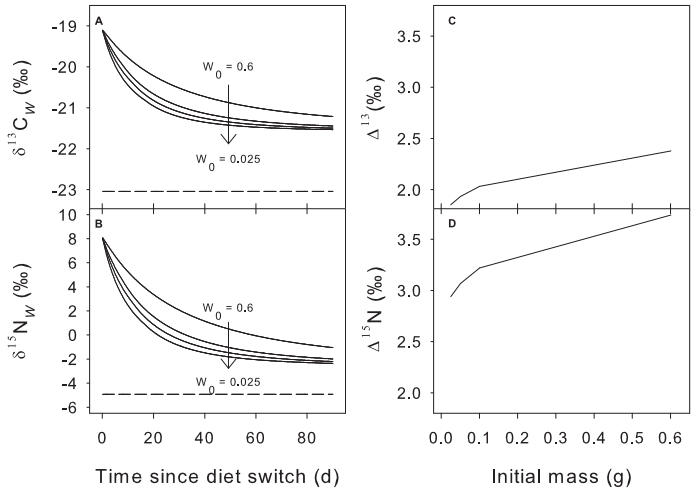

Figure 3.3: *Scenario S2*. *Left panels*: isotopic ratios of the oyster *Crassostrea gigas* tissues (solid lines) and of the food source (dashed lines) for different initial mass $W_0 = 0.025$, 0.05, 0.1, and 0.6 g of dry weight during a diet-switching simulation. *Right panels*: trophic-shift Δ values as a function of W_0. Graphs (A, C) and (B, D) relate to carbon and nitrogen stable isotopes, respectively. Scenario conditions are described in Table 3.5. Final masses are $W_f = 0.448$, 0.59, 0.81, and 2.18 g of dry weight for each initial mass tested.

3.3.4 S 3: effect of the isotopic ratio of the food source

When the model is forced by varying signals of food isotopic ratio over time ($\delta^{13}\mathrm{C}_X$ and $\delta^{15}\mathrm{N}_X$) the amplitude of the $\delta^{13}\mathrm{C}_W$ and $\delta^{15}\mathrm{N}_W$ variations of *C. gigas* soft tissues is smoothed down compared with the food source signal (Fig. 3.4). The half-life of the isotopic ratios also varies as shown by the time-lag between both signals (Fig. 3.4). Finally, the difference in the isotopic ratio between the oyster tissues and the food source tends to increase over time (Figs. 3.4 C and 3.4 D).

3.3.5 S 4: effect of a varying environment

As in the previous experiment, the amplitude of the variations in the food isotopic ratio is smoothed down in the animal tissues: strong variations of

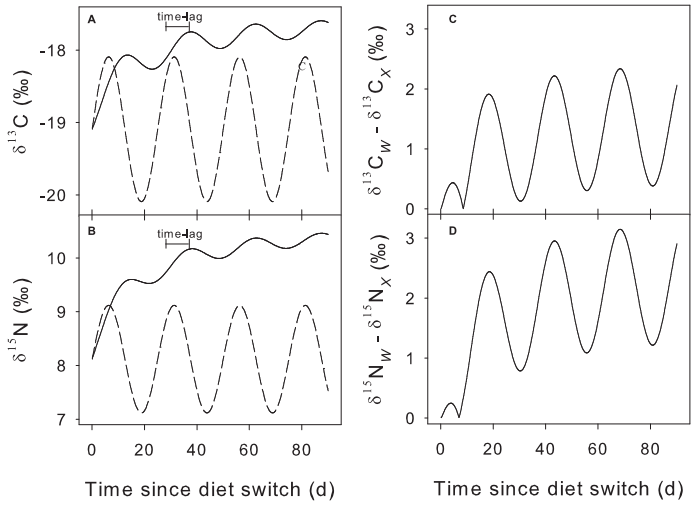

Figure 3.4: *Scenario S*3. *Left panels*: isotopic ratios of the oyster *Crassostrea gigas* tissues (solid lines) under varying conditions of food source signature (dashed lines). *Right panels*: difference in the isotopic ratio between the oyster tissues and the food source as a function of time. Graphs (A, C) and (B, D) relate to carbon and nitrogen stable isotopes respectively. Scenario conditions are described in Table 3.5. Final mass is $W_f = 0.59\,\mathrm{g}$ of dry weight.

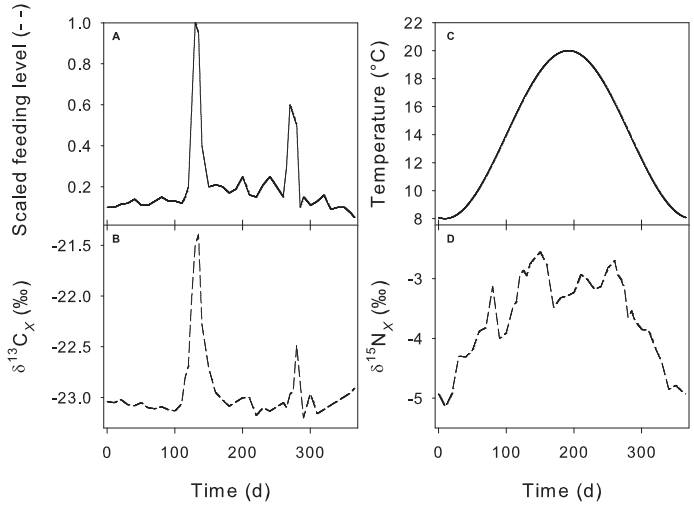

Figure 3.5: Forcing variables over time used for the scenario S 4. (A) f values, (B) isotopic ratio of food source for carbon (‰), (C) temperature (°C) and (D) isotopic ratio of food source for nitrogen (‰).

$\delta^{13}C_X$ (Fig. 3.5 B) over a short time period result in small variations in $\delta^{13}C_W$ in animal tissues (Fig. 3.6 A). The difference in the isotopic ratios between the individual tissues and the food ($\delta_W - \delta_X$) clearly varies over time with a range of 2.02 ‰ and 3.03 ‰ for carbon and nitrogen, respectively (Figs. 3.6 C and 3.6 D). During a spawning event (day 175), both $\delta^{13}C_W$ and $\delta^{15}N_W$ of oyster abruptly change regardless of the variations in the isotopic composition of food.

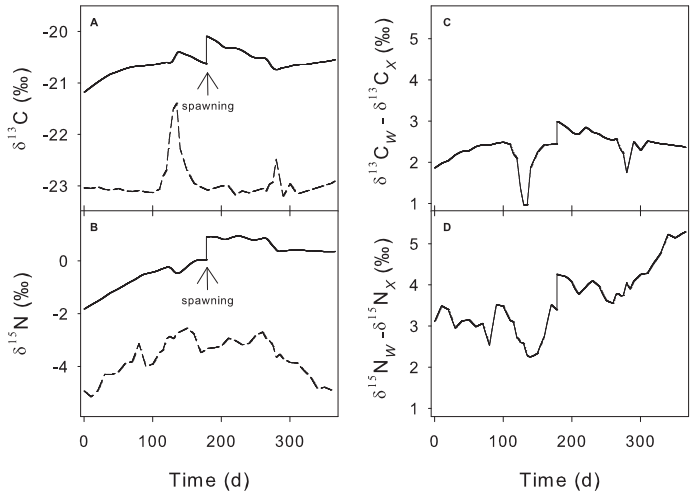

Figure 3.6: *Scenario S4*. *Left panels*: isotopic ratios of the oyster *Crassostrea gigas* tissues (solid lines) under varying conditions of scaled feeding level, temperature and food isotopic ratios (dashed lines). *Right panels*: difference in the isotopic ratio between the oyster tissue and the food source as a function of time. Graphs (A, C) and (B, D) relate to carbon and nitrogen stable isotopes respectively. Scenario conditions are described in Table 3.5. Final mass is $W_f = 0.18\,\mathrm{g}$ of dry weight.

3.4 Discussion

3.4.1 Variable trophic-shift

DEB theory (Kooijman, 2010) can be used to quantify variations in the trophic shift for a marine bivalve *C. gigas* in response to varying scaled feeding levels, initial mass of oyster, and isotopic ratio of the food. Stable isotope analysis has helped to understand the diet of natural and cultivated suspension-feeding bivalves in marine ecosystems (Marín Leal et al., 2008; Riera and Richard, 1996; Riera et al., 2002). These analyses assume that the organism is in equilibrium with its food source. To judge this, the trajectory of the isotopic signal of food and the enrichment factor must be known. Most ecological investigations

Table 3.6: Trophic-shift values (Δ, ‰) and half-life of the isotopic ratio ($t_\delta^{1/2}$, d) derived from the literature during diet-switching experiments carried out with different feeding levels. All Δ values refer to the enrichment of the whole body mass (non-defatted tissues) except for the study by Barnes et al. (2007) which is only on muscle. In the studies by Gaye-Siessegger et al. (2003, 2004b) and Focken (2001), Δ values are recalculated on the basis of dry flesh mass at the equilibrium state and the feeding level is expressed in $\mathrm{g.kg^{-0.8}.d^{-1}}$. f relates to the scaled feeding level (–), T relates to the temperature (°C), and W_0 relates to the initial mass of the organism (g of dry weight).

		Carbon $\delta^{13}C$		*Nitrogen* $\delta^{15}N$		*Experimental conditions*		
Study	Species	Δ	$t_\delta^{1/2}$	Δ	$t_\delta^{1/2}$	f	T	W_0
This study	*Crassostrea gigas*	3.01	13.1	5.46	22.1	$f = 0.2$	16	––
	〃	2.49	12.0	4.14	17.4	$f = 0.4$	16	––
	〃	2.22	10.3	3.59	14.2	$f = 0.6$	16	––
	〃	2.05	8.90	3.27	12.0	$f = 0.8$	16	––
	〃	1.93	7.9	3.06	10.3	$f = 1$	16	––
	〃	1.85	6.6	2.94	8.3	$f = 1$	16	0.025
	〃	1.93	7.9	3.06	10.3	$f = 1$	16	0.05
	〃	2.03	9.1	3.22	12.2	$f = 1$	16	0.1
	〃	2.37	12.0	3.73	19.4	$f = 1$	16	0.6
Barnes et al. (2007)	*Dicentrarchus labrax*	1.38 (±0.49)	–	4.02 (±0.43)	–	Low	16 (±0.03)	––
	〃	1.38 (±0.48)	–	3.92 (±0.46)	–	Medium	16 (±0.03)	––
	〃	1.55 (±0.43)	–	3.79 (±0.36)	–	High	16 (±0.03)	––
	〃	1.23 (±0.37)	–	4.23 (±0.27)	–	Low	11.1 (±0.05)	––
	〃	1.00 (±0.48)	–	4.82 (±0.30)	–	Medium	11.1 (±0.05)	––
	〃	1.09 (±0.56)	–	4.27 (±0.37)	–	High	11.1 (±0.05)	––
Gaye-Siessegger et al. (2003)	*Oreochromis niloticus*	2.34	–	5	–	2.5	27 (±0.1)	––
	〃	1.86	–	4.7	–	6.0	27 (±0.1)	––
	〃	1.34	–	4.5	–	10.0	27 (±0.1)	––
	〃	1.37	–	4.6	–	15.0	27 (±0.1)	––
Gaye-Siessegger et al. (2004b)	*Cyprinus carpio*	3.51	–	1.69	–	3.2	27 (±0.3)	––
	〃	2.19	–	1.44	–	9.6	27 (±0.3)	––
	〃	1.82	–	1.27	–	16	27 (±0.3)	––
	〃	1.65	–	1.13	–	22.4	27 (±0.3)	––
Focken (2001)	*Oreochromis niloticus*	0.69	–	0.6	–	5	27 (±0.2)	––
	〃	0.8	–	0.9	–	10	27 (±0.2)	––
	〃	1.05	–	1	–	20	27 (±0.2)	––

have used the concept of a constant trophic-shift because of the absence of an ecological tool to quantify the impact of different factors on the metabolism of the organism. A few studies have used bioenergetics-based models to investigate the impact of factors on the isotope dynamic of an organism (*e.g.* Harvey et al., 2002) or to estimate food-source contributions (Marín Leal et al., 2008). However, none of these studies described a dynamic and variable isotopic discrimination.

3.4.2 Link between trophic-shift and scaled feeding level

In our study, Δ^{13}C and Δ^{15}N were both affected by scaled feeding level. A five times increase of the scaled feeding level ($f = 0.2$ to $f = 1$) leads to a decrease of the Δ value of 35 % for carbon and 43 % for nitrogen (Fig. 3.2). These patterns and the range of variation of the Δ value are consistent with previous findings concerning *Cyprinus carpio* (Gaye-Siessegger et al., 2004b). A decrease of 52 % in Δ^{13}C and 33 % in Δ^{15}N was found between the lowest and highest feeding levels for this species. Another fish species (*Oreochromis niloticus*) showed a decrease of 41 % of the carbon trophic-shift when feeding level increased by a factor of 6 but no clear pattern was found for Δ^{15}N (Gaye-Siessegger et al., 2003). For the European sea bass (*Dicentrarchus labrax*) Barnes et al. (2007) showed a slight decrease of 5 % of the Δ^{15}N at 16 °C and a decrease of 11 % for Δ^{13}C at 11 °C between low and high feeding levels, although no clear pattern was observed for Δ^{13}C at 16 °C and Δ^{15}N at 11 °C. However, for *C. carpio* Focken (2001) found an increase of the Δ for both carbon and nitrogen with increasing feeding levels (Table 3.6). For the Δ^{15}N pattern, Focken (2001) suggested that a nutritional stress due to a high protein concentration in food may have occurred during the experiment. The authors further assumed that during the liponeogenesis that occurs at the highest feeding level, the newly formed lipids had a higher ^{13}C content than the lipids absorbed directly from food.

The fate of compounds through anabolism and catabolism, as well as the description of isotopic discrimination during metabolic transformations (assimilation, growth and dissipation) is critical to understand the impact of scaled feeding level on the isotopic ratio of an organism. During compound transformation, the probability of a molecule to be selected for the catabolic or anabolic route depends on its isotopic composition. In the present study, we assumed that the isotopic discrimination is equal for assimilation, growth, dissipation, and structure turn-over (see DIB model calibration section). The biochemical composition of reserve, structure, and reproduction buffer is constant over the life cycle (strong homeostasis assumption, Kooijman, 2010) implying that only the amount of the pools E, V, and E_R, and their respective isotopic ratios, can change over time according to the food characteristics (Kooijman, 2010). Therefore, for a given isotopic ratio of the food, the probability of a "light molecule" to be selected for the anabolic route is higher when $f = 1$ (high scaled feeding level) than when $f = 0.2$ (low scaled feeding level). This

phenomenon is supported by the fact that food and energy reserve cannot be considered as infinite (large) pools, *e.g.* as illustrated by the low level of primary production frequently observed in coastal marine ecosystems during winter. Isotopic discrimination related with maintenance of the organism, *i.e.* the somatic maintenance including structure turn-over, can also have a significant effect on the isotope dynamics of the whole body. In the standard DEB model, maintenance processes have priority over growth and maturation or reproduction. The importance of somatic maintenance relative to assimilation increases for decreasing ingestion levels. This leads to a strong enrichment of the whole body at low scaled feeding levels.

3.4.3 Link between trophic-shift and individual mass

An increase from 0.025 g to 0.6 g of the initial mass results in an enrichment of 22 ‰ for Δ^{13}C, and 21 ‰ for Δ^{15}N respectively (Fig. 3.3). This enrichment can be explained by the somatic maintenance because growing individuals increase their structural volume. In our model, the somatic maintenance flux is proportional to the structural volume. Since the structure turn-over selects for heavy isotopes during an animal's life, big individuals have a larger amount of structure to maintain and are consequently heavier in terms of isotopic ratio than small individuals.

Our results cannot be compared easily with literature data as, to our knowledge, no controlled diet-switching experiment, *e.g.* under constant conditions of feeding level and temperature, has been carried out on individuals of the same species with different initial body masses. Sweeting et al. (2007a,b) found a weak negative correlation between the δ^{13}C values and the mass of muscle and liver in *D. labrax* reared over a 2 year experiment under a constant isotopic ratio of food, though with seasonal variations of temperature and natural daylight cycle. The authors also found a correlation between the δ^{15}N values and liver mass, but this correlation was difficult to interpret. We think that this could have been due to confounding effects of mass, temperature, and experimental duration on sea bass metabolism. Trueman et al. (2005) showed that δ^{15}N varied inversely with growth rate in the Atlantic salmon *Salmo salar* during a controlled feeding experiment which is consistent with the fact that salmon were fed on a depleted diet at the start of the experiment.

Positive correlations of increasing age, length, and mass with the δ^{15}N enrichment of organisms have been frequently reported for marine fish species in field studies (Badalamenti et al., 2002; Lindsay et al., 1998, and references therein). However, for the δ^{13}C, this pattern is difficult to observe since the classical enrichment between two different trophic levels ranges from 0 ‰ to 1 ‰. This relationship for δ^{15}N should nevertheless be interpreted carefully due to the complexity of interactions between species and their environment. Indeed, an old individual can be enriched in heavy isotopes due to an increase in mass and/or a change in the trophic position, *i.e.* a change in the diet and/or in the size of prey. None of the current ecological tools makes it possible to

discriminate and quantify the effects of these two factors on the δ^{15}N enrichment across trophic levels. Jennings et al. (2002a,b) studied trophic network structures by applying stable isotope analysis on size-structured production. Dynamic energy and isotope budget models can be valuable in this context since isotopic discrimination is modeled mechanistically.

3.4.4 Half-life of the isotopic ratio

The half-life of the isotopic ratio in the whole body decreases when the scaled feeding level increases as explained in the scenario S 1. Indeed, when the scaled functional response remains constant, the scaled reserve density is equal to the scaled functional response, namely $e = f$. Moreover, J_{EC} is a function of the amount of energetic reserve M_E and of structural volume M_V. Consequently, when the scaled feeding level increases, e and J_{EC} increase, which leads to a rapid reserve mobilization and a decrease of the compound half-life of reserve.

For two individuals of the same species with different body masses, the larger one will have more reserve and structure than the smaller one under constant conditions. If the pools of reserve and structure are big, one compound of the pool will remain for longer before being mobilized and used for a particular metabolic function than in a small pool. This implies that the bigger the organism, the longer the residence time of a compound (see scenario S 2, Fig. 3.3).

The difference between $t^{1/2}_{\delta^{13}\mathrm{C}}$ and $t^{1/2}_{\delta^{15}\mathrm{N}}$ for both scenarios S 1 and S 2 can be partially explained by the difference in isotopic discrimination between carbon and nitrogen. There are different odds-ratio values for carbon and nitrogen with $\beta^{13}_{CW} < \beta^{15}_{NW}$, which implies that the $\delta^{13}\mathrm{C}_W$ reaches the equilibrium with the food source faster than the $\delta^{15}\mathrm{N}_W$ in a given pool. This effect is also increased because the reserve dynamic is faster than the structure dynamic. The biological composition is different (Table 3.2), though constant throughout the life span due to the strong homeostasis assumption (see Kooijman, 2010). Only the amounts of reserve and of structure can vary relative to each other, leading to the property that the chemical composition, and thus the C:N ratio of the whole body can change. This difference leads to different dynamics of isotopes among compartments. The use of two or more compartments is clearly an advantage to describe isotope dynamics (see review by Martínez del Rio et al., 2009).

3.4.5 Dynamic equilibrium between the food source and the individual

The trophic-sift value Δ is estimated when the isotopic ratio of an individual is constant compared with the isotopic ratio of the food, which is assumed to be constant. The scenario S 3 shows the possible errors that may be introduced into the estimation of Δ when δ_X varies. In controlled feeding experiments, bivalves are frequently fed on phytoplankton species which have complex and

variable isotope dynamics (Riera and Richard, 1997; Savoye et al., 2003; Malet et al., 2008; Bodineau et al., 1998). Even under controlled conditions, the complex life cycle of microalgae does not allow the attainment of a constant isotopic ratio during any experiment. This effect of the δ_X variations is well illustrated in Figure 3.1 where the $\delta^{13}C_X$ exhibits an increase of $\approx 3\,‰$ from day 0 to day 75 of the experiment, resulting in an enrichment of the whole body on the last sampling date. The effect of mass on the isotopic ratio of *C. gigas* is also well illustrated by Fig. 3.4. Indeed, the organism increases its body mass throughout the simulation. This results in: *i)* an increase of the mean difference between δ_W and δ_X, *i.e.* the oyster is heavier in terms of isotopic ratio than its food, and *ii)* a decrease of the rate of change in δ_W value in larger organisms.

In simulations of the natural environment over one year (Fig. 3.6) the discrimination of isotopes in *C. gigas* soft tissues results from the combined effects of organism mass, varying scaled feeding level, temperature, and isotopic ratio of food (see results of S 1, S 2 and S 3). Temperature that influences metabolic rates (assimilation, dissipation, and growth) should only affect the rate of isotopic discrimination in oyster tissues, but not the Δ value itself. For this reason, we considered a varying temperature for our study. The difference in the isotopic ratios between the individual tissues and the food in a dynamic environment, *i.e.* $\delta_W - \delta_X$, exhibits a range of variation of $2.02\,‰$ for carbon and $3.03\,‰$ for nitrogen (Figs. 3.6 C and 3.6 D). This range of variation emphasizes the potential errors that can occur when static traditional approaches are used to access to the contribution of food sources for interdidal suspension-feeders (Dubois et al., 2007a). Indeed, the isotopic ratio of a consumer is corrected from the discrimination factor Δ and then compared with the isotopic ratio of food sources with a $\delta^{13}C$ - $\delta^{15}N$ plot. A mixing model (Phillips, 2001) can then be used to quantify contribution of the different food sources to the consumer diet. The weakness of this method, which has been widely applied in coastal ecosystems to study the benthic invertebrate diets (*e.g.* Riera et al., 2004; Riera and Richard, 1996; Kang et al., 2003) is related to the estimation of the trophic-shift value. For example, Dubois et al. (2007a) report a difference of $0.85\,‰$ and $0.79\,‰$ for carbon and nitrogen Δ values (namely the difference between the commonly assumed: $\Delta^{13}C = 1.00\,‰$ and $\Delta^{15}N = 3.50\,‰$ and their estimations: $\Delta^{13}C = 1.85\,‰$ and $\Delta^{15}N = 3.79\,‰$) lead to a difference of 13 %, 11 %, and 9.4 % in the contribution of the microphytobenthos to the *C. gigas* diet for three data sets (see Dubois et al., 2007a). It is therefore understandable that a range of variation of $2.02\,‰$ and $3.03\,‰$ (Fig. 3.6) can introduce significant errors into the contribution of the food source. The equilibrium assumption of static mixing models does not consider food (isotope) assimilation flux as a dynamic process, which therefore introduces another bias into the estimation of the long-term effect of the diet. This is because the isotopic ratio of an organism reflects the isotopic ratio of past (recent) and present food.

The use of a standard DEB model is of increasing interest to capture the bioenergetics and physiology of molluscs, *e.g.* *Mytilus edulis* (Rosland et al., 2009; Van Haren and Kooijman, 1993) and *Crassostrea gigas* (Pouvreau et al., 2006; Bourlès et al., 2009; Bernard et al., 2011; Ren and Schiel, 2008) according to environmental fluctuations. Although most applications of DEB models deal with energy budgets, the DEB theory also specifies the elemental composition to access to a more detailed level of metabolic organization. Our description of the biochemical composition of *C. gigas* in a standard DEB model and the recent development of the dynamic isotope budget (Kooijman, 2010) concepts allow us to investigate two critical points in isotopic ecology: the impact of scaled feeding level and organism mass on isotope incorporation and discrimination. To our knowledge, the Dynamic Energy Budget theory is the first to propose a mechanistic description of isotope fluxes and discrimination among assimilation, growth, and dissipation in living organisms. Furthermore, the use of a dynamic isotope budget required only three more parameters than in the standard DEB models. Although estimation methods for DEB parameters are still in development, rapid progress has been made (Lika et al., 2011a). Our study gives a first calibration of the DIB model based on the data by Dubois et al. (2007a), but some improvements are still required in relation to both modeling and experimental procedures. For instance, a fractionation experiment involving two or more feeding levels during a growth survey of oyster could provide useful uni-variate data set (*i.e.* mass, length, C:N ratio against time) to refine the parameter estimation in the covariation method of Lika et al. (2011a).

Acknowledgments

We would like to thank Stanislas Dubois for providing the data set used in this study. We also thank Laure Pecquerie for her help in improving the quality of this manuscript and I. Bernard for his help. We also thank the anonymous reviewer for his/her comments. The members of the European Research Group AquaDEB (`http://www.ifremer.fr/aquadeb/`) are also gratefully acknowledged for their stimulating discussion. This work was supported by the Regional Council of Basse Normandie and Ifremer.

Chapter 4

Effect of the feeding level on the dynamics of stable isotopes δ^{13}C and δ^{15}N in soft tissues of the Pacific oyster *Crassostrea gigas*

Emmery, A.[a,b,c], Lefebvre, S.[b], Qéau, I.[c], LeBrun, L.[c], Bataillé, M.-P.[d], Alunno-Bruscia, M.[c].

Functional Ecology (in prep.)

[a] *Université de Caen Basse Normandie, CNRS INEE - FRE*3484 *BioMEA, Esplanade de la paix* 14032 *Caen cedex, France*

[b] *Université de Lille* 1 *Sciences et Technologies, UMR CNRS* 8187 *LOG, Station Marine de Wimereux,* 28 *avenue Foch,* 62930 *Wimereux, France*

[c] *Ifremer UMR* 6539, 11 *Presqu'île du Vivier,* 29840 *Argenton, France*

[d] *Université de Caen Basse Normandie, UMR INRA Ecophysiologie Végétale et Agronomie, Esplanade de la paix* 14032 *Caen cedex, France*

Abstract

1. Stable isotope analysis is a powerful tool used for reconstructing individual life histories, identifying food-web structures and tracking flow of elemental matter through ecosystems. However, contradictory results from the literature showed that both the isotopic ratios (δ, ‰) and the trophic fractionation (Δ, ‰) of organism tissues could be affected by the feeding level and the isotopic ratios of the food sources.

2. We carried out a fractionation experiment to investigate the effect of the feeding level on the dynamics of $\delta^{13}C_{W_d}$ and $\delta^{15}N_{W_d}$, of the marine bivalve

(*Crassostrea gigas*). Oysters were first reared under two different feeding levels over 108 d and then starved over 104 d.
3. The feeding level had a significant effect on $\delta^{13}C_{W_d}$ and $\delta^{15}N_{W_d}$ of the whole soft body tissues of oysters (W_d). At the end of the feeding period, tissues of oysters at high feeding level (HF) were depleted in ^{13}C by $\approx 6.15\,‰$ and in ^{15}N by $\approx 1.66\,‰$ compared to the tissues of oysters at low feeding level (LF). $\delta^{13}C_{W_d}$ and $\delta^{15}N_{W_d}$ in the organs of oysters, *i.e.* gills Gi, adductor muscle Mu and remaining tissues Re, were also significantly lower at HF compared to LF.
4. During the starvation period, temporal variations in $\delta^{13}C$ and $\delta^{15}N$ for the whole soft body tissues and for the different organs were similar at HF and LF levels. At the end of the starvation, the whole soft body tissues and the organs of oysters were slightly, but significantly enriched in heavy isotopes compared to the start of the starvation.
5. The model of Olive et al. (2003) was used to test the effect of the feeding level and the isotopic ratio of the diet on the trophic fractionation Δ_{W_d}. These two factors affected Δ_{W_d} but not in the same way. The higher the feeding level, the lower the Δ_{W_d}, *i.e.* $\Delta^{13}C_{W_d}$ and $\Delta^{15}N_{W_d}$. $\Delta^{13}C_{W_d}$ was inversely related to $\delta^{13}C_X$ while no clear trend was observed between $\Delta^{15}N_{W_d}$ and $\delta^{15}N_X$.

Keywords: feeding level; starvation; Pacific oyster; stable isotopes; trophic fractionation; isotopic ratios of the food

4.1 Introduction

Nitrogen and carbon stable isotope analysis are used to describe the trophic levels of individuals, populations and communities, to identify the diet components that support their growth and to understand trophodynamics in ecosystems (*e.g.* Fry, 2006). Field and laboratory observations showed that animal tissues reflect the isotopic ratio of their diet and are typically enriched in heavy isotopes, *i.e.* ^{13}C and ^{15}N (DeNiro and Epstein, 1978; Minagawa and Wada, 1984). This enrichment which is also called the trophic fractionation Δ_{W_d}, stands for the isotopic discrimination of isotopes between producers and consumers. Substantial variations in consumer-diet enrichment within this general pattern are however observed although underlying mechanisms are still poorly understood (Martínez del Rio et al., 2009). The metabolism of organisms plays a key role in the discrimination of isotopes (Pecquerie et al., 2010; Emmery et al., 2011) and different factors like nutritional status (Gaye-Siessegger et al., 2007), diet quality (Webb et al., 1998), protein turnover rates (Adams and Sterner, 2000), body size (Jennings et al., 2008), assimilation efficiency and excretion (Vanderklift and Ponsard, 2003), tissue type (Guelinckx et al., 2007), have been shown to account for variations in the Δ_{W_d}.

Trophic fractionation estimates are usually derived from captive feeding (fractionation) experiments where individuals are typically well fed and in good condition. Wild organisms can nevertheless experience strong seasonal variations in food availability with consequences on their feeding and physiological states. Only a few studies have investigated the effect of the feeding level on the ^{13}C and ^{15}N enrichment of organisms but the results are still contradictory. Focken (2001) found an increase of the $\delta^{13}C$ in the lipids and the lipid-free matter, as well as an increase in $\delta^{15}N$ with increasing feeding rate in the Nile tilapia (*Oreochromis niloticus*). Conversely, Gaye-Siessegger et al. (2003, 2004b) observed in both *Oreochromis niloticus* and *Cyprinus carpio* decreasing $\delta^{13}C$ and $\delta^{15}N$ of the whole body tissues with increasing feeding rate. Gaye-Siessegger et al. (2007) also reported low $\delta^{15}N$ values on *Oreochromis niloticus* fed at high food concentration. For the European sea bass (*Dicentrarchus labrax*), Barnes et al. (2007) observed a slight decrease in $\Delta^{15}N$ (at 16 °C) and in $\Delta^{13}C$ (at 11 °C) between low and high feeding levels, but no clear pattern for $\Delta^{13}C$ and $\Delta^{15}N$.

Starvation, which can be considered as a special case where the feeding level equal zero, has been shown to have effects on the isotopic composition of organisms, but in different ways according to the species and tissues types. Some organism tissues were enriched in both ^{13}C and ^{15}N during starvation phases on terrestrial invertebrates (hatchlings of the spider *Pardosa lugubris*, Oelbermann and Scheu, 2002), freshwater invertebrates (larvae of *Chironomus acerbiphilus*, Doi et al., 2007) and marine invertebrates (the larvae krill *Euphausia superba*, Frazer et al., 1997); marine worm *Nereis virens* (Olive et al., 2003). The anterior part of the flatworms *Arthurdendyus triangulatus* was significantly enriched in ^{15}N, but no clear pattern was observed for ^{13}C (Boag et al., 2006). Conversely, Haubert et al. (2005) found an increase in $\Delta^{15}N$ and a decrease in $\Delta^{13}C$ in starved Collembola *Protaphorura fimata*. In vertebrates, patterns are less clear. Hobson et al. (1993) found significant increase in ^{15}N in muscle and liver of starving snow geese (*Chen rossii*). Castillo and Hatch (2007) showed that $\delta^{15}N$ of the excreta increased significantly with the starvation duration in two species of lizards (*Anolis carolinensis* and *Uta stansburiana*), with no enrichment in the tail muscles. The excreta of the rattlesnake (*Crotalus atrox*) were also significantly enriched in $\delta^{15}N$ during long starvation period while $\delta^{15}N$ of the whole body remained rather constant.

Time-lags combined with changes in stable isotope ratios are essential information for accurate quantitative estimates of shifts in food habits and habitats (Marín Leal et al., 2008). The period over which isotopic ratio of tissues will reflect the one of a particular diet partly depends on the isotopic turnover rate and the biochemical composition of the tissues (*e.g.* Hobson et al., 1996; Webb et al., 1998; Miller, 2006; Guelinckx et al., 2007; Church et al., 2008). Knowledge of the isotope incorporation rate of different tissues (*i.e.* with high and low turnover rates) after a diet switch are crucial to better understand the migration dynamics of wild population (*e.g.* Hobson, 1999), the recruitment of marine fish (*e.g.* Guelinckx et al., 2008), the seasonal energy allocation between

tissues (*e.g.* Paulet et al., 2006) and the contribution of recent and past food source(s) to the diet of organisms (*e.g.* Kurle and Worthy, 2002).

Understanding and quantifying the effects of factors that influence the isotopic discrimination between diet and organisms is of primary importance for ecological studies since small changes in Δ value can affect estimates of trophic levels and/or food sources contributions (Marín Leal et al., 2008). living fixed on hard substrates, suspension feeders are sensitive to both quality/diversity and quantity of their food sources. They occupy an intermediate trophic niche between primary producers and consumers, providing a useful biological model to study trophic relationships. We thus carried out a diet switching experiment, over 212 days under controlled conditions of temperature and food concentrations, to *i)* investigate the effects of the feeding level and the starvation on the dynamics of δ^{13}C and δ^{15}N in the whole soft body tissues and organs of the Pacific oyster *Crassostrea gigas* and *ii)* to assesses consequences for diet reconstruction studies.

4.2 Material and methods

4.2.1 Experimental design

Biological material and rearing conditions. About 3300 natural spats of oyster *C. gigas* (mean shell length = 1.85(±0.44) cm, mean flesh dry mass = 0.013(±0.009) g, 8-months old) originating from Arcachon Bay (south-western France) were transferred on 29 March 2010 at the Ifremer laboratory in Argenton (Brittany, France). They were placed and further reared over 212 days in 280 L tanks supplied with 1 μm filtered running seawater at an average flow rate of *ca.* $D = 75(\pm 9)\,\mathrm{L.h^{-1}}$ (renewal time ≈ 6.4 h). In each tank, the water temperature was kept constant throughout the experiment, *i.e.* mean temperature $T = 14.3(\pm 0.4)$°C and the mean salinity was 34.2(±0.3) PSU on average. The tanks were washed twice a week to remove bio-deposits.

Feeding phase. After a 1-week acclimation phase, oysters were randomly split in two groups fed on a monoculture of *i.e. Skeletonema marinoï* (CCAP 1077/3) with depleted ^{13}C (obtained by bubbling CO_2 from a commercial cylinder into the medium culture). The first group was fed *ad libitum* (high food, HF) and received continuously a flux of $5.8\,10^9(\pm 1.8\,10^9)\,\mathrm{Nb\,cell.\,h^{-1}}$ of *S. marinoï*. The second group at a low food level (*i.e.* LF level) and received continuously a flux of $2.0\,10^9(\pm 7.2)\,10^8\,\mathrm{Nb\,cell.\,h^{-1}}$ of *S. marinoï*. For each food level, three replicate tanks were stocked with 550 oysters and were monitored daily for the micro-algae concentration by using an electronic particle counter (Beckman Multisizer III). Two additional empty tanks were used to control the incoming food concentration at both food levels. The feeding phase lasted for 108 days.

Starvation phase. At t_{109}, 200 individuals in each replicate tank per food level were randomly collected and pooled in a single 300 L tank. Thus, two

tanks containing each 600 individuals from the HF and LF levels and with no food input, were monitored for 104 days under the same rearing conditions (*e.g.* water temperature, salinity, flow, cleaning) than during the feeding phase. An additional empty tank was monitored simultaneously.

4.2.2 Food consumption

The micro-algae consumption C_X (expressed in number of cells per hour and per individuals, Nb cells.h^{-1}.ind^{-1}) was estimated for each tank with oysters at both food levels as followed:

$$C_X = \frac{[X]_{control} \times D_{control} - [X]_{oyster} \times D_{oysters}}{n_{ind}} \tag{4.1}$$

with $[X]_{oyster}$ and $[X]_{control}$ as the concentrations of cells of *S. marinoï* (Nb. cell. L^{-1}) in the tanks, respectively with oysters and without oyster; (D), the inflow rate (L^{-1}); and n_{ind}, the number of individuals per tank. Based on the high seawater renewal and mixing in the tanks, we assumed that the micro-algae sedimentation was similar among the tanks.

4.2.3 Sample collection and analysis

Oysters. The oyster sampling was conducted on days t_2, t_4, t_8, t_{16}, t_{30}, t_{50}, t_{60}, t_{85}, t_{108}, t_{130}, t_{188} and t_{212}. At each sampling date, 20 oysters for the feeding phase and 30 oysters for the starvation phase were collected in each tank so that the individual mass was representative of the mean population mass. Oysters were individually measured (shell length), opened for dissection of the whole body tissues and carefully cleaned with filtered seawater to remove any shell debris. Soft tissues were frozen (−20°C) and freeze-dried (48 h) before weighting the total flesh dry mass (W_d). Before dissection, 7 oysters were randomly selected for isotopic analysis and kept alive overnight in filtered sea water to evacuate the gut contents. Their were then dissected, frozen (−20°C) and freeze-dried (48 h) to measure their W_d and grounded to a homogeneous powder. From the sampling day t_{50}, the gills (Gi) and the adductor muscle (Mu) of the 7 oysters were dissected separately from the remaining tissues (Re), *i.e.* mantle, gonad, digestive gland and labial palps. The Gi, Mu and Re received the same treatment than for the whole soft body tissues. The total dry flesh mass was calculated as follows: $W_d = W_{dGi} + W_{dMu} + W_{dRe}$. All samples were store in safe light and humidity until isotopic analysis.

Food source. 60 mL of *i.e. S. marinoï* were sampled daily from the culture cylinder. The water sample was filtered onto pre-weighed, precombusted (450°C, 4 h) Whatmann GF/C (Ø = 47 mm) glass-fibre filters, immediately after sampling. Then the filters were frozen (−20°C), freeze-dried (60°C, 12 h), grounded to a powder using mortar and pestle and stored in safe light and humidity until isotopic analyses.

4.2.4 Elemental and stable isotope analyses

The samples of oysters tissues and food sources were analysed using a CHN elemental analyser (EuroVector, Milan, Italy) for the particulate organic carbon (POC) and particulate nitrogen (PN) in order to calculate their C/N atomic ratio (C_{at}/N_{at}). Analytical precision was estimated to be less than 2 % dry mass for POC and 6 % dry mass for PN. The resultant gas of elemental analyses was introduced online into an isotopic ratio mass spectrometer (IRMS, GV IsoPrime, UK) to determine carbon and nitrogen isotopes *i.e.* δ^{13}C and δ^{15}N. The isotopic ratio is expressed as the difference between the samples and the conventional standard Pee Dee Belemnite (PDB) for carbon and air N_2 for nitrogen, according to the following equation:

$$\delta^0_{ij} = \left(\frac{R_{\text{sample}}}{R_{\text{standard}}} - 1 \right) 1000 \tag{4.2}$$

where δ^0_{ij} (‰) is the isotope 0 (13 or 15) of element i (C or N) in a compound j. Subscript j stands for the total dry flesh mass W_d, the gills Gi, the adductor muscle Mu, the remaining tissues Re of *C. gigas* or the food source X. R is the $^{13}C/^{12}C$ or $^{15}N/^{14}N$ ratios. The standard values of R are 0.0036735 for nitrogen and 0.0112372 for carbon. When the organs were sampled, the isotopic ratio and the C/N ratio of the total dry flesh mass, *i.e.* $\delta^0_{iW_d}$ and C/N_{W_d} respectively, were calculated as followed:

$$\delta^0_{iW_d} = \frac{\delta^0_{iGi} W_{dGi} + \delta^0_{iMu} W_{dMu} + \delta^0_{iRe} W_{dRe}}{W_{dGi} + W_{dMu} + W_{dRe}} \tag{4.3}$$

$$C/N_{W_d} = \frac{C/N_{Gi} W_{dGi} + C/N_{Mu} W_{dMu} + C/N_{Re} W_{dRe}}{W_{dGi} + W_{dMu} + W_{dRe}} \tag{4.4}$$

The internal standard was the USGS 40 of the International Atomic Energy Agency ($\delta^{13}C = -26.2$; $\delta^{15}N = -4.5$). The typical precision in analyses was ±0.05 % for C and ±0.19 % for N. One tin caps per sample was analysed. The mean value of the isotopic ratio for the animal tissues (total dry flesh mass and organs) was considered.

4.2.5 Isotope dynamics and trophic fractionation estimation

The model of Olive et al. (2003) was used to calculate the isotopic ratios the total dry flesh mass ($\delta^0_{iW_d}$, ‰) of *C. gigas* after a shift in diet and the trophic fractionation: $\Delta^0_{iW_d} = \delta^0_{iW_d} - \delta^0_{iX}$, (‰). Both the variations in the feeding level and the variations in the isotopic ratio of the food source were considered. According to Olive et al. (2003), the $\delta^0_{iW_d}$ can be calculated as:

$$\frac{d\delta^0_{iW_d}}{dt} = \Omega_{i(t)} (q\delta^0_{iX(t)} - \delta^0_{iW_d(t)}) + Z_{i(t)} \tag{4.5}$$

with $\Omega_{\mathcal{X}(t)}$, the ratio of the mass of element (nitrogen, N or carbon C) in the ingested food over the mass element in the animal total dry flesh mass (d^{-1}); q, the absorption efficiency of an element in the food (--); and $Z_{\mathcal{X}(t)}$, the instantaneous rate of change in the isotopic ratio of an animal due to excretion ($‰ .d^{-1}$).

The general trends of the food consumption, *i.e.* described by the following equations: $y = 0.17x^4 - 70.53x^3 + 7.83\,10^3x^2 - 2.16\,10^5x + 4.13\,10^6$ at HF and $y = 0.08x^4 + -31.05x^3 + 3.23\,10^3x^2 + -7.31\,10^4x + 1.34\,10^6$ at LF (with y and x expressed in Nb cells.h^{-1}.ind^{-1}) where used to calculate $\Omega_{i(t)}$. The mass of the element in the food was divided by the mass of the same element in W_d (considering the percentage of C and N in both the food samples and in the total dry flesh mass). $\Omega_{i(t)}$ was then calculated for each replicate of the two feeding levels, *i.e.* $\Omega_{C_{HF}}$, $\Omega_{C_{LF}}$, $\Omega_{N_{HF}}$ and $\Omega_{N_{LF}}$. As no data were available to estimate the parameter q, we calibrated it and set up the value to 0.9 with $0 < q < 1$. $Z_{i(t)}$ was estimated using an unconstrained nonlinear optimization (under Matlab © using the fminsearch procedure) in order to minimize the sum of squares of deviations between observations and predictions. $Z_{i(t)}$ was estimated for both $\delta^{13}C$ and $\delta^{15}N$ and for each replicate of the two feeding levels (*i.e.* $Z_{C_{HF}}$, $Z_{C_{LF}}$, $Z_{N_{HF}}$ and $Z_{N_{LF}}$). According to the variations of the environment (*i.e.* $\Omega_{i(t)}$ and $\delta^0_{iX(t)}$) we assumed that $Z_{i(t)}$ was constant between two sampling days.

The equation (4.5) can be simplified for $t = \infty$ and was used to calculate the trophic fractionation $\Delta^0_{iW_d}$ as follows:

$$\Delta^0_{iW_d} = \frac{Z_{i(t)} + \Omega_{i(t)} q \delta^0_{iX(t)}}{\Omega_{i(t)}} - \delta^0_{iX(t)} \tag{4.6}$$

According to the variations in the environment (*i.e.* $\Omega_{i(t)}$ and $\delta^0_{iX(t)}$) and to the variations in $Z_{i(t)}$, we assumed that the average values of $\Omega_{i(t)}$ and $\delta^0_{iX(t)}$ between two sampling days could be considered as a "temporarily steady state" condition. All the model assumptions and equations are carefully described by Olive et al. (2003).

4.2.6 Statistical analyses

Firstly, comparisons of growth patterns and isotopic composition of the total dry flesh mass between HF and LF levels were based on the average individual dry flesh mass (W_d), the isotopic ratios $\delta^{13}C$ and $\delta^{15}N$ and the C/N ratios. Analyses of differences among W_d, $\delta^{13}C$, $\delta^{15}N$ and C/N were done as a two-way ANOVA with time (*i.e.* sampling day) and feeding levels (FL) as fixed factors for the feeding and starvation phase. Secondly, repeated measures ANOVAs were used to test for differences in the individual dry mass, the isotopic ratios and the C/N ratios among the different organs (gills, adductor muscle and remaining tissues) of *C. gigas*, with feeding level, time and tanks as the source of

variation among oysters (inter-individual) and organs as the source of variation within oysters (intra-individual). The W_d data for the whole soft and organs dry mass were square-root transformed to meet the normality assumption and the homogeneity of variance and/or the sphericity assumption were checked. Cases of significant ANOVA results were followed by a Tukey HSD post hoc test (Zar, 1996) to point out any significant differences in dry mass, isotopic ratios and C/N ratio for the total dry flesh mass and for each of the organs between the two feeding levels and/or among the different organs. Analyses of differences in the trophic fractionation $\Delta^0_{iW_d}$ were done as a two-way ANOVA with $\Omega_{i(t)}$ and $\delta^0_{iX(t)}$ as fixed factors for the feeding phase. Cases of significant ANOVA results were followed by a Tukey HSD post hoc test (Zar, 1996) to point out any significant differences in $\Delta^0_{iW_d}$.

4.3 Results

4.3.1 Variations in the micro-algae consumption and the total dry flesh mass W_d of oysters

Feeding phase. Strong differences in the micro-algae consumption between oysters fed at HF *Vs* LF levels were observed during the feeding phase. At HF, oysters consumed on average 2.8 times more phytoplankton cells than at LF (Fig. 4.1). A slight decrease of the consumption was observed during the first 15 days at HF, but the general pattern clearly showed an increase of the micro-algae consumption simultaneously to an increase in the oyster weight (Fig. 4.1 B) throughout the experiment at both HF and LF.

The whole dry flesh mass (W_d) of oysters increased till the end of the feeding phase by a factor of ≈ 8.2 at HF compared to a factor of ≈ 3.7 at LF. The final values of W_d were 0.10 ($\pm$0.05) g at HF and 0.04 ($\pm$0.02) g at LF (Fig. 4.1 B). Significant interaction between feeding levels and sampling days occurred for W_d (Table 4.1). From t_{16} to t_{108}, W_d of oysters at HF was significantly higher than W_d at LF ($P \leqslant 0.0075$).

The dry mass of the remaining tissues W_{dRe} represented $\approx 67\,\%$ (at HF) and $\approx 62\,\%$ (at LF) of W_d (Fig. 4.1 C). Significant interaction between feeding levels, sampling days and organs occurred for W_{dRe} W_{dGi} and W_{dMu} (Table 4.1). W_{dRe} was always significantly different between HF and LF levels ($P \leqslant 0.0003$). However, W_{dMu} differed significantly between HF and LF, but only at t_{60} ($P = 0.0056$) and at t_{108} ($P = 0.0002$), while W_{dGi} differed significantly between HF and LF at t_{108} ($P = 0.0009$).

Starvation phase. W_d of oysters was always significantly higher at HF than at LF (Table 4.1; Fig. 4.1 B). From t_{108} and t_{212}, W_d decreased from 0.10 ($\pm$0.05) g to 0.05 ($\pm$0.03) g at HF and from 0.04 ($\pm$0.02) g to 0.02 ($\pm$0.01) g at LF. The decrease in W_{dRe} between t_{108} and t_{130} was 61 % at HF and 58 % at LF but the lost of mass was sharper for oysters at HF than at LF (Fig. 4.1 C). W_{dRe}, W_{dGi} and W_{dMu} were significantly higher at HF than at LF ($P = 0.2260$,

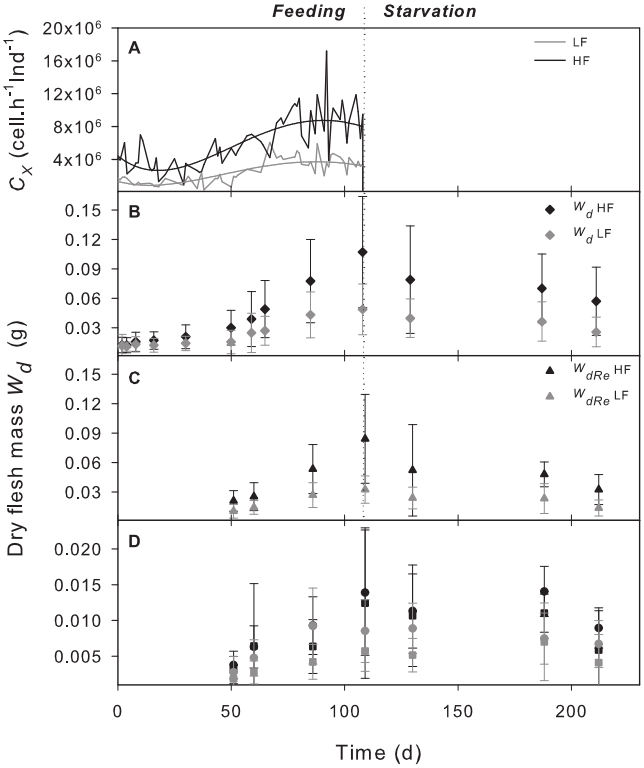

Figure 4.1: Temporal variations of *i)* the consumption of micro-algae *Skeletonema marinoï* (C_X, in cell. h^{-1} ind^{-1}, graph A) and *ii)* the dry flesh mass of the whole body (W_d, in g, graph B), the remaining tissues (W_{dRe}, in g, graph C) and the gills (W_{dGi}, in g) and the adductor muscle (W_{dMu}, in g, graph D) of *C. gigas* fed at two different feeding levels over 108 d. The black and grey colors stand for the high (HF) and low (LF) feeding levels. The vertical bars indicate $\pm$ SD of the mean for $n = 60$ (graph B, C, D, feeding phase), $n = 30$ (graph B, C, D, starvation phase).

Table 4.1).

4.3.2 Effect of the feeding level on $\delta^{13}C_{W_d}$ and $\delta^{15}N_{W_d}$

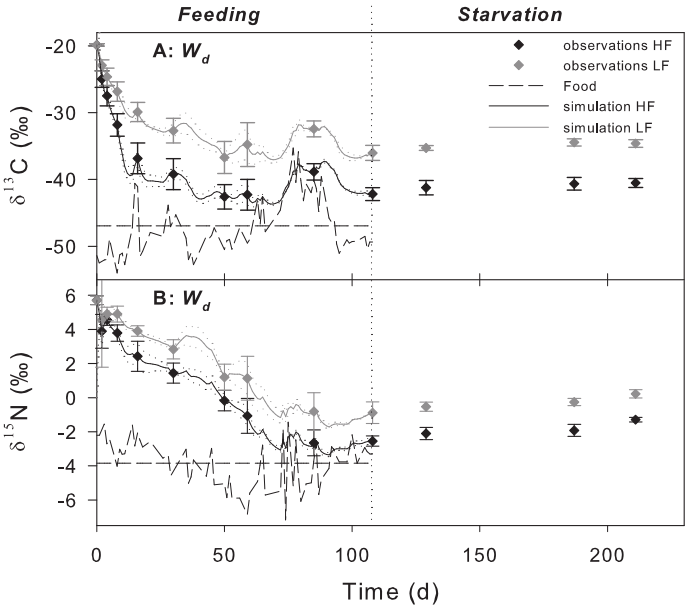

Figure 4.2: Variations in the mean isotopic ratios of the total dry flesh mass (δ_{W_d}) of *Crassostrea gigas* fed at two different feeding levels over 212 days. The observed $\delta^{13}C_{W_d}$ (‰, graph A) and $\delta^{15}N_{W_d}$ (‰, graph B) correspond to the black and grey symbols at high feeding (HF) *versus* low feeding (LF) levels, respectively. The simulated $\delta^{13}C_{W_d}$ and $\delta^{15}N_{W_d}$ are represented by the black and grey solid lines, respectively. The broken and straight dashed lines represent the variations of the isotopic ratio of the food source *i.e. Skeletonema marinoï* (δ_X, ‰) and the mean δ_X (‰), *i.e.* $\delta^{13}C_X = -46.93(\pm 4.39)$ and $\delta^{15}N_X = -3.85(\pm 1.35)$, respectively. The vertical bars indicate ± SD for $n = 21$ individuals.

Feeding phase. The isotopic ratios of the whole soft tissues ($\delta^{13}C_{W_d}$ and $\delta^{15}N_{W_d}$) of *C. gigas* decreased markedly after oysters start feeding on a δ_X depleted diet (Fig. 4.2). Significant interaction between feeding levels and sampling days occurred for $\delta^{13}C_{W_d}$ and $\delta^{15}N_{W_d}$ during the feeding phase (Table 4.1). Both $\delta^{13}C_{W_d}$ and $\delta^{15}N_{W_d}$ were always significantly higher at LF than at HF ($P \leqslant 0.0131$ and $P \leqslant 0.0321$ for $\delta^{13}C_{W_d}$ and $\delta^{15}N_{W_d}$ respectively). A sharp decrease in $\delta^{13}C_{W_d}$, from $-19.88(\pm 0.17)$ ‰ to $-42.51(\pm 0.79)$ ‰ (HF level) and from $-19.88(\pm 0.17)$ ‰ to $-36.73(\pm 0.31)$ ‰ (LF level), was observed till t_{50}. At t_{60} and t_{85} oysters became enriched in ^{13}C *i.e.* -40.65 ‰ at HF

Table 4.1: Statistical results of the multivariate ANOVA for the dry flesh mass (W_d), the C/N ratios and the isotopic ratios δ^{13}C and δ^{15}N of the whole body and organs of *C. gigas* during the feeding and starvation phases of the experiment. Time, feeding level (FL) and organs are fixed factors.

	feeding phase				starvation phase			
Sample & Source of variation	df_{Num}	df_{Den}	F	$P > F$	df_{Num}	df_{Den}	F	P
• W_d:								
FL	1	4	89.55	0.0007	1	173	64.19	0.0001
time	9	36	344.10	< 0.0001	2	173	7.09	< 0.0011
FL × time	9	36	27.23	< 0.0001	2	173	0.03	< 0.9744
• $\delta^{13}C_{W_d}$:								
FL	1	4	448.97	< 0.0001	1	33	551.95	< 0.0001
time	8	32	226.31	< 0.0001	2	33	3.38	0.0462
FL × time	8	32	5.77	0.0001	2	33	0.13	< 0.8769
• $\delta^{15}N_{W_d}$:								
FL	1	4	150.51	0.0003	1	33	281.33	< 0.0001
time	8	32	1137.68	< 0.0001	2	33	23.58	< 0.0001
FL × time	8	32	12.41	< 0.0001	2	33	0.22	0.8064
• C/N_{W_d}:								
FL	1	4	93.36	0.0006	1	33	26.35	< 0.0001
time	8	32	9.87	< 0.0001	2	33	3.46	0.0434
FL × time	8	32	12.09	< 0.0001	2	33	1.97	0.1554
• $\Delta^{13}C_{W_d}$:								
Ω	1	?	90.29	< 0.0001				
δ_X	7	?	135.12	< 0.0001				
$\Omega \times \delta_X$	7	?	12.02	< 0.0001				
• $\Delta^{15}N_{W_d}$:								
Ω	1	1	4.25	0.047				
δ_X	2	8	8.39	< 0.001				
$\Omega \times \delta_X$	2	?	1.02	0.436				
• $W_{dorgans}$:								
FL	1	4	71.24	0.0011	1	36	15.42	0.0004
time	3	12	159.69	< 0.0001	2	36	2.14	0.1328
organs	2	8	548.23	< 0.0001	2	69	168.57	< 0.0001
FL × time	3	12	11.55	0.0008	2	36	0.20	81.91
FL × organs	2	8	47.78	< 0.0001	2	69	8.16	0.0007
time × organs	6	24	44.05	< 0.0001	4	69	1.31	0.2751
FL × time × organs	6	24	7.64	0.0001	4	69	1.45	0.2260
• $\delta^{13}C_{organs}$:								
FL	1	4	237.31	0.0001	1	36	398.47	< 0.0001
time	3	12	24.77	< 0.0001	2	36	2.76	0.0768
organs	2	8	642.41	< 0.0001	2	68	122.26	< 0.0001
FL × time	3	12	0.88	0.4806	2	36	0.13	0.8815
FL × organs	2	8	9.66	0.0074	2	68	14.89	< 0.0001
time × organs	6	24	51.15	< 0.0001	4	68	0.99	< 0.4195
FL × time × organs	6	24	2.64	0.0415	4	68	0.21	< 0.9299
• $\delta^{15}N_{organs}$:								
FL	1	4	122.51	0.0004	1	36	153.92	< 0.0001
time	3	12	135.28	< 0.0001	2	36	12.55	< 0.0001
organs	2	8	409.43	< 0.0001	2	68	94.74	< 0.0001
FL × time	3	12	2.04	0.1616	2	36	0.49	0.6154
FL × organs	2	8	0.36	0.7053	2	68	5.09	0.0087
time × organs	6	24	28.24	< 0.0001	4	68	2.96	0.0257
FL × time × organs	6	24	1.33	0.2829	4	68	0.90	0.4669
• C/N_{organs}:								
FL	1	4	122.22	0.0004	1	36	32.12	< 0.0001
time	3	12	17.40	0.0001	2	36	3.69	0.0348
organs	2	8	579.66	< 0.0001	2	68	332.47	< 0.0001
FL × time	3	12	8.10	0.0032	2	36	3.99	0.0273
FL × organs	2	8	35.04	0.0001	2	68	12.57	< 0.0001
time × organs	6	24	3.08	0.0221	4	68	2.84	0.0308
FL × time × organs	6	24	2.98	0.0254	4	68	2.23	0.0752

and −34.46 ‰ at LF. At t_{108} the difference in oysters $\delta^{13}C_{W_d}$ between HF and LF was 6.15 ‰. $\delta^{15}N_{W_d}$ also exhibited a sharp decrease till t_{85} at both HF and LF, *i.e.* with values of −2.64(±0.19) ‰ (HF) and −0.79(±0.12) ‰ (LF), and then remained stable till the end of the feeding phase. At t_{108} oysters at LF were 1.66 ‰ higher in $\delta^{15}N$ compared to oysters at HF.

The variations observed in the simulated δ_{W_d} likely result from the variations in both δ_X and Ω. The model predicted an increase of $\delta^{13}C_{W_d}$ when $\delta^{13}C_X$ increased at *ca.* t_{75} (Fig. 4.2 A). A general decrease of the simulated $\delta^{15}N_{W_d}$ occurred all along the feeding phase (Fig. 4.2 B). Strong variations in $\delta^{15}N_X$ and $\delta^{13}C_X$ during short time increment induced rather small variations of δ_{W_d} as observed t_{60} and t_{85}.

$\delta^{13}C_X$ and $\delta^{15}N_X$ varied respectively in a magnitude range of 18.70 ‰ and 5.74 ‰ during the feeding phase. Most of the variations occurred over short time periods. $\delta^{13}C_X$ increased from t_{38} to t_{77} when the maximum value *i.e.* −35.31 ‰ was reached (Fig. 4.2 A). Conversely, $\delta^{15}N_X$ decreased of about ≈ 4.6 ‰ between t_0 and t_{59}, exhibiting next variations of more than 5 ‰ over three days (Fig. 4.2 B). The mean values of $\delta^{13}C_X$ and $\delta^{15}N_X$ in *S. marinoï* were −46.93(±4.39) ‰ and −3.85(±1.35) ‰ respectively.

Starvation phase. During the starvation phase, $\delta^{13}C_{W_d}$ and $\delta^{15}N_{W_d}$ were always significantly higher for oysters fed at LF than at HF level (Table 4.1; Fig. 4.2). This difference was also rather constant over time with a mean enrichment of ≈ 6.04 (±0.15) ‰ ($\delta^{13}C$) and ≈ 1.60 (±0.07) ‰ ($\delta^{15}N$) for the oysters at HF compared to LF. In the two feeding conditions, oysters were also significantly enriched in heavy isotopes at the end of the starvation phase compared to the start of the starvation phase for both carbon and nitrogen isotopes (Table 4.1).

4.3.3 Variations in $\delta^{13}C$ and $\delta^{13}N$ in the organs of *Crassostrea gigas*

Feeding phase. The nitrogen isotopic ratios in the organs of *C. gigas*, *i.e.* $\delta^{15}N_{Gi}$, $\delta^{15}N_{Mu}$ and $\delta^{15}N_{Re}$, were significantly higher for oysters at LF than at HF (Table 4.1; Fig.4.3 B, D and F). Although $\delta^{13}C_{Gi}$, $\delta^{13}C_{Mu}$ and $\delta^{13}C_{Re}$ varied differently over time and/or between feeding levels (Table 4.1), $\delta^{13}C$ of the organs was always significantly different between LF and HF ($P < 0.0001$; Fig.4.3 A, C and E). Both $\delta^{13}C_{Gi}$ and $\delta^{13}C_{Re}$ increased sharply between t_{50} and t_{85} *i.e.* ≈ 4.4 ‰ ($\delta^{13}C_{Gi}$ in LF and HF), ≈ 5.3 ‰ ($\delta^{13}C_{Re}$ in LF) and ≈ 4.8 ‰ ($\delta^{13}C_{Re}$ in HF; Fig.4.3 A and E). $\delta^{13}C_{Mu}$ remained rather constant between t_{50} and t_{85} with a mean value of −36.07 (±0.53) ‰ at LF and 30.08 (±0.41) ‰ at HF(Fig.4.3 C). A general decrease in $\delta^{15}N$ for each organ was observed from t_{50} and t_{108} (Fig.4.3 B, D and F). Differences in the final δ values of each organ and in the mean δ_X were more marked for $\delta^{13}C$ than for $\delta^{15}N$. Whatever the feeding level and for both $\delta^{13}C$ and $\delta^{15}N$, *Mu* was always heavier than *Gi* and/or *Re*. At HF, the gills were generally more enriched in ^{13}C and ^{15}N than the remaining tissues. At LF, $\delta^{13}C_{Gi}$ was lighter than $\delta^{13}C_{Re}$ while $\delta^{15}N_{Gi}$

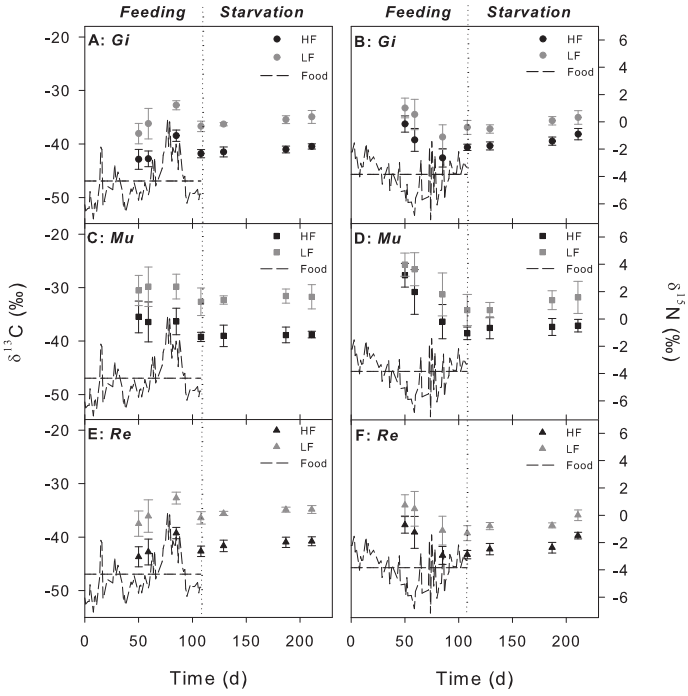

Figure 4.3: Variations of the isotopic ratios in the organs of *Crassostrea gigas* fed at two different feeding levels over 212 days. The left and right panels stand for δ^{13}C (‰) and δ^{15}N (‰), respectively. Graphs A and B stand for the gills Gi, graphs C and D stand for the adductor muscle Mu and the graphs E and F stand for the remaining tissues Re (including the mantle, the gonad, the digestive gland and the labial palps). The black and grey symbols stand for the high (HF) and low (LF) feeding levels, respectively. The broken and straight dashed line represent the variations of the isotopic ratio of the food source *i.e. Skeletonema marinoï* (δ_X, ‰) and the mean δ_X (‰), *i.e.* $\delta^{13}C_X = -46.93(\pm 4.39)$ and $\delta^{15}N_X = -3.85(\pm 1.35)$, respectively. The vertical bars on the symbols indicate ± SD for $n = 21$ individuals.

was conversely heavier than the $\delta^{15}N_{Re}$.

Starvation phase. In terms of $\delta^{13}C$ and $\delta^{15}N$, the organs of oysters were significantly enriched in heavy isotopes at LF compared to HF (Table 4.1; Fig. 4.3). Regardless of the organ type, the enrichment in heavy isotopes between HF and LF levels remained rather stable during the starvation phase with a mean value of 6.12 ($\pm$0.77) ‰ for $\delta^{13}C$ and of 1.57 ($\pm$0.20) ‰ for $\delta^{15}N$. All the organs also exhibited an increase in their isotopic ratio for both $\delta^{13}C$ and $\delta^{15}N$ resulting in an enrichment in heavy isotopes between the start and the end of the starvation. This enrichment was significant for $\delta^{15}N$ ($P < 0.0001$), but not for $\delta^{13}C$ ($P = 0.0768$). δ_{Mu} was always heavier than δ_{Gi} and δ_{Re}, but $\delta^{13}C_{Gi}$ was lighter than $\delta^{13}C_{Re}$ and $\delta^{15}N_{Gi}$ was heavier than $\delta^{15}N_{Re}$.

4.3.4 Effect of variations in Ω and δ_X on $\Delta^{13}C_{W_d}$ and $\delta^{15}N_{W_d}$

For both the carbon and nitrogen isotopes, Δ_{W_d} varied between and within feeding levels (Fig. 4.4). The use of a mean Ω and δ_X values for each sampling intervals resulted in estimating variableΔ values for the carbon and nitrogen isotopes. $\Delta^{15}N_{W_d}$ ranged from 0.7($\pm$0.1) ‰ to 8.2($\pm$3.5) ‰ while $\Delta^{13}C_{W_d}$ exhibited stronger variations, *i.e.* from 2.1($\pm$0.2) ‰ to 25.9($\pm$2.0) ‰.

Significant interaction between Ω_C and $\delta^{13}C_X$ occurred for $\Delta^{13}C_{W_d}$ during the feeding phase (Table 4.1). $\Delta^{13}C_{W_d}$ differed significantly between $\Omega_{C_{HF}}$ and $\Omega_{C_{LF}}$ during the feeding phase ($P \leqslant 0.01$, Table 4.1) except from t_0 to t_2 ($P = 0.9837$) and from t_4 to t_8 ($P = 0.4008$; Fig. 4.4 A). At LF level, the estimated $\Delta^{13}C_{W_d}$ corresponding to the lowest values of $\delta^{13}C_X$, *i.e.* between t_0 and t_8, did not differ significantly from each other ($0.7188 \leqslant P \leqslant 1.0000$). $\Delta^{13}C_{W_d}$ estimations for the highest $\delta^{13}C_X$ values, *i.e.* between t_8 and t_{108}, did not differ significantly from each other ($0.4392 \leqslant P \leqslant 1.0000$). However, the estimated $\Delta^{13}C_{W_d}$ differed significantly between these two groups ($0.0000 \leqslant P \leqslant 0.0004$; Fig. 4.4 A). At HF, the estimated $\Delta^{13}C_{W_d}$ for the highest $\delta^{13}C_X$ values, *i.e.* between t_8 and t_{108}, were not significantly different each other ($0.0744 \leqslant P \leqslant 1.0000$). $\Delta^{13}C_{W_d}$ estimated for the lowest $\delta^{13}C_X$ values *i.e.* between t_0 and t_8 was not significantly different each other ($0.0744 \leqslant P \leqslant 1.0000$) but was significantly different from all other $\Delta^{13}C_{W_d}$ estimations ($0.0000 \leqslant P \leqslant 0.0311$, Fig. 4.4 A).

No significant interaction between Ω_N values and $\delta^{15}N_X$ occurred for $\Delta^{15}N_{W_d}$ during the feeding phase (Table 4.1). $\Delta^{15}N_{W_d}$ estimates based on the $\Omega_{N_{LF}}$ values were always significantly higher than the $\Delta^{15}N_{W_d}$ estimated with $\Omega_{N_{HF}}$ values. However, no clear trend was observed between the variations in $\Delta^{15}N_{W_d}$ and those of $\delta^{15}N_X$ (Fig. 4.4 B).

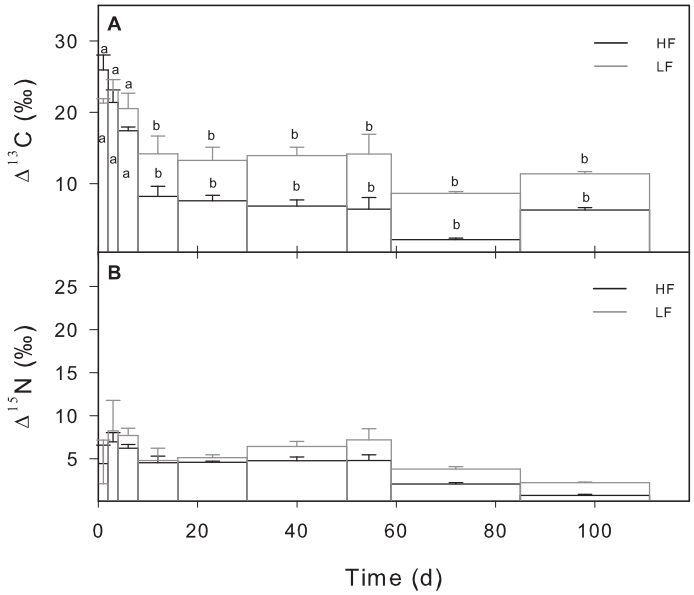

Figure 4.4: Variations in the values of trophic fractionation Δ (‰) between the food source, *i.e.* *Skeletonema marinoï*, and the total dry flesh mass of *Crassostrea gigas*. Graphs (A) and (B) correspond to the carbon and nitrogen isotopes and the black and grey bar charts stand for the HF and LF levels, respectively. Δ values were estimated using the mean values of Ω (d^{-1}) and δ_X (‰) between each sampling. The different subscripts within each condition indicate significant differences of diet isotopic ratio on the Δ estimations. The vertical bars indicate $\pm$ SD ($n = 3$ replicates).

4.3.5 Variations in the C/N ratios of *Crassostrea gigas* tissues

Feeding phase. Significant interaction between feeding levels and sampling day occurred for C/N_{W_d} (Fig. 4.5 and Table 4.1). From t_8, C/N_{W_d} of oysters at HF was significantly higher than C/N_{W_d} of oysters at LF ($P \leqslant 0.01$). The highest variations in C/N_{W_d} were observed at HF with values from 4.05 ($\pm$0.17) to 5.01 ($\pm$0.21). C/N_{W_d} increased till t_{85}, and decreased from 5.01 ($\pm$0.21) to 4.60 ($\pm$0.15) between t_{85} and t_{108}.

Significant interaction between feeding levels, sampling days and organs occurred for the C/N_{Re}, C/N_{Gi} and C/N_{Mu} (Table 4.1). Except for C/N_{Mu} for which no significant difference was observed between the two feeding levels, C/N_{Re} and C/N_{Gi} were always higher for HF than at LF ($P \leqslant 0.0426$). The highest variations of the C/N ratio of *C. gigas* organs were observed for the remaining tissues and ranged from 4.09 to 5.51 (Fig 4.5).

Starvation phase. C/N_{W_d}, C/N_{Re}, C/N_{Gi} and C/N_{Mu} were significantly higher at HF than at LF (Table 4.1). At both HF and LF, C/N_{W_d}, C/N_{Re}, C/N_{Gi} exhibited a decrease from t_{108} to t_{130} and then a slight increase till t_{188} (Fig. 4.5). Nevertheless, C/N_{W_d} and C/N_{Re} of the oysters at HF exhibited the strongest decrease during the starvation, *i.e.* from 4.60 ($\pm$0.15) (at t_{108}) to 3.91 ($\pm$0.01) (at t_{212}) for C/N_{W_d} and from 4.97 ($\pm$0.18) (at t_{108}) to 4.09 ($\pm$0.19) (at t_{212}) for C/N_{Re}. C/N_{Mu} remained rather constant throughout the starvation period with no difference between feeding levels ($P = 0.5448$).

4.4 Discussion

4.4.1 The δ_{W_d} of oysters depend on the feeding level

The amount of consumed food had a strong and significant effect on the dynamics of the isotopes in *Crassostrea gigas* total dry flesh mass. Oysters reared at HF consumed *ca.* 2.8 times more food than oysters at LF (Fig. 4.1) resulting in a difference of 6.15‰ for the $\delta^{13}C$ and of 1.66‰ for $\delta^{15}N$ at the end of the feeding phase (Fig. 4.2). Our results also revealed that the higher the feeding rate, the lower the isotopic ratios of oysters. Oyster at HF increased in mass faster than oysters reared at LF (Fig. 4.1 B), resulting in a higher Ω. Although Ω varied over time and between feeding levels, our results are in agreement with the sensitivity analysis of Olive et al. (2003) who found decreasing δ values with increasing Ω values. We estimated Ω values from 0.05 to 0.44 for C and from 0.04 to 0.36 for nitrogen, which are consistent with the Ω values of 0.05 for C and 0.25 for N in the marine worm *Nereis virens*. Olive et al. (2003) estimated. However, our values for N differed from lower Ω values from 0.017 to 0.031 found in three different herbivorous fish species (Mill et al., 2007).

Our results are consistent with the results on *Oreochromis niloticus* and *Cyprinus carpio* (Gaye-Siessegger et al., 2003, 2004b). For these two species the final $\delta^{13}C$ values of the lipids and the lipid-free matter and the final $\delta^{15}N$

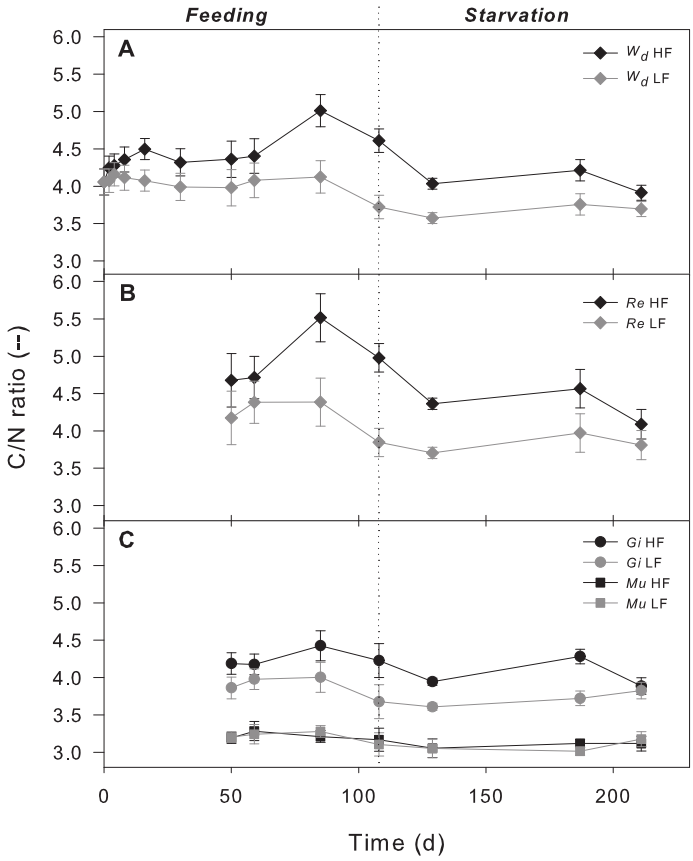

Figure 4.5: Temporal variations of the mean individual C/N ratios of *Crassostrea gigas* whole soft body tissues (W_d, in g, graph A) and organs, *i.e.* the remaining tissues (W_{dRe}, in g, graph B) and the gills (W_{dGi}, in g, graph C) and the adductor muscle (W_{dMu}, in g, graph C) fed at two different feeding levels over 108 d. The black and grey colors stand for the high (HF) and low (LF) feeding levels. The vertical bars indicate $\pm$ SD of the mean for $n = 21$ individuals.

values both decreased with increasing feeding rate. Gaye-Siessegger et al. (2003, 2004b) suggested that the anabolic to catabolic ratio may change with feeding level, affecting indirectly the amount of molecules (and isotopes) available for the different biochemical reactions. According to Emmery et al. (2011), however, we were expected that a fixed fraction of the substrate molecules (and isotopes) available to fuel a particular metabolic function (*i.e.* assimilation of food compounds) was routed through the catabolic pathway, the remaining material being routed through anabolism. The different metabolic functions may possibly have different anabolic to catabolic ratios *e.g.* according to growth, maintenance, respiration, tissues recycling, resulting in varying δ^{13}C and δ^{15}N values at the whole body scale. The increase in δ values of the oyster tissues linked with decreasing food conditions has been already reported by Emmery et al. (2011). However, the relationship between the enrichment in heavy isotopes and the feeding levels was only studied in fish species and results are still contradictory. Carleton and Del Rio (2010) did not observe any clear pattern between muscle and liver $\delta^{13}C_{\infty}$ on the Nile tilapia (*Oreochromis niloticus*) fed at three different feeding levels. These authors also reported mean δ^{13}C increasing with increasing feeding level, while the opposite pattern was observed for δ^{15}N in the European sea bas *Dicentrarchus labrax* (Barnes et al., 2007).

The oysters reared at HF showed a lower δ_{W_d} than oysters at LF; but they grew faster and had a higher C/N ratio than at LF (Fig. 4.1 B and Fig 4.5). In suspension-feeders high feeding conditions are usually resulting in periods of high growth (*e.g.* Laing, 2000; Rico-Villa et al., 2009) and in an increase of the main biochemical compounds, *i.e.* protein, lipids and carbohydrates in animal tissues (Deslous-Paoli and Héral, 1988; Dridi et al., 2007; Flores-Vergara et al., 2004). Bodin et al. (2007), Post et al. (2007) and Sweeting et al. (2006) observed a strong positive relationship between the increase of the lipid content in animal tissues and the increase of their C/N ratio. However, *C. gigas* stores energy mainly as glycogen (*e.g.* Deslous-Paoli and Héral, 1988) and the differences in C/N_{W_d} between HF and LF seem to be to small (*i.e* less than 1.5) to account for the strong differences observed between $\delta^{13}C_{W_d}$ and $\delta^{15}N_{W_d}$. Indeed, oysters at HF grew faster, suggesting an faster synthesis of new tissues and utilization of energetic reserves compared to oysters at LF.

4.4.2 Effect of the starvation on δ_{W_d} of oysters

At the end of the starvation, $\delta^{13}C_{W_d}$ and $\delta^{15}N_{W_d}$ of *C. gigas* were slightly, but significantly, higher compared to the start of starvation for each feeding level. At the start of the starvation, both the mass and the C/N ratio of oysters decreased, suggesting that the starved oysters firstly used compounds depleted in heavy isotopes such as lipids (for δ^{13}C).

The same pattern was described by Haubert et al. (2005) for the collembolan *Protaphorura fimata* and by Doi et al. (2007) for the deposit-feeding chironomid larvae *Chironomus acerbiphilus*. Increasing $\delta^{15}N_{W_d}$ values were observed for the spider *Pardosa lugubris*, (Oelbermann and Scheu, 2002), the polychaete

Nereis virens (Olive et al., 2003), and for birds and mammals (Hobson and Clark, 1992; Hobson et al., 1993). Although changes in the isotopic composition of $\delta^{15}N_{W_d}$ due to excretion processes are poorly studied in suspension feeders, it is well accepted that the types of nitrogenous waste, associated to the protein metabolism (*i.e.* synthesis, recycling and excretion), strongly influence the isotopic composition of an organism under nutritional stress (*e.g.* Hobson et al., 1993).

The temporal variations in $\delta^{15}N_{W_d}$ and $\delta^{13}C_{W_d}$ during starvation were identical between the two feeding levels (Fig. 4.2, right part). This suggests that oysters were likely using a minimal and necessary amount of "reserve compounds" to maintain their structural body components (*i.e.* protein recycling) and to stay alive. This phenomenon, acting as a turnover process, should certainly be considered to better understand isotope dynamics in living systems (Pecquerie et al., 2010). The monitoring of stable isotopes over a longer starvation period could help to better understand metabolic changes during this stressful period and to provide explanation for the discrepancy with some patterns reported in literature.

4.4.3 Effect of the feeding level on the dynamics of δ in the organs of oysters

The feeding level had a strong and significant effect on δ_{Gi}, δ_{Mu} and δ_{Re} for both the C and N isotopic ratios (Fig. 4.3). Firstly, the higher the feeding level, the lower the isotopic ratios of the different organs, which is consistent with the patterns observed for the total dry flesh mass. This difference between δ_{LF} and δ_{LF} appeared to be rather constant among organs over the whole experience (for feeding and starvation periods) with a mean value of 1.56 ($\pm$0.31)‰ for δ^{15}N and 6.09 ($\pm$0.69)‰ for δ^{13}C. As previously discussed, it suggests that the different organs of an individual likely require a proportion of reserve compounds to allow their own development and some structural compounds (*e.g.* structural proteins) that involve maintenance and/or recycling (Kooijman, 2010; Pecquerie et al., 2011). Secondly, δ_{Mu} was always higher than δ_{Gi} and δ_{Re} regardless of the feeding level. Although patterns between δ_{Gi} and δ_{Re} were less clear, the average isotopic ratio δ in the different organs ranked as follows, $\delta_{Mu} > \delta_{Gi} > \delta_{Re}$ during the whole experiment. Since Tieszen et al. (1983), numerous studies have shown significant differences in isotope discrimination among organs in fish (*e.g.* Guelinckx et al., 2007; Pinnegar and Polunin, 1999; Suzuki et al., 2005; Sweeting et al., 2007a), in birds (*e.g.* Ogden et al., 2004; Pearson et al., 2003) and in mammals (*e.g.* MacAvoy et al., 2005; Voigt et al., 2003).

For suspension feeders, our findings are in agreement with the results of previous studies. Malet et al. (2007) found that δ^{13}C and δ^{15}N were higher in the adductor muscle than in the mantle, in the digestive gland and in the gonad of diploid and triploid *C. gigas*. Paulet et al. (2006) found that the adductor muscle had higher δ values than the gills and the gonad of oysters at

the start of an experimental shift in $\delta^{13}C_X$. Yokoyama et al. (2005b) pointed out that $\delta^{15}N_{Mu}$ of *C. gigas* was higher than $\delta^{15}N_{Gi}$ after equilibrium with the food source during a fractionation experiment. Conversely, the C/N ratios among the different organs ranked in the inverse order, namely $C/N_{Mu} < C/N_{Gi} < C/N_{Re}$ (Fig 4.5), suggesting that the biochemical composition of organs likely influenced the discrimination of isotopes within the organism. These two patterns, *i.e.* the relative order in both δ and C/N ratios, match with the existing knowledge of the different physiological roles of organs. Namely *C. gigas* stores energy (mainly lipids and glycogen) in the digestive gland, in the gonad and in the mantle (Berthelin et al., 2000) which correspond to the remaining tissues *Re* in our study. The low δ values associated with high values of the C/N ratio supports the role of *Re* as a storage tissue. Conversely, *Mu* which exhibited the highest δ values and the lowest C/N ratios, is mostly composed of proteins (Berthelin et al., 2000; Costil et al., 2005; Ren et al., 2003) and likely plays a minor role in the processes of energy storage.

4.4.4 Consequences of the variations in δ_X on the isotopic ratios of oyster whole soft tissues and organs

According to equation (4.5) the δ_{W_d} depends on the variations of Ω and δ_X. In our experiment δ_X exhibited important temporal variations (Fig. 4.2). As observed by Pennock et al. (1996), isotope fractionation in *S. marinoï* may be influenced by the concentration of nutrients (*e.g.* ammonium and nitrate) and can exhibit strong and fast variations (within few hours/days) in batch culture. This phenomenon can explain the variations in $\delta^{13}C_X$ and $\delta^{15}N_X$ of *S. marinoï* observed during the feeding phase. It also suggests a varying isotopic ratio of food rather than a constant mean value to describe the dynamics of isotopes in the total dry flesh mass of *C. gigas*. Although δ_X is often considered constant during diet switching experiment, some variations in δ_X were already observed by Yokoyama et al. (2008). Emmery et al. (2011) used varying values of δ_X to describe the dynamics of δ_{W_d} in *C. gigas*.

Consequences of the variations in δ_X on δ_{W_d} strongly depend on their intensity and duration. From t_{60} to t_{85}, an increase of $\approx 2.3‰$ (LF level) and $\approx 3.4‰$ (HF level) of $\delta^{13}C_{W_d}$ occurred consecutively to an increase by $\approx 13‰$ of $\delta^{13}C_X$ (Fig. 4.2 A). Nevertheless, the variations in δ_X are smoothed down by oyster tissues between trophic levels as observed by Harvey et al. (2002, and references therein). The variations in $\delta^{13}C_X$ may also explain the enrichment in heavy isotopes observed for $\delta^{13}C_{Mu}$, $\delta^{13}C_{Gi}$ and $\delta^{13}C_{Re}$ between t_{60} to t_{85} (Fig. 4.3 A, C, E). However, the fastness of the variations in the isotopic ratios of oyster organs consecutively to the $\delta^{13}C_X$ variations differed among the organs. $\delta^{13}C_{Mu}$ exhibited the lowest variations compared to $\delta^{13}C_{Gi}$ and $\delta^{13}C_{Re}$, which is consistent with the existing knowledge about the low turnover rate of this organ (Lefebvre et al., 2009a).

4.4.5 Trophic fractionation depends on feeding level and δ_X

According to equation (4.6) the trophic fractionation, *i.e.* $\Delta_{W_d} = \delta_{W_d} - \delta_X$, depends on both the variations in Ω and δ_X. As Z, and therefore δ_{W_d}, also varied over time according to these two factors, we here calculated Δ_{W_d} values between each sampling day. We assumed that the mean values of Ω and δ_X could be considered as a "temporarily steady state" condition of the individual with respect to its food source (Fig. 4.4). According to our results, the two factors did not influence the trophic fractionation in the same way; Ω likely explained most of the variations in Δ^{13}C and in Δ^{15}N. As observed for the dynamics of δ_{W_d}, the higher the feeding level (higher Ω) the lower Δ for both C and N isotopic ratios. Our results are consistent with those of Gaye-Siessegger et al. (2003, 2004b). According to Emmery et al. (2011), the quantification of compounds (and isotopes) through catabolism and anabolism could be helpful to understand this trend.

The clearest effect of the isotopic ratio of the food on the values of Δ is observed for C isotopes since $\delta^{13}C_X$ exhibited stronger variations than $\delta^{15}N_X$. Our results revealed that the lower $\delta^{13}C_X$, the higher Δ^{13}C (Fig. 4.4 A). Although the effect of δ_X on Δ remains rather unknown and hardly studied in the literature, our results are consistent with the trends observed by Caut et al. (2008a) who found decreasing Δ^{13}C and Δ^{15}N for the liver, the muscle and the hair of the rat (*Rattus rattus*) with increasing $\delta^{13}C_X$ and $\delta^{15}N_X$, respectively. Dennis et al. (2010) also pointed out a strong inverse relationship between increasing isotopic ratios of the food source and increasing trophic fractionation, for both C and N isotopes, in the guppies *Poecilia reticulata* under controlled conditions. However, conversely to the experimental protocol of Dennis et al. (2010), our experiment was not initially designed to demonstrate the effect of δ_X on Δ. This may account for the lack of clear relationship between $\delta^{15}N_X$ and Δ^{15}N in our experiment.

The effect of the isotopic ratio of the food source on Δ could be explained in different ways. Dubois et al. (2007a) carried out a diet switching experiment on *C. gigas*, using the same species of micro-algae as food source and under approximately the same experimental conditions (Table 4.2). These authors estimated trophic fractionation value of 1.85 ‰ for Δ^{13}C. Following the classical approach to calculate the trophic fractionation, we considered *i)* the overall mean of Z and Ω (over time for the two feeding levels) and *ii)* the mean $\delta^{13}C_X$ value over time. It resulted in an enrichment in heavy isotopes of 7.25‰ between oysters and *S. marinoï* for δ^{13}C at HF. The difference in the trophic fractionation value between Dubois et al. (2007a) study and our study may be due to the isotopic ratio of the food source. In our experiment oysters incorporated a lower $\delta^{13}C_X$ compared to the oysters in the experiment of Dubois et al. (2007a) (Table 4.2)

Table 4.2: Comparison between the fractionation experiment carried out in this study and the one carried out by Dubois et al. (2007a). T and W_{di} are respectively the water temperature (°C) and the initial flesh dry mas of oysters (g). δ_{min}, δ_{max} and δ_{mean} stand for the minimal, the maximal and the mean isotopic ratios of the food source respectively (‰); δ_i and δ_f are the initial and final isotopic ratios of *Crassostrea gigas* (‰, total dry flesh mass). Δ is the trophic fractionation (‰). The values of δ and Δ used in this study come from oysters reared at high feeding (HF) level.

	This study		Dubois et al. (2007a)	
Duration	108		90	
T	14.27(±0.36)		15.9(±0.6)	
Salinity	34.2(±0.3)		31.9(±1.7)	
W_{di}	0.013(±0.009)		0.05*	
Feeding level	HF		*ad libitum*	
	Carbon ^{13}C	*Nitrogen* ^{15}N	*Carbon* ^{13}C	*Nitrogen* ^{15}N
Food source: Skeletonema marinoï				
δ_{min}	−54.01	−7.17	−24.54	−8.81
δ_{max}	−35.31	−1.43	−20.24	−11.56
$\delta_{max} - \delta_{min}$	18.7	5.74	4.32	20.37
δ_{mean}	−46.93(±4.39)	−3.85(±)1.35	−23.04(±0.97)	−4.93(±1.09)
Oysters: Crassostrea gigas				
δ_i	−19.88(±0.17)	5.70(±)0.27	−19.09	8.11
δ_f	−42.18(±0.48)	−2.54(±)0.19	−20.82	−0.93
Δ	7.25	3.37	1.85	3.79

*: assuming that the total dry flesh mas equal 20 % of the total wet flesh mass

4.4.6 Conclusion

Our results show that isotopic ratios and trophic fractionation estimations for *C. gigas* strongly depend on both the feeding level (*i.e* no food, low food high food) and the isotopic ratio of the food source. We observe that *i)* the higher the feeding level, the lower δ_{W_d} and Δ_{W_d}, and *ii)* the higher the isotopic ratio of the food source, the lower δ^{13}C and Δ^{13}C. The temporal evolution observed for the different organs are similar to the total dry flesh mass. Our results also suggest that the individual metabolism (metabolic functions and biochemical composition) likely play an important role in discriminating the stable isotopes. The underlying mechanisms explaining the isotopic incorporation rates and the isotopes discrimination remain, however, poorly understood. Indeed, the model of Olive et al. (2003) considers the individual as a "single black box" and discrimination of isotopes during excretion as a single mechanism. However, more complex mechanisms and metabolic functions may certainly occur and should be considered simultaneously to fully describe and understand mass and isotope fluxes within organisms (*e.g.* Martínez del Rio et al., 2009; Carleton and Del Rio, 2010; Pecquerie et al., 2010, and references therein). In this context, the Dynamic Energy Budget theory (*i.e.* DEB theory, Kooijman, 2010) offers a new set of assumptions and a single model framework to describe fluxes of energy, mass (including biochemical composition of organisms) and isotopes in living systems (Emmery et al., 2011; Kooijman, 2010; Pecquerie et al., 2010).

4.5 Acknowledgment

We would like to thank Stanislas Dubois for his critical comments on this study. We also would like to thank Gaétan Daigle for his help with the statistical analyses. Pierrick Le Souchu, Christian Mingant, Bruno Petton and Stéphane Pouvreau from the Ifremer laboratory in Argenton are also gratefully acknowledged for their useful technical advices to set up our experiment. The participants of the 8$^{\text{th}}$ ISOECOL conferences are also gratefully acknowledged for their stimulating discussion.

Chapter 5

Effect of the ingestion rate on the dynamics of stable isotopes δ^{13}C and δ^{15}N in soft tissues of the Pacific oyster *Crassostrea gigas*: investigation through dynamic energy budget (DEB) model

Emmery, A.[a,b,c], Lefebvre, S.[b], Alunno-Bruscia, M.[c], Kooijman, S.A.L.M.[d] (in prep).

[a] *Université de Caen Basse Normandie, CNRS INEE - FRE*3484 *BioMEA, Esplanade de la paix* 14032 *Caen cedex, France*

[b] *Université de Lille* 1 *Sciences et Technologies, UMR CNRS* 8187 *LOG, Station Marine de Wimereux,* 28 *avenue Foch,* 62930 *Wimereux, France*

[c] *Ifremer UMR* 6539, 11 *Presqu'île du Vivier,* 29840 *Argenton, France*

[d] *Vrije Universiteit, Dept. of Theoretical Biology, de Boelelaan* 1085 1081 *HV Amsterdam, The Netherlands*

Abstract

In order to better understand the effect of the ingestion rate on the dynamics of stable isotopes in the Pacific oyster *Crassostrea gigas*, we fed oysters with a depleted diet in ^{13}C and ^{15}N of *Skeletonema marinoï* at two different feeding levels over 108 d. Results revealed that the higher the ingestion rate, the higher the growth (total dry flesh mass) and the lower δ^{13}C and δ^{15}N of the oyster

tissues. The dynamic energy and isotope budget model (IsoDEB) we used satisfactory describes both the total dry flesh mass and the isotopic compositions of oysters *i)* under the two different feeding conditions and *ii)* under varying isotopic ratios of *S. marinoï* (δ^{13}_X). According to the model framework, the selection of compound and isotopes through anabolism and catabolism played a major role in the discrimination of isotopes processes and in the understanding of patterns we observed. However, model simulations were less accurate during strong variations of the $\delta^{13}C_X$, suggesting a possible misleading consideration of the biochemical composition of *C. gigas*. Although the set of parameters estimated using the covariation methods originates from a full description of the life cycle of *C. gigas*, further developments are still required to refine estimation of parameters linked to reproduction.

Keywords: *Crassostrea gigas*; stable isotopes; ingestion rate; DEB theory; trophic fractionation

5.1 Introduction

Introduced in Europe for aquaculture purpose in the early 1970s, the Pacific oyster *Crassostrea gigas* became an important ecological and economical species in natural marine ecosystems and marine aquaculture (Buestel et al., 2009). *C. gigas* is a non-indigenous bivalve in the north-western coast of Europe that is considered as an invasive species (Troost et al., 2010). Its important filtration activity associated to the lack of natural predators and the diversity of food sources that composed its diet (*e.g.* Marín Leal et al., 2008), allowed *C. gigas* to established successfully in natural contrasting environments (*e.g.* Troost, 2010, and references therein), competing for space and resources with other suspension feeders (Dubois et al., 2007b; Riera et al., 2002). These key ecological and economical roles of the Pacific oyster stimulated scientific interests in development of modeling tools, *i.e.* such as bioenergetic models, to better understand the factors underlying its growth and reproduction performances (*e.g.* Alunno-Bruscia et al., 2011).

Over the last decays, increasing interests have been paid on the use of dynamic energy budget (DEB) models (from Kooijman, 2010) to better understand ecophysiology of bivalves species according to environment variations, *i.e.* food availability and temperature (*e.g.* Cardoso et al., 2006a; Ren and Ross, 2005; Pouvreau et al., 2006; Rosland et al., 2009; Handå et al., 2011). Since the first application by Pouvreau et al. (2006) of DEB model to the Pacific oyster, different studies were performed on a wild range of environmental (and experimental) conditions. Ren and Schiel (2008) validated the model on growth data set of *C. gigas* reared at two different depths in the New waters during winter. Alunno-Bruscia et al. (2011) successfully describes the oyster growth

in six different farming areas throughout the French Atlantic coast from 1993 to 2008. The original DEB oyster, based on individual response, was adapted by Bacher and Gangnery (2006) to study *C. gigas* population growth in Thau lagoon and by Grangeré et al. (2009a) at the ecosystem scale to understand year-to-year variability of oysters in the Bay of Veys. Bourlès et al. (2009) and Bernard et al. (2011), respectively, improved the initial set of parameters estimated by Van der Veer et al. (2006), although these parameters are estimated in joule (energy dimension) without considering elemental composition of oyster tissues thanks to moles (number dimension). Most of the studies above cited focused their investigations on adult stage of *C. gigas*, frequently on (natural) shellfish farming area, while Rico-Villa et al. (2010) re-estimated, thanks to experimental data, some parameters in order to better understand larvae stage development of *C. gigas*. Although food availability (*i.e.* phytoplankton) and temperature explain most of the spatial and temporal variations in growth patterns between and within ecosystems, the problem of estimating food resources available to suspension feeding bivalves, as well as their consequences on their growth, remains however a major problem in modeling bivalves energetics (*e.g.* Grant and Bacher, 1998; Marín Leal et al., 2008; Pouvreau et al., 2006; Flye-Sainte-Marie et al., 2007; Rosland et al., 2009).

An alternative approach for understanding bivalve ecophysiology lies in the use of stable isotopes analysis, *i.e.* δ^{13}C and δ^{15}N, as a tracer of organic matter fluxes in food webs (*e.g.* Fry and Sherr, 1984). In coastal marine ecosystems, the trophic ecology of suspension feeding bivalves relative to the diversity and availability of the potential food sources has been extensively studied. It was shown that phytoplankton (*e.g.* Yokoyama et al., 2005b), as well as benthic micro-algae (*e.g.* Kang et al., 2006), terrestrial matter from rivers uptakes and decomposing macro-algae (*e.g.* Marín Leal et al., 2008) and sewage organic material (*e.g.* Piola et al., 2006) could contribute differently, but significantly to the diet of *C. gigas*. However, a weakness of these approaches still lies in the lack of tools allowing an accurate consideration of the incorporation rates of trophic resource and factors that influence isotope fractionation between food source(s) and consumer(s). The recent developments of dynamic isotope budgets (DIB, Kooijman, 2010) were used by Pecquerie et al. (2010) and Emmery et al. (2011) to investigate impacts of metabolism or feeding levels on the dynamics of stable isotopes in organisms. Based on biological, physical and chemical assumptions, this model provides *i)* a generic framework to describe the uptake and use of energy, compounds and isotopes by living organisms and *ii)* new mechanisms to describe discrimination of isotopes by living organisms. However, the use of this type of model remains rare in isotopic ecology. To our knowledge, no studies have already investigated the link between mass and isotope in *C. gigas* tissues by coupling DEB and DIB models (IsoDEB model).

The aim of this study was therefore to better understand the effect of feeding level on the growth and the dynamics of δ^{13}C and δ^{15}N in *C. gigas* by applying the IsoDEB model to experimental data.

5.2 Material and methods

5.2.1 Diet-switching experiment

The experimental design, *i.e.* including both feeding and starvation phases and sample treatments are fully described by Emmery et al. (in prep.). Briefly, *ca.* 3300 individuals of natural spat of oyster (mean shell length = 1.85 ± 0.44 cm, mean flesh dry mass = 0.013 ± 0.009 g, 8-months old) originating from Arcachon Bay (south-western France) were transferred on 29 March 2010 at the Ifremer laboratory in Argenton (Brittany, France). They were randomly split in two groups, placed and further reared over 212 days in 280 L tanks supplied with filtered running seawater. The two groups of oyster were fed on a monoculture *Skeletonema marinoï* (CCAP 1077/3) during the first 108 d under two different feeding levels, *i.e.* HF (high food level, *i.e.* 8 % of dry mass of microalgae per dry mass of oyster) and LF (Low food level, *i.e.* 8 % of dry mass of microalgae per dry mass of oyster). They were then starved over the last 104 d. In each tank, the water temperature was kept constant throughout the experiment, *i.e.* mean temperature $T = 14.3(\pm 0.4)$°C and mean salinity was $34.2(\pm 0.3)$ PSU. At each sampling date, 20 oysters per tank for the feeding phase and 30 oysters per tank for the starvation phase were collected, measured, dissected and freeze-dried to measure the total dry flesh mass W_d of individuals. Before dissection, 7 oysters per tank were randomly selected for isotopic analysis.

5.2.2 Dynamic energy and isotope budget model (IsoDEB)

The IsoDEB model describes the growth of the total dry flesh mass of *C. gigas* (W_d, g) and the isotopic composition of the total whole soft body tissues (dry flesh mass) *i.e.* $\delta^{13}C_{W_d}$ and $\delta^{15}N_{W_d}$ (‰) over time according to three forcing variables: the food availability, the temperature and the isotopic composition of the food source *i.e.* $\delta^{13}C_X$ and $\delta^{15}N_X$. The model equations were modified according to Sousa et al. (2010) and Pecquerie et al. (2010) to follow the same model framework and assumptions. Nevertheless, our approach slightly differ from the one of Sousa et al. (2010) in the way that we here consider the ingestion of microalgae (J_{XA}, mol.d^{-1}) as a forcing variable of the model, by converting the number of cells (of microalgae) consumed per hour and per individual in moles per hour and per individual as follows: $J_{XA} = C_X M_X$ (Fig. 5.1 and Table 5.1). During starvation, somatic maintenance has priority over growth (*i.e.* increase of structure) and maturity maintenance has priority over maturation or reproduction. When reserve is not sufficient enough to cover maintenance costs, energy accumulated in the reproduction buffer is used. Finally, if the reproduction buffer is empty, maintenance costs are paid from the structure.

Since Emmery et al. (2011), the parameter estimation for the DEB model was improved by using the covariation method (Lika et al., 2011a). Emmery

et al. (2011), estimated parameters based on both zero-variate data and pseudo-data. The zero variate data consists in measurable quantities such as age (a), physical length (L) and weight wet (W_w) on particular stages of *C. gigas* development, *i.e.* birth (start of feeding), puberty (start of reproduction) and adult stage (when individuals feed and reproduce) (see the Table. 4 in Emmery et al., 2011). The pseudo data consists of typical (primary) parameter values of a "generalized animal", *i.e.* based on a large collection of estimated parameters from various data sets and from a wide variety of species (*e.g.* Kooijman, 2010; Lika et al., 2011a). The main difference between the two sets of parameters estimated previously by Emmery et al. (2011) lies in the integration of several uni-variate data in the covariation method: length over time for larvae stage (from Rico-Villa et al., 2009, 2010; Collet et al., 1999); oxygen consumption rate over length and flesh (dry) weight over time for larvae stage (from Goulletquer et al., 2004); length, flesh (wet) weight, flesh (dry) weight, ingestion rate and clearance rate over time for adult stage (this study); total (wet) weight over time and length over time for (early) adult stage (unpublished data); total (wet) weight over time, length over time and gonad (wet) weight over time for adult stage (from Fabioux et al., 2005). The diversity of the uni-variate data used for the parameter estimation allowed the characterization of the full life cycle of *C. gigas*, *i.e.* from birth to adult stages including the larvae metamorphosis. A module for development acceleration has also been implemented for larvae by including a V1-morphic stage from settlement till metamorphosis.

Detail description of the method is given by Lika et al. (2011a). The routines used for the estimations, *i.e.* the DEBtool package and the 3 files for *C. gigas* species (mydata_Crassostrea_gigas.m, predict_Crassostrea_gigas.m and pars_Crassostrea_gigas.m) are available at `http://www.bio.vu.nl/thb/deb/deblab/debtool/` and `http://www.bio.vu.nl/thb/deb/index.html`, respectively.

To investigate how parameter values can potentially affect both growth and isotopic composition of *C. gigas*, we applied the IsoDEB model to a single data set with two different sets of parameters. The first set of parameter (*i.e.* parameters a) originates from the covariation method procedure Lika et al. (2011a). The second set of parameter (*i.e.* parameters b) originates from Bernard et al. (2011). This latter was converted from energy to mole using volume-based, mole-based and energy based relationship (Kooijman, 2010). Parameters (a) and (b) stand for an oyster after metamorphosis that feeds and reproduces Table 5.1.

Table 5.1: Set of parameters estimated for *Crassostrea gigas* using (*a*) the covariation method from Lika et al. (2011a) and (*b*) from Bernard et al. (2011). X, V, E, E_R and P stand for generalized compounds of food, structure, reserve, reproduction buffer and feces, respectively. The reference temperature for rates is 20°C.

Symbol	Unit	Value (*a*)	Value (*b*)	Interpretation
Core parameters of the DEB model:				
$\{\dot{F}m\}$	$dm^{-3}.d^{-1}.cm^{-2}$	11.97	–	max surf-area-spec. searching rate
$\{\dot{J}_{EAm}\}$	$mol.d^{-1}.cm^{-2}$	1.28×10^{-4}	0.0016	max surf-area-spec. assimilation rate
$[\dot{J}_{EM}]$	$mol.d^{-1}.cm^{-3}$	2.67×10^{-5}	9.27×10^{-5}	vol-spec somatic maintenance rate
M_H^b	mol	9.56×10^{-10}	–	maturity at birth
M_H^p	mol	1.80×10^{-6}	–	maturity at puberty
$\dot{v}$	$cm.d^{-1}$	8.02×10^{-3}	0.183	energy conductance
κ	–	0.29	0.45	fraction of mobilized reserve allocated to soma
κ_R	–	0.95	0.75	reproduction efficiency
$\dot{k}_J$	d^{-1}	1.72×10^{-4}	0.002*	maturity maintenance rate coefficient
y_{EX}	$mol.mol^{-1}$	0.36	0.79	yield of E on X
y_{PX}	$mol.mol^{-1}$	0.24	0.22	yield of P on X
y_{VE}	$mol.mol^{-1}$	0.75	0.80	yield of V on E
$\dot{h}_a$	d^{-2}	2.368×10^{-7}	0.80	Weibull aging acceleration
Compound parameters:				
L_m	cm	8.85	7.76	maximum volumetric structural length
Auxiliary parameters:				
$[M_V]$	$mol.cm^{-3}$	0.0043	0.0066	vol-spec structural mass
δ_M	–	0.1209	0.175	shape coefficient
M_X	$mol.cell^{-1}$	7.61×10^{-13}	1.14×10^{-12}	mass of a cell of *Skeletonema marinoï*
T_A	K	8000	5800	arrhenius temperature
T_L,	K	–	281	lower boundary tolerance range
T_H	K	–	298	upper boundary tolerance range
T_{AL}	K	–	75000	arrhenius temperature for lower boundary
T_{AH}	K	–	30000	arrhenius temperature for upper boundary
Specific parameters of the DIB model:				
κ_L	–	0.8	0.8	fraction of volume-specific maintenance allocated to structure turnover
κ_{Lr}	–	0.4762	0.4762	fraction of structure that is recycled
y_{VE}^L	–	0.63	0.63	yield of V from E in turnover of structure
β_{CX}^{13Aa}, β_{NX}^{15Aa}	–	0.978, 0.997	1.006, 1.006	odds ratio for ^{13}C and ^{15}N in assimilation
$\beta_{CE_R}^{13Ra}$, $\beta_{NE_R}^{15Ra}$	–	1.0002, 1.0008	1.006, 1.006	odds ratio for ^{13}C and ^{15}N in reproduction
β_{CV}^{13Ga}, β_{NV}^{15Ga}	–	1.0002, 1.0008	1.006, 1.006	odds ratio for ^{13}C and ^{15}N in growth
β_{CE}^{13L1a}, β_{NE}^{15L1a}	–	1.02, 1.006	1.004, 1.0015	odds ratio for ^{13}C and ^{15}N in production of renewed structure
β_{CV}^{13L2a}, β_{NV}^{15L2a}	–	1.02, 1.006	1.004, 1.0015	odds ratio for ^{13}C and ^{15}N in degradation of structure
α_{EX}^{CA}, α_{EX}^{NA}	–	0.5115, 0.3580	0.79, 0.553	reshuffling coeff. for C and N from X to E in assimilation
$\alpha_{E_RE}^{ER}$, $\alpha_{E_RE}^{NR}$	–	1, 1	1, 1	reshuffling coeff. for C and N from E to E_R in reproduction
α_{VE}^{CG}, α_{VE}^{NG}	–	0.8059, 0.8655	0.80, 0.8592	reshuffling coeff. for C and N from E to V in growth
α_{VE}^{CL1}, α_{VE}^{NL1}	–	0.63, 0.6766	0.63, 0.6766	reshuffling coeff. for C and N from E to V in structure turnover
α_{VV}^{CL1}, α_{VV}^{NL1}	–	0.4762, 0.4762	0.4762, 0.4762	reshuffling coeff. for C and N from V to V in structure turnover

*: values of a "generalized" animal

5.3 Results

5.3.1 Ingestion rate and dry flesh mass W_d of *Crassostrea gigas*

The ingestion rate of oysters was on average 2.8 times higher in HF than in LF (Fig. 5.1 A). During the first 50 days, J_{XA} was rather stable at the two feeding levels *i.e.* ≈ 0.66 and ≈ 0.22 mol.d^{-1} ind.$^{-1}$ for HF and LF, respectively. Then, J_{XA} exhibited an increase till the end of the experiment, that was concomitant to an increase in W_d for both HF and LF levels (Fig. 5.1 B). Simulations with parameters (b) led to a stronger value of J_{XA} (*i.e.* by a factor M_X) compared to the simulations made with parameters (a).

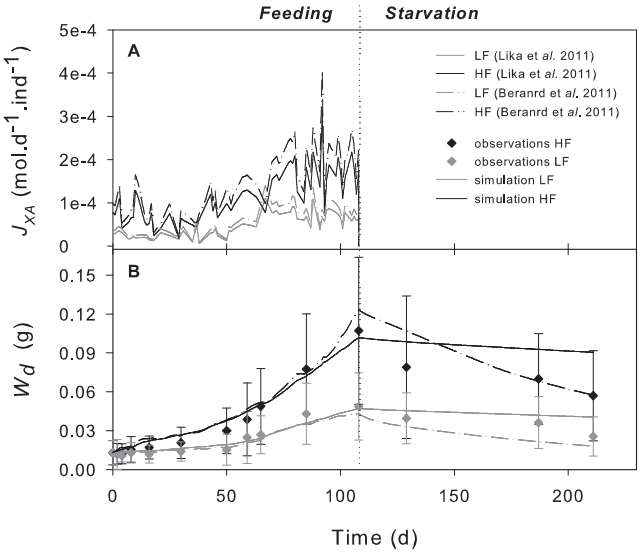

Figure 5.1: Ingestion rate of micro-algae (mol.d^{-1} ind.$^{-1}$, graph A) and temporal variation of the total dry flesh mass W_d (g, graph B) of *Crassostrea gigas* during the diet-switching experiment (212 d). The black and grey plots stand for the high and low feeding levels. The black and grey symbols stand for the observations. The solid lines stand for the model simulations based on parameters estimated with the covariation method; the dashed lines stand for the model simulations based on parameter estimated by Bernard et al. (2011). The vertical bars indicate ± SD of the mean for $n = 60$ (feeding phase) and $n = 21$ (starvation phase).

For both HF and LF levels, W_d increased till the end of the feeding phase (Fig. 5.1). The oysters reared at HF reached a final dry flesh mass (*i.e.* at

t_{108}) of 0.10(±0.05) g and were 2.5 times bigger than oysters at LF. For the two feeding levels, the two sets of parameters used in the IsoDEB model led to a rather good fit between simulations and observations. A low growth phase can be observed during the first 50 days of the feeding phase followed then by a phase of faster mass increase from t_{50} to t_{108}. These two phases were rather well described by parameters (a) and (b). Nevertheless, at t_{108}, the simulations based on parameters (b) slightly overestimated W_d at HF level while the simulations with parameters (a) fitted properly with the observations.

During the starvation phase, none of the two sets of parameters could provide simulations that fitted properly the observations. The simulations based on parameters (a) predicted a small and constant decrease in mass compared to the observations. Although simulations based on parameters (b) were overestimating W_d at HF and underestimating W_d at LF, the overall trends in simulations given by the model were nevertheless more consistent with observations than simulations based on parameters (a).

5.3.2 Effect of the ingestion rate on $\delta^{13}C_{W_d}$ and $\delta^{15}N_{W_d}$

Feeding phase. The model, with parameters (a) and (b), predicted a higher $\delta^{13}C_{W_d}$ and $\delta^{15}N_{W_d}$ for oysters at LF than at HF level over the whole experiment (Fig. 5.2 A and B). The mean difference between $\delta_{W_{d\,HF}}$ and $\delta_{W_{d\,LF}}$ during the feeding phase was, for $\delta^{13}C$, 5.98(±2.16) (parameters a) and 5.16 ± 2.40 (parameters b). For $\delta^{15}N$, it was 1.85 ± 0.63 (parameters a) and 1.30 ± 0.56 (parameters b).

The best fit between simulations and observations was obtained with parameters (b) from t_0 to t_{60} for both $\delta^{13}C_{W_d}$ and $\delta^{15}N_{W_d}$. Over that period, the model closely matched the observations by smoothing the variations in the food source. However, the accuracy of the model predictions decreased from $\approx t_{85}$ for both $\delta^{13}C_{W_d}$ and $\delta^{15}N_{W_d}$, but with different patterns between LF and HF for C and N isotopes. The enrichment of $\delta^{13}C_X$ (between $\approx t_{70}$ and $\approx t_{90}$) was not properly reproduced by the model at LF, leading to a rather strong underestimation of $\delta^{13}C_{W_d}$ compared to the observations till the end of the experiment. A similar phenomenon occurred for $\delta^{15}N_{W_d}$, but with a lower extent at HF, leading to an overestimation of $\delta^{15}N_{W_d}$.

The simulations obtained with parameters (a) led to a stronger smoothing of isotopes trajectories for both $\delta^{13}C_{W_d}$ and $\delta^{15}N_{W_d}$ compared to the simulations based on parameters (b). The effect of rapid fluctuations of δ_X on δ_{W_d} over a rather long period ($\approx 10 - 20$ d) decreased while W_d increased. As for the simulations with parameters (b), the best illustration of this phenomenon occurred at the sampling date t_{85} where $\delta^{13}C_{W_d}$ was strongly overestimated for both LF and HF levels. The best fit between simulations and observations was obtained with parameters (a) for $\delta^{15}N_{W_d}$ at HF.

Starvation phase. During the starvation the model, whatever the two set of parameters, predicted a slight enrichment in heavy isotopes (Fig. 5.2). The difference observed at the end of the feeding part of the experiment between

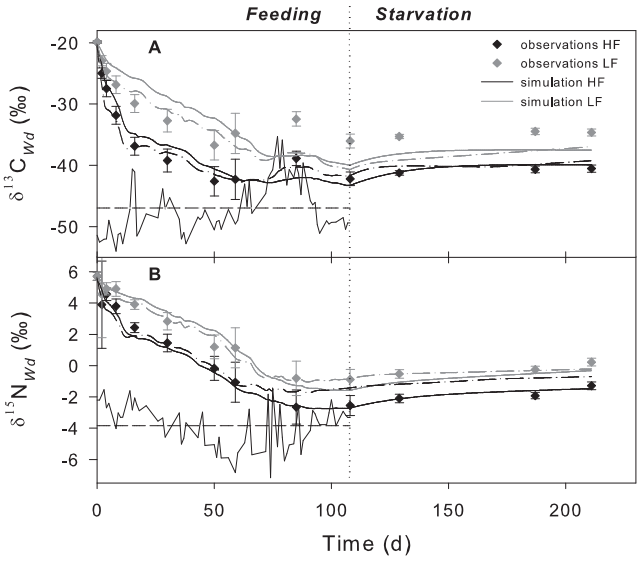

Figure 5.2: Temporal variations of the mean isotopic ratios of *Crassostrea gigas* whole soft body tissues (δ_{W_d}) fed at two different feeding levels (HF, black symbols; LF, grey symbols) during a diet-switching experiment (212 d). Graph (A) and (B) stand for the $\delta^{13}C_{W_d}$ (‰) and $\delta^{15}N_{W_d}$ (‰) respectively. The symbols stand for the observations and the lines stand for the model simulations obtained with two different sets of parameter: parameters estimated with the covariation method (solid lines) and parameters estimated by Bernard et al. (2011) (dashed lines). The vertical bars indicate $\pm$SD of the mean for $n = 21$ individuals.

$\delta^{13}C_{W_d}$ and $\delta^{15}N_{W_d}$ remained unchanged till t_{212} for both simulations performed with parameters (a) and (b). For simulations performed with parameters (b), $\delta^{13}C_{W_d}$ at LF was underestimated while $\delta^{15}N_{W_d}$ at HF was overestimated. The model run with parameters (b) also predicted a slight change in the isotopes trajectories just before t_{188}, while simulations based on parameters (a) showed a slight and (almost) constant enrichment throughout the starvation period (Fig. 5.2).

5.4 Discussion

Effect of the feeding level on δ_{W_d} of oysters

Our results show that the amount of food assimilated by oysters had a strong effect on growth and dynamics of stable isotopes in oyster tissues, throughout the experiment. The higher the feeding level, the higher the increase of W_d, and the lower the values of $\delta^{13}C_{W_d}$ and $\delta^{15}N_{W_d}$ (Fig. 5.1 and 5.2). This pattern was well predicted by the IsoDEB model with the two different sets of parameters and in agreement with Emmery et al. (2011).

The fate of compounds (and isotopes) through anabolic or catabolic route during metabolic transformation (assimilation, growth and dissipation) played a key role to understand the effect of the ingestion rate on the dynamics of $\delta^{13}C_{W_d}$ and $\delta^{15}N_{W_d}$ (Emmery et al., 2011). The different compounds have different probabilities to be selected for anabolic or catabolic route according to their isotopic composition. The compounds containing light isotopes have weaker binging and could be more easily broken down and selected for catabolic purpose (*e.g.* Fry, 2006). According to the DEB theory, the selection of compounds through anabolism or catabolism is at random. This implies that the frequency distribution of heavy isotopes follows a Fisher non central hypergeometric distribution, and compounds containing heavy isotopes have a deviating probabilities, *i.e.* odds ratio β, to be selected for a particular route. Odds ratios > 1 (as calibrated in this study, Table 5.1) imply that compounds containing light isotopes have a lower probability to be selected for anabolic purpose than compounds containing heavier isotopes (Pecquerie et al., 2010; Kooijman, 2010). In our experiment, oysters ingested the same food source (*i.e.* from an isotopic point of view), but in different quantities. The set of parameters being the same between the two feeding conditions, the probability of light compounds to be selected for anabolic purpose was therefore higher at LF than at HF, leading to "lighter" organism as predicted by the model (Fig. 5.2).

During the starvation period, the whole soft body tissues of oysters, as well as the model predictions, followed the trends frequently observed in the literature in terms of δ values (*e.g.* Boag et al., 2006; Doi et al., 2007; Frazer et al., 1997), with an enrichment in heavy isotopes for $\delta^{13}C_{W_d}$ and $\delta^{15}N_{W_d}$. During starvation animals stop feeding ($J_{XA} = 0$). Thus, $\delta^{13}C_{W_d}$ and $\delta^{15}N_{W_d}$ predicted by the model (with parameters (a) and (b)) only depended on the

discrimination of isotopes during growth and dissipation reactions. The model simulations performed with parameters (*b*) exhibited (slight) different rates of enrichment, *i.e.* a switch during starvation phase. This may result from *i)* the amount of reserve and reproduction buffer available (at start of starvation) to fuel metabolic reactions and *ii)* the effect of the structure turnover of the organism. During the whole experiment, the reserve was lighter in δ^{13}C and δ^{15}N than the reproduction buffer, that is lighter than the structure throughout the experiment. It resulted in the observed enrichment of the whole soft body tissues (from $\approx t_{108}$ to $\approx t_{170}$) once reserve was depleted (Fig. 5.2, HF). The switch that next occurred (*i.e.* at t_{170}) resulted from the depletion of both the reserve and the reproduction buffer. Somatic maintenance was paid from the structure only (also called shrinking). The structure turnover did not lead to any net production of structure ($J_{VrL} = \kappa_{L2a} \times J_{VL2} = -\kappa_{L2a} \times J_{VL1}$), but influenced the isotopic composition since both J_{VrL} and J_{VL1} have different isotopic composition. As the structure turnover discriminates against light isotopes ($\beta_{iE}^{0L1a} > 1$ and $\beta_{iV}^{0L2a} > 1$), the whole soft body tissues become enriched in heavy isotopes. In the LF level, the switch between the maintenance costs paid from reserve and the maintenance costs paid from structure, occurred earlier than in the HF level (*i.e.* $\approx t_{120}$), since oysters did not allocate matter to the reproduction buffer. Although our formulation exhibited realistic and expected trends, more complex rules during starvation may occur, such as extra cost-conversion efficiency of structure to energy and rejuvenation processes (Augustine et al., 2011b; Sousa et al., 2010).

5.4.1 Allocation to reproduction influenced δ_{W_d}

The amount of matter allocated to the maturity and reproduction influenced the dynamics of $\delta^{13}C_{W_d}$ and $\delta^{15}N_{W_d}$. One of the main differences between parameters (*a*) and (*b*) lies in the κ values. The (rather) low κ value estimated with the covariation method (*i.e.* $\kappa = 0.24$, Table 5.1) led to a strong and early increase of M_{E_R} compared to the κ value used by Bernard et al. (2011). One major effect of M_{E_R} on $\delta^{13}C_{W_d}$ and $\delta^{15}N_{W_d}$ was the smoothing of isotopes trajectories throughout the experiment. The general underestimations of the models simulations from *ca.* t_{70} till *ca.* t_{212} for $\delta^{13}C_{W_{dLF}}$, $\delta^{13}C_{W_{dHF}}$ and the $\delta^{15}N_{W_{dLF}}$ (Fig. 5.2 A and B) might be due to the "light" isotopic composition of compounds in E_R compared to the isotopic composition of the structure. Although stable isotopes have been previously used to trace nutrient allocation to reproduction in birds (Hobson et al., 2000, 2004, 2005) and bivalves (Malet et al., 2007; Paulet et al., 2006), the patterns predicted by the model remain difficult to compare to the literature results. Indeed the reproduction buffer is part of energetic reserve that was not converted into eggs (no overheads) and had the same biochemical composition than E. Moreover, the discrimination of isotopes depended only on the flux J_{E_R} since, as a first approximation, we assumed that parameters y_{EE_R}, $\alpha_{E_RE}^{iR}$ and κ_{Ra} were equal to 1. As stated by Bernard et al. (2011), the dissociation of reproduction buffer compartment from

the gonad compartment with different biochemical composition each, as well as the consideration of a gonad maintenance flux could be helpful to improve model predictions in terms of both mass and isotopes trajectories.

5.4.2 Relationships between δ_X, δ_{W_d} and Δ_{W_d}: what is going on?

The model successfully predicted different $\delta^{13}C_{W_d}$ and $\delta^{15}N_{W_d}$ at the two feeding levels and for the two different sets of parameters. However, the model underestimated the observed values of $\delta^{13}C_{W_d}$ from $\approx t_{70}$ at LF while simultaneously $\delta^{13}C_X$ was increasing of $\approx 12.5\,‰$ compared to the mean value ($\delta^{13}C_{X_{mean}} = -46.93(\pm 4.39)\,‰$, Fig. 5.2 A). Recent studies on the rate *Rattus rattus* (Caut et al., 2008b), on the guppie *Poecilia reticulata* Dennis et al. (2010) as well as a review on *ca.* 86 species (Caut et al., 2009) showed that the trophic fractionation *i.e.* $\Delta_{W_d} = \delta_{W_d} - \delta_X$ (Martínez del Rio et al., 2009) seems to be affected by the isotopic ratio of the food source with the following pattern: the lower δ_X, the higher Δ_{W_d} for both C and N stable isotopes. Under constant conditions of food and isotopic ratios of food source, our model predicts the same trends as the ones observed by the authors above cited but in lower extent for $\delta^{13}C_{W_d}$ and $\delta^{15}N_{W_d}$. An explanation of this pattern could be that, for oysters feeding a "lighter" food source, the probability of a "light compounds" to be selected for anabolic purpose during assimilation, growth and dissipation is higher than for oysters consuming an "heavier" food source. The same phenomenon was simultaneously observed for $\delta^{15}N_{W_d}$ with, contrary to the $\delta^{13}C_{W_d}$ case, an overestimation of the IsoDEB model at HF (Fig. 5.2 B). This duality of the model simulations between $\delta^{13}C_{W_d}$ and $\delta^{15}N_{W_d}$ and between the two feeding levels could potentially originate from the biochemical composition of reserve, structure and reproduction buffer. The number of atoms of H, O, and N relative to that of C (n_{ij}) were different between X, E and E_R and V. As the reshuffling parameters depend on n_{ij} parameters during assimilation, growth and dissipation, the differences between n_{iE}, n_{iE_R} and n_{iV} were possibly not enough contrasted to allow sufficient variations of the biochemical composition of the whole soft body tissues and thus of the δ_{W_d} consecutive to the δ_X variations.

To conclude, our study showed that the ingestion rate had a strong effect on the growth and the dynamics of stable isotopes in *C. gigas* tissues. The higher the feeding rate, the higher the growth and the lower the values of $\delta^{13}C_{W_d}$ and $\delta^{15}N_{W_d}$ of oysters. The IsoDEB model satisfactory described growth of oysters under the two different feeding levels as well as the stable isotope trajectories consecutive to the diet switch. However, the model simulations for $\delta^{13}C_{W_d}$ were less accurate during strong variations in $\delta^{13}C_X$ (enrichment), suggesting a possible inaccurate characterization of the biochemical composition of *C. gigas*. The differences between the two sets of parameters tested led to (very) different

pattern from a mass and isotopes point view. Although the set of parameters by Bernard et al. (2011) led to a more accurate description of the oyster mass and isotopic composition, the parameter estimations (based on the covariation method) led to a full characterization of the life cycle of *C. gigas* from birth to adult stage. The reserve allocation to maturity and reproduction remains however inconsistent with the knowledge on the biology of this species and further developments are required to improve the parameter estimation for *C. gigas*.

Chapter 6

General conclusion

The quantification of stable isotopic ratios in organic matter confers to stable isotope analysis (SIA) the role of tracing origin and fate of energy at different levels of biological organisation (molecule, individuals, populations, ecosystems). However, applications of SIA still suffer from a lack of appropriate (bioenergetic) models that consider both the physiological plasticity and the fluctuations of environment. The simplicity of existing models frequently limits the interpretation of stable isotope patterns in living organisms. This limitation is particularly true for the interpretation of the variations in trophic fraction value Δ_{W_d}, *i.e.* the difference between the isotopic ratios of the consumer and the source. As long ago observed, all living organisms basically handle, ingest and assimilate food (substrates) to meet their physiological needs *i.e.* growth and reproduction. In marine ecosystems, sessile organisms, *i.e.* living fixed at the interface between benthic and pelagic compartments, are fully dependent on both trophic and abiotic environment fluctuations. Sensitive to both the quantity and the quality of the trophic resource, suspension feeders like *Crassostrea gigas* generally have a broad trophic niche and thus integrate all changes like a recorder of the ecosystem state.

The general objective of this thesis was thus to understand the influence of the trophic resources (*i.e.* quantity and diversity of food) on the dynamics of stable isotopes δ^{13}C and δ^{15}N in the soft tissues of the Pacific oyster *Crassostrea gigas*. I combined both experimental (under natural and controlled conditions) and DEB modeling approaches to decipher the role of oyster metabolism relatively to stable isotopes discrimination. Based on this simple and generic observation, the amount and the diversity of trophic resources consumed by oysters has been quantified (see chapters 3 and 5) and shown (see chapters 2 and 4) throughout this work, as one of the major factor influencing both the growth and the dynamics of stable isotopes of oyster tissues.

6.1 From *in situ* observations to modeling investigations

The Bays of Veys (BDV, Normandy, France) and the Bay of Brest (BH, Britany, France) exhibit contrasted trophic environments in terms of food availability and diversity (chapter 2, *in situ* monitoring). In BDV, the chlorophyll-*a* concentration ([Chl-*a*]) was 3 times higher than in BH on average over the year. This difference likely account for the higher growth and CN ratios observed in BDV compared to BH for both, whole soft body tissues (W_d) and organs (gills, G_i, muscle adductor M_u and remaining tissues R_e). BDV is also characterized by the presence of phytoplankton (PHY) and microphytobenthos (MPB) while in BH the trophic resource is mainly dominated by the presence of PHY. Isotopic ratios in oyster whole soft body tissues (δ_{W_d}) exhibited opposite patterns between the two site with, on average, a higher $\delta^{13}C_{W_d}$ in BH compared to BDV and a lower $\delta^{15}N_{W_d}$ in BH compared to BDV. The $\delta^{13}C_{Gi}$, $\delta^{13}C_{Mu}$ and $\delta^{13}C_{Re}$ exhibited similar temporal variations, and in the same order of magnitude, in the two ecosystems. They also exhibited clear differences in their isotopic enrichment levels with $\delta_{Mu} > \delta_{Gi} > \delta_{Re}$ regardless of the studied area and season. I concluded that phenotypic plasticity in the physiology of the oyster is important to understand the different isotope patterns in the bays of Veys and Brest. However, there is also a role for spatial and temporal variations in food sources (in terms of availability and isotopic ratios). Variations in trophic resources doubtlessly cause variations in trophic fractionation Δ (‰). To test and understand the effect of the amount of food consumed by organisms on the dynamics of C and N stable isotopes, I concluded on the necessity to couple different approaches, *i.e.* experiment and modeling to simplify the complexity of natural environment.

The challenge was thus to select appropriate tool(s) and approach(es) to take into account both the temporal variations of trophic resources (*i.e.* amount and diversity of food) and oyster metabolism, to understand their respective contribution to a given isotopic trajectory. The DEB model for the physiology and the DIB model for isotope dynamics were combined in the IsoDEB model, which became an important research tool. Based on physical and chemical rules, the DEB model quantifies the state of the individual under varying food and temperature regimes (Kooijman, 2010; Sousa et al., 2006). It delineates catabolic and anabolic aspects of assimilation, maintenance and growth. It makes explicit use of balances of the chemical elements C, H, O and N. The DIB model further exploits the DEB concepts of strong homeostasis (generalised compounds) and macrochemical reaction equations to follow isotopes that are subjected to mixing (always) and fractionation (sometimes). It allows for routing , where particular atoms in substrate molecules (partially) map on particular atoms in product molecules (*i.e.* atom reshuffling). The separation of anabolic and catabolic pathways is key to fractionation.

Our theoretical study (chapter 3) demonstrated that the relative feeding

level impacted both the dynamics of stable isotopes and trophic fractionation value. The higher the feeding level, the lower the Δ value; an increase by a factor 5 of the feeding level leads to a decrease of $\approx 1\,‰$ and $\approx 2.4\,‰$ for the $\Delta^{13}C_{W_d}$ and $\Delta^{15}N_{W_d}$ respectively. The organism mass partly compensates this effect. An increase by a factor 24 of the initial W_d (*i.e.* at the beginning of the simulation) leads to an increase in Δ of hardly $0.52\,‰$ for carbon and $0.79\,‰$ for the nitrogen. This weak influence of organism's mass on δ_{W_d} can not fully explain the trophic enrichment generally observed in field. The results of the chapter 3 also revealed that energetic reserve of oyster play a key role to smooth down the variations of the diet isotopic ratios (δ_X). The bigger the organism, the stronger the attenuation of the δ_X variations. Additionally to the fact that the IsoDEB model allows to investigate the effect of metabolism on stable isotope dynamics (Pecquerie et al., 2010), the isotope discrimination mechanisms developed by Kooijman (2010) provide the powerful advantage that the simulated $\delta^{13}C_{W_d}$ and $\delta^{15}N_{W_d}$ are, for each time step of the individual life cycle, already "corrected" from the trophic fractionation value (*i.e.* the later being "implicit") according to both environment variations and metabolism effects. However, although our theoretical study (chapter 3) confirmed our interpretation of *in situ* observations and some of literature results (both experimental and theoretical), an experimental approach was nevertheless required to validate the model (chapter 4).

6.2 A simple trophic relationship: experimental and model validations

During the experiment, the oysters spat was fed at two different feeding levels (high food, HF; low food, LF) with a monospecific culture of *Skeletonema marinoï* depleted in ^{13}C and ^{15}N (chapter 4). Our experimental results confirmed the simulated trends given by the model. At the end of the feeding phase, significant differences between HF and LF conditions were observed for the growth and C/N ratios of the whole soft body tissues on the one hand, and organs *i.e.* gills, adductor muscle and remaining tissues, on the other hand. Both growth and C/N ratios were higher at HF compared to LF level. Conversely, the oysters spat reared at HF level exhibited significantly lower $\delta^{13}C_{W_d}$ and $\delta^{15}N_{W_d}$ compared to those reared at LF throughout the experiment duration. These differences were nevertheless more important compared to the trends simulated by the model (chapter 3) for the $\delta^{13}C_{W_d}$, with a final difference of $\approx 6\,‰$ between $\delta^{13}C_{W_dHF}$ and $\delta^{13}C_{W_dLF}$. During the starvation phase, all the different organs of oysters were significantly enriched in heavy isotopes compared to the end of the feeding phase. Another important result of our experiment lies in the rather strong temporal variations of the diet isotopic ratios for both carbon and nitrogen stable isotopes and their consequences for trophic shift estimations. The empirical model of Olive et al. (2003) highlighted that δ and Δ values depended on both the temporal variations of the feeding

level and the diet isotopic ratios. The use of a constant Δ value seems thus to be wrong for diet reconstruction purpose. As observed during the *in situ* monitoring (chapter 2), the rather constant differences between δ_{HF} and δ_{LF} among organs, as well as their relative enrichment rate (*i.e.* $\delta_{Mu} > \delta_{Gi} > \delta_{Re}$) over the whole experiment (feeding and starvation phases) suggest that reserve and organ structure, and their respective biochemical composition, should be considered to fully understand isotopic fractionation phenomenon (*i.e.* discrimination factor) among organs.

The effect of the ingestion rate on the growth and the dynamics of stable isotopes in oyster tissues was successfully described by the IsoDEB model, *i.e.* with the higher the ingestion rate, the higher the growth and the lower the $\delta^{13}\mathrm{C}_{W_d}$ and $\delta^{15}\mathrm{N}_{W_d}$. The model properties allowed to show that the anabolic and catabolic components of metabolic reactions (*i.e.* mass fluxes) and the dynamic of reserves relative to the dynamic of structure, played a major role for the dynamic of stable isotopes in oyster tissues. The mechanisms of fractionation and reshuffling allowed an accurate description of isotope mixing among organism compartments, *i.e.* energetic reserve, structure and reproduction buffer. The different metabolic reactions do not affect isotope ratios in the whole body in the same way. This is well-recognized by the mechanisms that are implemented in the model. However, model simulations were less accurate during strong variations in the isotopic ratios of the diet for both $\delta^{13}\mathrm{C}_{W_d}$ and $\delta^{15}\mathrm{N}_{W_d}$. This deviation might link to an inaccurate estimation of the elemental composition of reserve and structure. It might also be that fast changes can only be captured accurately with much more complex models. At the end of the feeding phase, the strong difference in the average isotopic ratios between the diet and the oyster soft tissues was not correctly simulated by the model, letting the question of the effect of the diet isotopic ratio on the trophic fractionation value open.

6.3 Perspectives

6.3.1 Modeling tools for diet reconstruction studies: new insights

Our results show that the coupling of DEB and DIB modeling with mixing models (*e.g.* Isosource, SIAR) constitutes an innovative and relevant method to characterize trophic environments of *C. gigas* within the context of diet reconstruction studies. To our knowledge, only the studies by Van Haren and Kooijman (1993), Cardoso et al. (2006b), Freitas et al. (2011) used the DEB framework to reconstruct feeding conditions experienced by different bivalve species. However, not all of these studies consider the diversity of the different food sources that compose their diet. Indeed, different steps are required to assess the contribution of the different food sources to the diet and growth of *C. gigas*. Based on individual growth (*e.g.* shell length, mass) and tempera-

ture monitoring, the first step would be to back calculate the scaled functional response f that links food availability (*i.e.* trophic resources) and the energy assimilated to the reserve. At a first approximation, the potential food sources can be simplified as an homogeneous bulk (*i.e.* a mixture) of food items that remain constant (in terms of quantity and quality) between two sampling dates. This allows the back calculation of an average f value between two growth observations (Cardoso et al., 2006b). Following the assumption that food is composed of a mixture of different food items which proportions can vary over time, the second step would be then to back calculate the $\delta^{13}C_X$ and $\delta^{15}N_X$ of this mixture using the DIB framework. The difference between mixture and tissues isotopic ratios implicitly represents the trophic fractionation values between consumer and food. Finally, contributions of food items (in %) to the mixture assimilated by *C. gigas* can be estimated thanks to the isotopic ratios of the food sources measurments and mixing model (*i.e.* IsoSource, SIAR). By assuming that assimilation efficiencies are known, this method would allow to link temporal variations of the trophic resources (*i.e.* quatity and diversity) to temporal variations of growth observations.

As pointed out by Marín Leal et al. (2008), the application and generalization of this method would bring different relevant insights for stable isotopes analyses and applications (SIA). First, the back calculation of feeding conditions with the IsoDEB model shows that oysters are not in "isotopic equilibrium" with their food source(s). Indeed, the DEB model considers the temporal variations in both the mixture assimilation rate and the diet isotopic ratios. The consideration of these variations implies that the time scale over which the mixture is assimilated and used consecutively to a natural diet switch varies over time. Second, the DIB module allows to remedy the problems raised by the use of constant trophic fractionation values since it is dynamically calculated by the model according to environment variations, metabolism and physiological state of consumer (Emmery et al., 2011; Pecquerie et al., 2010). For the diet reconstruction studies, this imply that the (temporal and spatial) variations in the contributions of the different food sources can be linked to the variations of the trophic fractionation over time, and thus indirectly to the plasticity of oyster's physiology. Extending this method by considering variations of both the growth and the isotopic ratios of different organs (with different turnover rates) would also bring valuable information on the time scale over which a given food source is assimilated and contributes to the growth of a given organ (Guelinckx et al., 2007, 2008). Application of this type of approach at large spatial scale in shellfish culture areas (*i.e.* Normandy, Brittany, Thau lagoon, *etc.*) would allow an accurate temporal characterization of trophic environment variations and their consequences for the physiological performances of *C. gigas* and, in general, for bivalves. Static and dynamic generalisations of DEB's kappa-rule can be used to quantify the growth of body parts, such as organs (Kooijman, 2010). One has to be prepared, however, that this extension involves a considerable increase in numbers of parameters that have to estimated from data.

6.3.2 Trophic functioning of benthic communities

Describe the trophic environment of *C. gigas* may also imply to describe the trophic relationships between oysters, co-occurring suspension feeders and other benthic species (Dubois et al., 2007b; Levesque et al., 2003). Hard substrates on which oysters live (*i.e.* rocks, reefs, oysters shells, rearing tables, *etc.*) and their surrounding areas, constitute ideal natural and/or artificial habitats for a lot of benthic invertebrates belonging to the same suspension-feeding guild. These benthic invertebrates (*e.g.* scallop *Pecten maximus*, mussels *Mytilus edulis*, polychaete *Pomatoceros lamarcki*, barnacle *Elminius modestus*, ascidian *Asciidiella aspersa*, *etc.*) are frequently considered as potential trophic competitors of natural and cultivated oysters (Riera et al., 2002; Lesser et al., 1992). Based on the assumption that organisms feeding on the same food source(s) would have similar isotopic ratios, the use of SIA to assess this type of trophic relationships still remains one of the most relevant and easiest approaches. According to the results presented in this thesis, suspension feeders consuming the same food source(s) can however exhibit dissimilar isotopic ratios due to effects of metabolism, amount of food consumed, large trophic plasticity, food particle selection.

Many bivalve species have been studied under natural conditions (*e.g.* mussels (Dubois et al., 2007a), scallops (Lorrain et al., 2002; Paulet et al., 2006), clams (Flye-Sainte-Marie et al., 2007, 2009), cockles (Troost et al., 2010; Wijsman and Smaal, 2011)). Nevertheless, too few species-specific experiments (under controlled conditions) are available for this class of organisms that investigate how metabolism and trophic resources influence both physiological performances and stable isotope discrimination processes. Prior theoretical investigations and parametrization with the IsoDEB model help to design experiments and sampling protocols. According to DEB theory, differences in physiological plasticity of species originate from differences in parameter values (Kooijman, 2010; Lika et al., 2011a). Species that differ in life traits (*e.g.* age, length, weight at birth and at puberty, maximum length and reproduction rate), so in their physical and biochemical parameters, typically exhibit different physiological responses to environmental fluctuations. They are expected to have different patterns in their stable isotope dynamics. Extending theoretical investigations based on DEB theory to other classes (and phyla) and trophic networks, *e.g.* herbivorous and carnivorous, autotrophs and heterotrophs, marine and terrestrial, benthic and pelagic, would allow to characterize the isotopic commonalities between living organisms.

6.3.3 Characterization of organisms life cycles

Interspecific comparison of stable isotope dynamics within the context of DEB theory requires knowledge of the set of parameters. To this end, the covariation method (Lika et al., 2011a,b) has been developed to estimate all parameter from sets of ecophysiological data. Basically, the full life cycle of a species is

considered, *i.e.* embryo, juvenile and adult stages, being consistent with the concepts and rules of the DEB theory. The life traits of species, but also a large diversity of zero- and uni-variate data set can be included (*i.e.* growth, respiration, reproduction, ingestion, *etc.*) to accurately capture physiological characteristics of species (*e.g.* Saraiva et al., 2011a). Another important aspect of this method lies, as for SIA, in its generic formulation, allowing interspecific comparison on the basis of standardized parameters. So far, *ca.* 168 species, representatives of most large phyla, are included in the "Add-my-pet" data base [1]. Although the method was developed recently, six studies used this method to estimate parameters for the mussel *Mytilus edulis* (Saraiva et al., 2011a), the fish *Danio rerio* (Augustine et al., 2011a), the Lizard *Sceloporus undulatus* (Kearney, 2012), the frogs *Crinia nimbus*, *Crinia georgiana*, *Geocrinia vitellina* and *Pseudophryne bibronii* (Mueller et al., 2012), the tuna *Thunnus orientalis* (Jusup et al., 2011) and the chinook salmon *Oncorhynchus tshawytscha* (Pecquerie et al., 2011).

We also applied the covariation method of estimating parameters to *C. gigas*. To this end we not only used data on larval growth and respiration, but also juvenile and adult ingestion, wet weight, dry weight, length growth, gonadal production, nitrogen waste and pseudo-faeces production, feeding and growth data from our experiments and life history data such as size at birth and puberty and ultimate size. The covariation method also allows to perform sensitivity analyses and comparisons on the (published) parameter values, to unify the numerous and diverse biological knowledge and information we already have for this species. The large flexibility of the method, in terms of the diversity of both data that can be included in routines and processes that can be modeled, could be also extended to consider the dynamics of both C/N ratios and stables isotopes.

6.3.4 Theoretical investigation of stable isotopic patterns using DEB theory

The consideration of dynamic isotope budget within the context of DEB theory still remains, to my point of view, a new and innovating tool based on mechanisms for isotope discrimination by living organisms. The different tools developed in the context of the DEB theory (*e.g.* DIB extension, software package DEB tool, covariation method, DEB book and courses), can be used to design experimental protocols for factors influencing stable isotopes dynamics. They should be considered with increasing interest for future research requiring the use of SIA as an ecological tool. To our knowledge, only the studies by Pecquerie et al. (2010) and Emmery et al. (2011) used this type of model to assess stable isotope patterns, the later being the first application on experimental observations. Numerous applications and factors, known to influence stable isotope patterns, still remain to investigate and explore within the

[1] http://www.bio.vu.nl/thb/deb/deblab/add_my_pet/index.php

context of DEB theory. For instance, starvation formulation can be improved according to the developments by Augustine et al. (2011a). The description of the reproduction processes (*i.e.* gamete production, atresia phenomenon and spawning events) by Bernard et al. (2011) where the reproduction buffer is dissociated from the gonadal compartment could be an interesting way to accurately describe and investigate the effect of gamete production and release by oysters on the isotopic ratios of the individual (Hobson et al., 2004, 2005). As developed by Kooijman (2006), the quantification of pseudofeces and then feces production by oysters could be helpful *i)* to refine the stable isotopes discrimination during ingestion and assimilation fluxes and *ii)* to check the assumption that feces is enriched in heavy isotopes compared to assimilated material (*e.g.* Steele and Daniel, 1978; Altabet and Small, 1990).

In this work, only the modeling of growth and stable isotope ratios in the whole soft body tissues have been considered (chapter 5). As previously discussed, formalizing the dynamics of growth and stable isotopes of organs within the context of DEB theory would bring valuable information on the past and recent assimilated diet, allowing finest estimations of the contribution of potential food source(s) to the diet of an organism (*e.g.* Kurle and Worthy, 2002; Lorrain et al., 2002). Additionally, modeling the growth and stable isotopes dynamics in different organs may also provide a powerful tool (from a technical point of view) to investigate the preferential allocation of nutrients to a given organ(s) (*e.g.* Kelly and del Rio, 2010; McMahon et al., 2010). These type of investigation can also be used to explore the concept of atom reshuffling (Kooijman, 2010). This concept quantifies the fraction of an atom, in given substrate (compound) that ends up in a given product. Since substrate molecules are not necessarily fully disassembled into their elemental components to form products, partial reshuffling quantifies to what extend atoms in substrates travel together in the transformation at the molecular level to products (Kooijman, 2010; Pecquerie et al., 2010).

Modeling the dynamics of the C/N ratios in consumers according to the C/N ratios of the food would also be an important scientific progress. The C/N ratio can be considered as a proxy of energetic reserves of an organism since it generally represents the amount of lipids and carbohydrates over the amount of proteins. Although it is well known that lipids are depleted in ^{13}C (Post, 2002) and they constitute a common form of energetic reserves among animals, energetic reserves of oysters for reproduction are mainly formed by carbohydrates (Berthelin et al., 2000). On the assumption that the mass of oysters is mainly composed by the mass of lipids, proteins and carbohydrates, investigating the temporal variations of these biochemical components within the context of DEB theory would be a relevant way to estimate their contribution to a given isotope trajectory, refine reproduction formulation in the case of oysters, *etc.* The theory for the dynamics of these compounds is ready for use, we "only" need systematic experimental testing.

The dynamics of $\delta^{13}C$ and $\delta^{15}N$ within the context of DEB theory constitute a key tool to validate some assumptions of the theory itself. In DEB

theory, energetic reserve acts as a buffer and smooths down the variations of the environment. It constitutes the first compartment wherein matter (and isotopes) enters the organism, and it is used to fuels the growth, the reproduction and the maintenance of the organisms. The dynamic of reserve is faster than the one of structure which implies that the isotopic composition of the whole body mainly resembles the one of the energetic reserve for a given diet isotopic ratio. Compare the values of the residence times of δ_{W_d} (*i.e.* $t_{\delta_{W_d}}$) calculated thanks to empirical model (*e.g.* Dubois et al., 2007a), with the $t_{\delta_{W_d}}$ of energetic reserve calculated from DEB formulation would allow to check the consistency of the strong assumption that energetic reserve can be considered as a well mixed pool.

Bibliography

Adams, T., Sterner, R., 2000. The effect of dietary nitrogen content on trophic level ^{15}N enrichment. Limnol. Oceanogr. 45, 601–607.

Altabet, M., Small, L., 1990. Nitrogen isotopic ratios in fecal pellets produced by marine zooplankton. Geochim. Cosmochim. Acta 54, 155–163.

Alunno-Bruscia, M., Bourlès, Y., Maurer, D., Robert, S., Mazurié, J., Gangnery, A., Goulletquer, P., Pouvreau, S., 2011. A single bio-energetics growth and reproduction model for the oyster *Crassostrea gigas* in six atlantic ecosystems. J. Sea Res. 66, 340–348.

Augustine, S., Gagnaire, B., Floriani, M., Adam-Guillermin, C., Kooijman, S., 2011a. Developmental energetics of zebrafish, *Danio rerio*. Comp. Biochem. Physiol., Part A: Mol. Integr. Physiol. 159, 275–283.

Augustine, S., Litvak, M., Kooijman, S., 2011b. Stochastic feeding of fish larvae and their metabolic handling of starvation. J. Sea Res. 66, 411–418.

Bacher, C., Gangnery, A., 2006. Use of dynamic energy budget and individual based models to simulate the dynamics of cultivated oyster populations. J. Sea Res. 56, 140–155.

Badalamenti, F., D'Anna, G., Pinnegar, J., Polunin, N., 2002. Size-related trophodynamic changes in three target fish species recovering from intensive trawling. Mar. Biol. 141, 561–570.

Barillé, L., Lerouxel, A., Dutertre, M., Haure, J., Barillé, A., Pouvreau, S., Alunno-Bruscia, M., 2011. Growth of the pacific oyster (*Crassostrea gigas*) in a high-turbidity environment: Comparison of model simulations based on scope for growth and dynamic energy budgets. J. Sea Res. 66, 392 – 402. <ce:title>The AquaDEB project (phase II): what we've learned from applying the Dynamic Energy Budget theory on aquatic organisms</ce:title>.

Barnes, C., Sweeting, C., Jennings, S., Barry, J., Polunin, N., 2007. Effect of temperature and ration size on carbon and nitrogen stable isotope trophic fractionation. Funct. Ecol. 21, 356–362.

Bayne, B., 2004. Phenotypic flexibility and physiological tradeoffs in the feeding and growth of marine bivalve molluscs. Integr. Comp. Biol. 44, 425–432.

Ben-David, M., Flynn, R., Schell, D., 1997. Annual and seasonal changes in diets of martens: evidence from stable isotope analysis. Oecologia 111, 280–291.

Bernard, I., de Kermoysan, G., Pouvreau, S., 2011. Effect of phytoplankton and temperature on the reproduction of the pacific oyster *Crassostrea gigas*: Investigation through DEB theory. J. Sea Res. 66, 349–360.

Berthelin, C., Kellner, K., Mathieu, M., 2000. Storage metabolism in the Pacific oyster (*Crassostrea gigas*) in relation to summer mortalities and reproductive cycle (West Coast of France). Comp. Biochem. Physiol., Part B: Biochem. Mol. Biol. 125, 359–369.

Boag, B., Neilson, R., Scrimgeour, C., 2006. The effect of starvation on the planarian *Arthurdendyus triangulatus* (Tricladida: Terricola) as measured by stable isotopes. Biol. Fert. Soils 43, 267–270.

Bodin, N., Le Loc'h, F., Hily, C., 2007. Effect of lipid removal on carbon and nitrogen stable isotope ratios in crustacean tissues. J. Exp. Mar. Biol. Ecol. 341, 168–175.

Bodineau, L., Thoumelin, G., Béghin, V., Wartel, M., 1998. Tidal time-scale changes in the composition of particulate organic matter within the estuarine turbidity maximum zone in the macrotidal Seine estuary, France: the use of fatty acid and sterol biomarkers. Estuar. Coast. Shelf. Sci. 47, 37–49.

Boecklen, W.J., Yarnes, C.T., Cook, B.A., James, A.C., 2011. On the use of stable isotopes in trophic ecology. Annu. Rev. Ecol. Evol. Syst. 42, 411–440.

Bourlès, Y., Alunno-Bruscia, M., Pouvreau, S., Tollu, G., Leguay, D., Arnaud, C., Goulletquer, P., Kooijman, S., 2009. Modelling growth and reproduction of the Pacific oyster *Crassostrea gigas*: Advances in the oyster-DEB model through application to a coastal pond. J. Sea Res. 62, 62–71.

Brown, M., 2002. Nutritional value and use of microalgae in aquaculture. Avances en Nutrición Acuícola VI. Memorias del VI Simposium Internacional de Nutrición Acuícola 3, 281–292.

Buestel, D., Ropert, M., Prou, J., Goulletquer, P., 2009. History, Status, and Future of Oyster Culture in France. J. Shellfish. Res. 28, 813–820.

Canuel, E., Cloern, J., Ringelberg, D., Guckert, J., Rau, G., 1995. Molecular and isotopic tracers used to examine sources of organic matter and its incorporation into the food webs of San Francisco Bay. Limnol. Oceanogr. 40, 67–81.

Carassou, L., Kulbicki, M., Nicola, T., Polunin, N., 2008. Assessment of fish trophic status and relationships by stable isotope data in the coral reef lagoon of New Caledonia, southwest Pacific. Aquat. Living Resour. 21, 1–12.

Cardoso, J., Van der Veer, H., Kooijman, S., 2006a. Body-size scaling relationships in bivalve species: A comparison of field data with predictions by the Dynamic Energy Budget (DEB) theory. J. Sea Res. 56, 125–139.

Cardoso, J., Witte, J., Van der Veer, H., 2006b. Intra-and interspecies comparison of energy flow in bivalve species in dutch coastal waters by means of the Dynamic Energy Budget (DEB) theory. J. Sea Res. 56, 182–197.

Carleton, S., Del Rio, C., 2010. Growth and catabolism in isotopic incorporation: a new formulation and experimental data. Funct. Ecol. 24, 805–812.

Castillo, L., Hatch, K., 2007. Fasting increases δ^{15}N-values in the uric acid of *Anolis carolinensis* and *Uta stansburiana* as measured by non-destructive sampling. Rapid Commun. Mass Spectrom. 21, 4125–4128.

Caut, S., Angulo, E., Courchamp, F., 2008a. Caution on isotopic model use for analyses of consumer diet. Can. J. Zool. 86, 438–445.

Caut, S., Angulo, E., Courchamp, F., 2008b. Discrimination factors (δ^{15}N and δ^{13}C) in an omnivorous consumer: effect of diet isotopic ratio. Funct. Ecol. 22, 255–263.

Caut, S., Angulo, E., Courchamp, F., 2009. Variation in discrimination factors (Δ^{15}N and Δ^{13}C): the effect of diet isotopic values and applications for diet reconstruction. J. Appl. Ecol. 46, 443–453.

Chauvaud, L., Donval, A., Thouzeau, G., Paulet, Y.M., Nézan, E., 2001. Variations in food intake of *Pecten maximus* (L.) from the Bay of Brest (France): influence of environmental factors and phytoplancton species composition. Life Sci. 324, 743–755.

Christensen, V., Pauly, D., 1992. Ecopath II – a software for balancing steady-state ecosystem models and calculating network characteristics. Ecol. Model. 61, 169–185.

Church, M., Ebersole, J., Rensmeyer, K., Couture, R., Barrows, F., Noakes, D., 2008. Mucus: a new tissue fraction for rapid determination of fish diet switching using stable isotope analysis. Can. J. Fish. Aquat. Sci. 66, 1–5.

Cloern, J., 1982. Does the benthos control phytoplankton biomass in south San Francisco Bay. Mar. Ecol. Prog. Ser. 9, 191–202.

Cloern, J., Jassby, A., 2008. Complex seasonal patterns of primary producers at the land–sea interface. Ecol. Lett. 11, 1294–1303.

Collet, B., Boudry, P., Thebault, A., Heurtebise, S., Morand, B., Gérard, A., 1999. Relationship between pre-and post-metamorphic growth in the Pacific oyster *Crassostrea gigas* (Thunberg). Aquaculture 175, 215–226.

Costil, K., Royer, J., Ropert, M., Soletchnik, P., Mathieu, M., 2005. Spatio-temporal variations in biological performances and summer mortality of the Pacific oyster *Crassostrea gigas* in Normandy (France). Helgol. Mar. Res. 59, 286–300.

Cugier, P., Ménesguen, A., Guillaud, J., 2005. Three-dimensional (3d) ecological modelling of the Bay of Seine (English Channel, France). J. Sea Res. 54, 104–124.

Dame, R., 1996. Ecology of marine bivalves: an ecosystem approach. 254p , 254.

Dang, C., Sauriau, P., Savoye, N., Caill-Milly, N., Martinez, P., Millaret, C., Haure, J., de Montaudouin, X., 2009. Determination of diet in Manila clams by spatial analysis of stable isotopes. Mar. Ecol. Prog. Ser. 387, 167–177.

Dawson, T., Mambelli, S., Plamboeck, A., Templer, P., Tu, K., 2002. Stable isotopes in plant ecology. Annual Review of Ecology and Systematics , 507–559.

Decottignies, P., Beninger, P.G., Rincé, Y., Robins, R.J., Riera, P., 2007. Exploitation of natural food sources by two sympatric, invasive suspension-feeders: *Crassostrea gigas* and *Crepidula fornicata*. Mar. Ecol. Prog. Ser. 334, 179–192.

DeNiro, M., Epstein, S., 1978. Influence of diet on the distribution of carbon isotopes in animals. Geochim. Cosmochim. Acta 42, 495–506.

DeNiro, M., Epstein, S., 1981. Influence of diet on the distribution of nitrogen isotopes in animals. Geochim. Cosmochim. Acta 45, 341–351.

Dennis, C.A., MacNeil, M.A., Rosati, J.Y., Pitcher, T.E., Fisk, A.T., 2010. Diet discrimination factors are inversely related to δ^{15}N and δ^{13}C values of food for fish under controlled conditions. Rapid Commun. Mass Spectrom. 24, 3515–3520.

Deslous-Paoli, J., Héral, M., 1988. Biochemical composition and energy value of *Crassostrea gigas* (Thunberg) cultured in the bay of Marennes-Oléron. Aquat. Living Resour. 1, 239–249.

Deudero, S., Cabanellas, M., Blanco, A., Tejada, S., 2009. Stable isotope fractionation in the digestive gland, muscle and gills tissues of the marine mussel *Mytilus galloprovincialis*. J. Exp. Mar. Biol. Ecol. 368, 181–188.

Doering, P., Oviatt, C., 1986. Application of filtration rate models to field populations of bivalves: an assessment using experimental mesocosms. Mar. Ecol. Prog. Ser. 31, 265–275.

Doi, H., Chang, K.H., Obayashi, Y., Yoshihara, M., Shime, M., Yamamoto, T., Nishibe, Y., S-i., N., 2008. Attached microalgae contribute to planktonic food webs in bays with fish and pearl oyster farms. Mar. Ecol. Prog. Ser. 353, 107–113.

Doi, H., Kikuchi, E., Takagi, S., Shikano, S., 2007. Changes in carbon and nitrogen stable isotopes of chironomid larvae during growth, starvation and metamorphosis. Rapid Commun. Mass Spectrom. 21, 997–1002.

Dridi, S., Romdhane, M., et al., 2007. Seasonal variation in weight and biochemical composition of the Pacific oyster, *Crassostrea gigas* in relation to the gametogenic cycle and environmental conditions of the Bizert lagoon, Tunisia. Aquaculture 263, 238–248.

Dubois, S., Blin, J.L., Bouchaud, B., Lefebvre, S., 2007a. Isotope trophic-step fractionation of suspension-feeding species: implications for food partitioning in coastal ecosystems. J. Exp. Mar. Biol. Ecol. 351, 121–128.

Dubois, S., Orvain, F., Marin-Leal, J.C., Ropert, M., Lefebvre, S., 2007b. Small-scale spatial variability of food partitioning between cultivated oysters and associated suspension-feeding species, as revealed by stable isotopes. Mar. Ecol. Prog. Ser. 336, 151–160.

Emmery, A., Lefebvre, S., Alunno-Bruscia, M., Kooijman, S., 2011. Understanding the dynamics of δ^{13}C and δ^{15}N in soft tissues of the bivalve *Crassostrea gigas* facing environmental fluctuations in the context of dynamic energy budgets (DEB). J. Sea Res. 66, 361–371.

Emmery, A., Lefebvre, S., Alunno-Bruscia, M., Qéau, I., Lebrun, L., Bataillé, M.P., in prep. Effect of the feeding level on the dynamics of stable isotopes δ^{13}C and δ^{15}N in soft tissues of the pacific oyster *Crassostrea gigas*.

Ernande, B., Clobert, J., McCombie, H., Boudry, P., 2003. Genetic polymorphism and trade-offs in the early life-history strategy of the Pacific oyster, *Crassostrea gigas* (Thunberg, 1795): a quantitative genetic study. J. Evol. Biol. 16, 399–414.

Fabioux, C., Huvet, A., Le Souchu, P., Le Pennec, M., Pouvreau, S., 2005. Temperature and photoperiod drive *Crassostrea gigas* reproductive internal clock. Aquaculture 250, 458–470.

Fleeger, J., Carman, K., Nisbet, R., 2003. Indirect effects of contaminants in aquatic ecosystems. Sci. Total Environ. 317, 207–233.

Fleury, P.G., Simonne, C., Claude, S., Palvadeau, H., Guilpain, P., D'Amico, F., Le Gall, P., Vercelli, C. Pien, C., 2005a. REseau MOllusques des Rendements Aquacoles (REMORA - huître creuse); résultats des stations NATIONALES; année 2003. http://archimer.ifremer.fr/doc/00000/2412/.

Fleury, P.G., Simonne, C., Claude, S., Palvadeau, H., Guilpain, P., D'Amico, F., Le Gall, P., Vercelli, C. Pien, C., 2005b. REseau MOllusques des Rendements Aquacoles (REMORA - huître creuse); résultats des stations NATIONALES; année 2004. http://archimer.ifremer.fr/doc/00000/2413/.

Flores-Vergara, C., Cordero-Esquivel, B., Ceron-Ortiz, A., Arredondo-Vega, B., 2004. Combined effects of temperature and diet on growth and biochemical composition of the Pacific oyster *Crassostrea gigas* (Thunberg) spat. Aquacult. Res. 35, 1131–1140.

Flye-Sainte-Marie, J., Jean, F., Paillard, C., Ford, S., Powell, E., Hofmann, E., Klinck, J., 2007. Ecophysiological dynamic model of individual growth of *Ruditapes philippinarum*. Aquaculture 266, 130–143.

Flye-Sainte-Marie, J., Jean, F., Paillard, C., Kooijman, S., 2009. A quantitative estimation of the energetic cost of brown ring disease in the manila clam using dynamic energy budget theory. J. Sea Res. 62, 114–123.

Focken, U., 2001. Stable isotopes in animal ecology: the effect of ration size on the trophic shift of C and N isotopes between feed and carcass. Isotopes Environ. Health Stud. 37, 199–211.

Forsberg, B., Araujo-Lima, C., Martinelli, L., Victoria, R., Bonassi, J., 1993. Autotrophic carbon sources for fish of the central Amazon. Ecology , 644–652.

Fossi, M., 1994. Nondestructive biomarkers in ecotoxicology. Environ. Health Perspect. 102, 49.

Frazer, T., Ross, R., Quetin, L., Montoya, J., 1997. Turnover of carbon and nitrogen during growth of larval krill, *Euphausia superba* Dana: a stable isotope approach. J. Exp. Mar. Biol. Ecol. 212, 259–275.

Freitas, V., Lika, K., Witte, J., van der Veer, H., 2011. Food conditions of the sand goby *Pomatoschistus minutus* in shallow waters: An analysis in the context of Dynamic Energy Budget theory. J. Sea Res. 66, 440–446.

Fry, B., 2006. Stable isotope ecology. Springer Verlag.

Fry, B., Arnold, C., 1982. Rapid 13 C/12 C turnover during growth of brown shrimp (Penaeus aztecus). Oecologia 54, 200–204.

Fry, B., Sherr, E., 1984. δ^{13}C measurements as indicators of carbon flow on marine and freshwater ecosystems. Contrib. Mar. Sci. 27, 13–47.

Gannes, L., del Rio, C., Koch, P., 1998. Natural abundance variations in stable isotopes and their potential uses in animal physiological ecology. Comp. Biochem. Physiol., Part A: Mol. Integr. Physiol. 119, 725–737.

Gannes, L.Z., O'Brien, D.M., Rio, C.M.d., 1997. Stable isotopes in animal ecology: Assumptions, caveats, and a call for more laboratory experiments. Ecology 78, 1271–1276.

Gaye-Siessegger, J., Focken, U., Abel, H., Becker, K., 2003. Feeding level and diet quality influence trophic shift of C and N isotopes in Nile tilapia (*Oreochromis niloticus* (L.)). Isotopes Environ. Health Stud. 39, 125.

Gaye-Siessegger, J., Focken, U., Abel, H., Becker, K., 2004a. Individual protein balance strongly influences δ^{15}N and δ^{13}C values in Nile tilapia, *Oreochromis niloticus*. Naturwissenschaften 91, 90–93.

Gaye-Siessegger, J., Focken, U., Abel, H., Becker, K., 2007. Starvation and low feeding levels result in an enrichment of ^{13}C in lipids and ^{15}N in protein of Nile tilapia *Oreochromis niloticus* L. J. Fish Biol. 71, 90–100.

Gaye-Siessegger, J., Focken, U., Muetzel, S., Abel, H., Becker, K., 2004b. Feeding level and individual metabolic rate affect δ^{13}C and δ^{15}N values in carp: implications for food web studies. Oecologia 138, 175–183.

Gearing, J., Gearing, P., Rudnick, D., Requejo, A., Hutchins, M., 1984. Isotopic variability of organic carbon in a phytoplankton-based, temperate estuary. Geochim. Cosmochim. Acta 48, 1089 – 1098.

Gili, J., Coma, R., 1998. Benthic suspension feeders: their paramount role in littoral marine food webs. Trends Ecol. Evol. 13, 316–321.

González-Araya, R., Quéau, I., Quéré, C., Moal, J., Robert, R., 2011. A physiological and biochemical approach to selecting the ideal diet for *Ostrea edulis* (l.) broodstock conditioning (part A). Aquacult. Res. 42, 710–726.

Goulletquer, P., Wolowicz, M., Latala, A., Brown, C., Cragg, S., 2004. Application of a micro-respirometric volumetric method to respiratory measurements of larvae of the pacific oyster *Crassostrea gigas*. Aquat. Living Resour. 17, 195–200.

Grangeré, K., Lefebvre, S., Ménesguen, A., Jouenne, F., 2009a. On the interest of using field primary production data to calibrate phytoplankton rate processes in ecosystem models. Estuar. Coast. Shelf. Sci. 81, 169–178.

Grangeré, K., Ménesguen, A., Lefebvre, S., Bacher, C., Pouvreau, S., 2009b. Modelling the influence of environmental factors on the physiological status of the Pacific oyster *Crassostrea gigas* in an estuarine embayment; The Baie des Veys (France). J. Sea Res. 62, 147–158.

Grant, J., Bacher, C., 1998. Comparative models of mussel bioenergetics and their validation at field culture sites. J. Exp. Mar. Biol. Ecol. 219, 21–44.

Guarini, J., Gros, P., Blanchard, G., Richard, P., Fillon, A., 2004. Benthic contribution to pelagic microalgal communities in two semi-enclosed, European-type littoral ecosystems (Marennes-Oléron Bay and Aiguillon Bay, France). J. Sea Res. 52, 241–258.

Guelinckx, J., Maes, J., Geysen, B., Ollevier, F., 2008. Estuarine recruitment of a marine goby reconstructed with an isotopic clock. Oecologia 157, 41–52.

Guelinckx, J., Maes, J., Van Den Driessche, P., Geysen, B., Dehairs, F., Ollevier, F., 2007. Changes in δ^{13}C and δ^{15}N in different tissues of juvenile sand goby *Pomatoschistus minutus*: a laboratory diet-switch experiment. Mar. Ecol. Prog. Ser. 341, 205.

Handå, A., Alver, M., Edvardsen, C.V., Halstensen, S., Olsen, A.J., Øie, G., Reitan, K.I., Olsen, Y., Reinertsen, H., 2011. Growth of farmed blue mussels (*Mytilus edulis* l.) in a Norwegian coastal area; comparison of food proxies by DEB modeling. J. Sea Res. 66, 297–307.

Harvey, C., Hanson, P., Essington, T., Brown, P., Kitchell, J., 2002. Using bioenergetics models to predict stable isotope ratios in fishes. Can. J. Fish. Aquat. Sci. 59, 115–124.

Haubert, D., Langel, R., Scheu, S., Ruess, L., 2005. Effects of food quality, starvation and life stage on stable isotope fractionation in collembola. Pedobiologia 49, 229–237.

Hayes, J., 2002. Practice and principles of isotopic measurements in organic geochemistry. Organic geochemistry of contemporaneous and ancient sediments .

Hesslein, R., Hallard, K., Ramlal, P., 1993. Replacement of sulfur, carbon, and nitrogen in tissue of growing broad whitefish (*Coregonus nasus*) in response to a change in diet traced by δ^{34}s, δ^{13}c, and δ^{15}n. Can. J. Fish. Aquat. Sci. 50, 2071–2076.

Hobson, K., 1999. Tracing origins and migration of wildlife using stable isotopes: a review. Oecologia 120, 314–326.

Hobson, K., Alisauskas, R., Clark, R., 1993. Stable-nitrogen isotope enrichment in avian tissues due to fasting and nutritional stress: implications for isotopic analyses of diet. Condor 95, 388–394.

Hobson, K., Atwell, L., Wassenaar, L., Yerkes, T., 2004. Estimating endogenous nutrient allocations to reproduction in Redhead Ducks: A dual isotope approach using δD and δ^{13}C measurements of female and egg tissues. Funct. Ecol. 18, 737–745.

Hobson, K., Schell, D., Renouf, D., Noseworthy, E., 1996. Stable carbon and nitrogen isotopic fractionation between diet and tissues of captive seals: implications for dietary reconstructions involving marine mammals. Can. J. Fish. Aquat. Sci. 53, 528–533.

Hobson, K., Sirois, J., Gloutney, M., 2000. Tracing nutrient allocation to reproduction with stable isotopes: a preliminary investigation using colonial waterbirds of Great Slave Lake. Auk 117, 760–774.

Hobson, K., Thompson, J., Evans, M., Boyd, S., 2005. Tracing nutrient allocation to reproduction in Barrow's Goldeneye. J. Wildl. Manage. 69, 1221–1228.

Hobson, K.A., Clark, R.G., 1992. Assessing avian diets using stable isotopes I: turnover of $\delta^{13}C$ in tissues. Condor 94, 181 – 188.

Hyslop, E., 1980. Stomach contents analysis – a review of methods and their application. Journal of fish biology 17, 411–429.

Jackson, J., Kirby, M., Berger, W., Bjorndal, K., Botsford, L., Bourque, B., Bradbury, R., Cooke, R., Erlandson, J., Estes, J., et al., 2001. Historical overfishing and the recent collapse of coastal ecosystems. Science 293, 629–637.

Jennings, S., Maxwell, T., Schratzberger, M., Milligan, S., 2008. Body-size dependent temporal variations in nitrogen stable isotope ratios in food webs. Mar. Ecol. Prog. Ser. 370, 199–206.

Jennings, S., Pinnegar, J., Polunin, N., Warr, K., 2002a. Linking size-based and trophic analyses of benthic community structure. Mar. Ecol. Prog. Ser. 226, 77–85.

Jennings, S., Warr, K., 2003. Environmental correlates of large-scale spatial variation in the δ^{15}N of marine animals. Mar. Biol. 142, 1131–1140.

Jennings, S., Warr, K., Mackinson, S., 2002b. Use of size-based production and stable isotope analyses to predict trophic transfer efficiencies and predator-prey body mass ratios in food webs. Mar. Ecol. Prog. Ser. 240, 11–20.

Jouenne, F., Lefebvre, S., Veron, B., Lagadeuc, Y., 2007. Phytoplankton community structure and primary production in small intertidal estuarine-bay ecosystem (eastern English Channel, France). Mar. Biol. 151, 805–825.

Jusup, M., Klanjscek, T., Matsuda, H., Kooijman, S., 2011. A full lifecycle bioenergetic model for bluefin tuna. PloS one 6, e21903.

Kang, C., Kim, J., Lee, K., Kim, J., Lee, P., Hong, J., 2003. Trophic importance of benthic microalgae to macrozoobenthos in coastal bay systems in Korea: dual stable C and N isotope analyses. Mar. Ecol. Prog. Ser. 259, 79–92.

Kang, C., Lee, Y., Choy, E., Shin, J., Seo, I., Hong, J., 2006. Microphytobenthos seasonality determines growth and reproduction in intertidal bivalves. Mar. Ecol. Prog. Ser. 315, 113–127.

Kang, C., Sauriau, P., Richard, P., Blanchard, G., 1999. Food sources of the infaunal suspension-feeding bivalve *Cerastoderma edule* in a muddy sandflat of Marennes-Oléron Bay, as determined by analyses of carbon and nitrogen stable isotopes. Mar. Ecol. Prog. Ser. 187, 147–158.

Kearney, M., 2012. Metabolic theory, life history and the distribution of a terrestrial ectotherm. Funct. Ecol. 26, 167–179.

Kelly, L., del Rio, C., 2010. The fate of carbon in growing fish: an experimental study of isotopic routing. Physiol. Biochem. Zool. 83, 000–000.

Kooijman, S., Sousa, T., Pecquerie, L., van der Meer, J., Jager, T., 2008. From food-dependent statistics to metabolic parameters, a practical guide to the use of the dynamic energy budget theory. Biol. Rev. 83, 533–552.

Kooijman, S.A.L.M., 2006. Pseudo-faeces production in bivalves. J. Sea Res. 56, 103 – 106.

Kooijman, S.A.L.M., 2010. Dynamic Energy Budgets theory for metabolic organisation. Third edition. Cambridge University Press edition.

Kurle, C., Worthy, G., 2002. Stable nitrogen and carbon isotope ratios in multiple tissues of the Northern fur seal *Callorhinus ursinus*: implications for dietary and migratory reconstructions. Mar. Ecol. Prog. Ser. 236, 289–300.

Laing, I., 2000. Effect of temperature and ration on growth and condition of king scallop (*Pecten maximus*) spat. Aquaculture 183, 325–334.

Lefebvre, S., Harma, C., Blin, J., 2009a. Trophic typology of coastal ecosystems based on δ^{13}C and δ^{15}N ratios in an opportunistic suspension feeder. Mar. Ecol. Prog. Ser. 390, 24–37.

Lefebvre, S., Marín Leal, J., Dubois, S., Orvain, F., Blin, J., Bataillé, M., Ourry, A., Galois, R., 2009b. Seasonal dynamics of trophic relationships among co-occurring suspension-feeders in two shellfish culture dominated ecosystems. Estuar. Coast. Shelf. Sci. 82, 415–425.

Lejart, M., Hily, C., 2010. Differential response of benthic macrofauna to the formation of novel oyster reefs (*Crassostrea gigas*, thunberg) on soft and rocky substrate in the intertidal of the bay of brest, france. J. Sea Res. In Press, Corrected Proof, –.

Lesser, M., Shumway, S., Cucci, T., Smith, J., 1992. Impact of fouling organisms on mussel rope culture: interspecific competition for food among suspension-feeding invertebrates. J. Exp. Mar. Biol. Ecol. 165, 91–102.

Levesque, C., Juniper, S.K., Marcus, J., 2003. Food resource partitioning and competition among alvinellid polychaetes of Juan de Fuca Ridge hydrothermal vents. Mar. Ecol. Prog. Ser. 246, 173–182.

Lika, K., Freitas, V., van der Veer, H., van der Meer, J., Wijsman, J., Pecquerie, L., Kearney, M., Kooijman, S., 2011a. The "covariation method" for estimating the parameters of the standard Dynamic Energy Budget model I: phylosophy and approach. J. Sea Res. 66, 270–277.

Lika, K., Kearney, M., Kooijman, S., 2011b. The "covariation method" for estimating the parameters of the standard Dynamic Energy Budget model II: properties and preliminary patterns. J. Sea Res. 66, 278–288.

Lika, K., Kooijman, S., 2011. The comparative topology of energy allocation in budget models. J. Sea Res. 66, 381–391.

Lindeman, R., 1942. The trophic-dynamic aspect of ecology. Ecology 23, 399–417.

Lindsay, D.J., Minagawa, M., Mitani, I., Kawaguchi, K., 1998. Trophic shift in the Japanese anchovy *Engraulis japonicus* in its early life history stages as detected by stable isotope ratios in Sagami Bay, Central Japan. Fish. Sci. 64, 403–410.

Lorrain, A., 2002. Utilisation de la coquille Saint-Jacques comme traceur environnemental: approches biologiques et biogéochimiques. Thï£¡se de Doctorat. Université de Bretagne Occidentale. Brest.

Lorrain, A., Paulet, Y.M., Chauvaud, L., Savoye, N., Donval, A., Saout, C., 2002. Differential δ^{13}C and δ^{15}N signatures among scallop tissues: implications for ecology and physiology. J. Exp. Mar. Biol. Ecol. 275, 47–61.

Lorrain, A., Paulet, Y.M., Chauvaud, L., Savoye, N., Nézan, E., Guérin, L., 2000. Growth anomalies in *Pecten maximus* from coastal waters (Bay of Brest, France): relationship with diatom blooms. J. Mar. Biol. Ass. U.K. 80, 667–673.

Lorrain, A., Savoye, N., Chauvaud, L., Paulet, Y.M., Naulet, N., 2003. Decarbonation and preservation method for the analysis of organic C and N contents and stable isotope ratios of low-carbonated suspended particulate material. Anal. Chim. Acta 491, 125–133.

MacAvoy, S., Macko, S., Arneson, L., 2005. Growth *versus* metabolic tissue replacement in mouse tissues determined by stable carbon and nitrogen isotope analysis. Can. J. Zool. 83, 631–641.

Malet, N., Sauriau, P.G., Faury, N., Soletchnik, P., Guillou, G., 2007. Effect of seasonal variation in trophic conditions and the gametogenic cycle on δ^{13}C and δ^{15}N levels of diploid and triploid Pacific oysters *Crassostrea gigas*. Mar. Ecol. Prog. Ser. 346, 203–217.

Malet, N., Sauriau, P.G., Ryckaert, M., Malestroit, P., Guillou, G., 2008. Dynamics and sources of suspended particulate organic matter in the Marennes-Oléron oyster farming bay: insights from stable isotopes and microalgae ecology. Estuar. Coast. Shelf. Sci. 78, 576–586.

Marín Leal, J.C., Dubois, S., Orvain, F., Galois, R., Blin, J.L., Ropert, M., Bataille, M.P., Ourry, A., Lefebvre, S., 2008. Stable isotopes (δ^{13}C, δ^{15}N) and modelling as tools to estimate the trophic ecology of cultivated oysters in two contrasting environments. Mar. Biol. 153, 673–688.

Mariotti, A., 1983. Atmospheric nitrogen is a reliable standard for natural ^{15}n abundance measurements. Nature 303, 685–687.

McCutchan Jr, J., Lewis Jr, W., Kendall, C., McGrath, C., 2003. Variation in trophic shift for stable isotope ratios of carbon, nitrogen, and sulfur. Oikos 102, 378–390.

McMahon, K., Fogel, M., Elsdon, T., Thorrold, S., 2010. Carbon isotope fractionation of amino acids in fish muscle reflects biosynthesis and isotopic routing from dietary protein. J. Anim. Ecol. 79, 1132–1141.

Mill, A.C., Pinnegar, J.K., Polunin, N.V.C., 2007. Explaining isotope trophic-step fractionation: why herbivorous fish are different. Comp. Biochem. Physiol., Part A: Mol. Integr. Physiol. 146, 71 – 77.

Miller, T., 2006. Tissue-specific response of δ^{15}N in adult Pacific herring (*Clupea pallasi*) following an isotopic shift in diet. Environ. Biol. Fish. 76, 177–189.

Minagawa, M., Wada, E., 1984. Stepwise enrichment of ^{15}N along food chains: further evidence and the relation between δ^{15}N and animal age. Geochim. Cosmochim. Acta 48, 1135 – 1140.

Mirón, M., Herrera, M., Ramirez, P.N., Hobson, K.A., 2006. Effect of diet quality on carbon and nitrogen turnover and isotopic discrimination in blood of a New World nectarivorous bat. J. Exp. Biol. 209, 541–548.

Monserrat, J., Martínez, P., Geracitano, L., Lund Amado, L., Martinez Gaspar Martins, C., Lopes Leães Pinho, G., Soares Chaves, I., Ferreira-Cravo, M., Ventura-Lima, J., Bianchini, A., 2007. Pollution biomarkers in estuarine animals: critical review and new perspectives. Comparative Biochemistry and Physiology Part C: Toxicology & Pharmacology 146, 221–234.

Mueller, C., Augustine, S., Kooijman, S., Kearney, M., Seymour, R., 2012. The trade-off between maturation and growth during accelerated development in frogs. Comp. Biochem. Physiol., Part A: Mol. Integr. Physiol. 163, 95–102.

Myers, R., Baum, J., Shepherd, T., Powers, S., Peterson, C., 2007. Cascading effects of the loss of apex predatory sharks from a coastal ocean. Science 315, 1846–1850.

Newell, R., 2004. Ecosystem influences of natural and cultivated populations of suspension-feeding bivalve molluscs: a review. J. Shellfish Res. 23, 51–62.

Nisbet, R., Muller, E., Lika, K., Kooijman, S., 2000. From molecules to ecosystems through dynamic energy budget models. J. Anim. Ecol. 69, 913–926.

Odum, E., 1969. The strategy of ecosystem development. Science 164, 262–270.

Oelbermann, K., Scheu, S., 2002. Stable isotope enrichment (δ^{15}N and δ^{13}C) in a generalist predator (*Pardosa lugubris*, Araneae: Lycosidae): effects of prey quality. Oecologia 130, 337–344.

Officer, C., Smayda, T., Mann, R., 1982. Benthic filter feeding: a natural eutrophication control. Mar. Ecol. Prog. Ser. 9, 203–210.

Ogden, L., Hobson, K., Lank, D., 2004. Blood isotopic (δ^{13}C and δ^{15}N) turnover and diet-tissue fractionation factors in captive dunlin (*Calidris alpina pacifica*). Auk 121, 170–177.

Olive, P., Pinnegar, J., Polunin, N., Richards, G., Welch, R., 2003. Isotope trophic-step fractionation: a dynamic equilibrium model. J. Anim. Ecol. 72, 608–617.

Paine, R., 1980. Food webs: linkage, interaction strength and community infrastructure. J. Anim. Ecol. 49, 667–685.

Paulet, Y.M., Lorrain, A., Richard, J., Pouvreau, S., 2006. Experimental shift in diet δ^{13}C: A potential tool for ecophysiological studies in marine bivalves. Org. Geochem. 37, 1359–1370.

Pearson, S., Levey, D., Greenberg, C., Martinez del Rio, C., 2003. Effects of elemental composition on the incorporation of dietary nitrogen and carbon isotopic signatures in an omnivorous songbird. Oecologia 135, 516–523.

Pecquerie, L., Johnson, L.R., Kooijman, S., Nisbet, R.M., 2011. Analyzing variations in life-history traits of pacific salmon in the context of Dynamic Energy Budget (DEB) theory. J Sea Res 66, 424–433.

Pecquerie, L., Nisbet, R., Fablet, R., Lorrain, A., Kooijman, S., 2010. The impact of metabolism on stable isotope dynamics: a theoretical framework. Phil. Trans. R. Soc. B 365, 3455–3468.

Pennock, J., Velinsky, D., Ludlam, J., Sharp, J., Fogel, M., 1996. Isotopic fractionation of ammonium and nitrate during uptake by *Skeletonema costatum*: Implications for δ^{15}N dynamics under bloom conditions. Limnol. Oceanogr. , 451–459.

Pernet, F., Malet, N., Pastoureaud, A., Vaquer, A., QuÃľrÃľ, C., Dubroca, L., 2012. Marine diatoms sustain growth of bivalves in a mediterranean lagoon. J. Sea Res. 68, 20–32.

Phillips, D., 2001. Mixing models in analyses of diet using multiple stable isotopes: a critique. Oecologia 127, 166–170.

Phillips, D., Gregg, J., 2001. Uncertainty in source partitioning using stable isotopes. Oecologia 127, 171–179.

Phillips, D., Gregg, J., 2003. Source partitioning using stable isotopes: coping with too many sources. Oecologia 136, 261–269.

Phillips, D., Koch, P., 2002. Incorporating concentration dependence in stable isotope mixing models. Oecologia 130, 114–125.

Pilditch, C., Grant, J., 1999. Effect of temperature fluctuations and food supply on the growth and metabolism of juvenile sea scallops (*Placopecten magellanicus*). Mar. Biol. 134, 235–248.

Pinnegar, J., Polunin, N., 1999. Differential fractionation of δ^{13}C and δ^{15}N among fish tissues: implications for the study of trophic interactions. Funct. Ecol. 13, 225–231.

Piola, R.F., Moore, S.K., Suthers, I.M., 2006. Carbon and nitrogen stable isotope analysis of three types of oyster tissue in an impacted estuary. Estuar. Coast. Shelf. Sci. 66, 255 – 266.

Post, D., Layman, C., Arrington, D., Takimoto, G., Quattrochi, J., MontaÃśa, C., 2007. Getting to the fat of the matter: models, methods and assumptions for dealing with lipids in stable isotope analyses. Oecologia 152, 179–189.

Post, D.M., 2002. Using stable isotopes to estimate trophic position: models, methods, and assumptions. Ecology 83, 703–718.

Pouvreau, S., Bourlès, Y., Lefebvre, S., Gangnery, A., Alunno-Bruscia, M., 2006. Application of a dynamic energy budget model to the Pacific oyster, *Crassostrea gigas*, reared under various environmental conditions. J. Sea Res. 56, 156–167.

Raikow, D., Hamilton, S., 2001. Bivalve diets in a midwestern us stream: A stable isotope enrichment study. Limnol. Oceanogr. 46, 514–522.

Ren, J., Marsden, I., Ross, A., Schiel, D., 2003. Seasonal variation in the reproductive activity and biochemical composition of the Pacific oyster (*Crassostrea gigas*) from the Marlborough Sounds, New Zealand. N. Z. J. Mar. Freshw. Res. 37, 171–182.

Ren, J.S., Ross, A.H., 2005. Environmental influence on mussel growth: A dynamic energy budget model and its application to the greenshell mussel *Perna canaliculus*. Ecol. Model. 189, 347–362.

Ren, J.S., Schiel, D.R., 2008. A dynamic energy budget model: parameterisation and application to the Pacific oyster *Crassostrea gigas* in New Zealand waters. J. Exp. Mar. Biol. Ecol. 361, 42–48.

Rico-Villa, B., Bernard, I., Robert, R., Pouvreau, S., 2010. A dynamic energy budget (DEB) growth model for Pacific oyster larvae, *Crassostrea gigas*. Aquaculture 305, 84–94.

Rico-Villa, B., Pouvreau, S., Robert, R., 2009. Influence of food density and temperature on ingestion, growth and settlement of Pacific oyster larvae, *Crassostrea gigas*. Aquaculture 287, 395–401.

Riera, P., 2007. Trophic subsidies of *Crassostrea gigas*, *Mytilus edulis* and *Crepidula fornicata* in the Bay of Mont Saint Michel (France): A δ^{13}C and δ^{15}N investigation. Estuar. Coast. Shelf. Sci. 72, 33–41.

Riera, P., Richard, P., 1996. Isotopic determination of food sources of *Crassostrea gigas* along a trophic gradient in the estuarine bay of Marennes-Oléron. Estuar. Coast. Shelf. Sci. 42, 347–360.

Riera, P., Richard, P., 1997. Temporal variation of δ^{13}C in particulate organic matter and oyster *Crassostrea gigas* in Marennes-Oléron Bay (France): effect of freshwater inflow. Mar. Ecol. Prog. Ser. 147, 105–115.

Riera, P., Stal, L., Nieuwenhuize, J., 2002. δ^{13}C *versus* δ^{15}N of co-occurring molluscs within a community dominated by *Crassostrea gigas* and *Crepidula fornicata* (Oosterschelde, The Netherlands). Mar. Ecol. Prog. Ser. 240, 291–295.

Riera, P., Stal, L., Nieuwenhuize, J., 2004. Utilization of food sources by invertebrates in a man-made intertidal ecosystem (Westerschelde, The Netherlands): a δ^{13}C and δ^{15}N study. J. mar. biol. Ass. U.K. 84, 323–326.

Riera, P., Stal, L., Nieuwenhuize, J., Richard, P., Blanchard, G., Gentil, F., 1999. Determination of food sources for benthic invertebrates in a salt marsh (Aiguillon Bay, France) by carbon and nitrogen stable isotopes: importance of locally produced sources. Mar. Ecol. Prog. Ser. 187, 301–307.

Martínez del Rio, C., Wolf, N., Carleton, S., Gannes, L., 2009. Isotopic ecology ten years after a call for more laboratory experiments. Biol. Rev. 84, 91–111.

Rosland, R., Strand, Ø., Alunno-Bruscia, M., Bacher, C., Strohmeier, T., 2009. Applying dynamic energy budget (DEB) theory to simulate growth and bio-energetics of blue mussels under low seston conditions. J. Sea Res. 62, 49–61.

Salas, F., Marcos, C., Neto, J., Patrício, J., Pérez-Ruzafa, A., Marques, J., 2006. User-friendly guide for using benthic ecological indicators in coastal and marine quality assessment. Ocean & coastal management 49, 308–331.

Saraiva, S., van der Meer, J., Kooijman, S., Sousa, T., 2011a. DEB parameters estimation for *Mytilus edulis*. J. Sea Res. 66, 289 – 296.

Saraiva, S., van der Meer, J., Kooijman, S., Sousa, T., 2011b. Modelling feeding processes in bivalves: A mechanistic approach. Ecol. Model. 222, 514–523.

Sauriau, P., Kang, C., 2000. Stable isotope evidence of benthic microalgae-based growth and secondary production in the suspension feeder *Cerastoderma edule* (Mollusca, Bivalvia) in the Marennes-Oléron Bay. Hydrobiologia 440, 317–329.

Savoye, N., Aminot, A., Tréguer, P., Fontugne, M., Naulet, N., Kérouel, R., 2003. Dynamics of particulate organic matter δ^{15}N and $\delta^{13}C$ during spring phytoplankton blooms in a macrotidal ecosystem (Bay of Seine, France). Mar. Ecol. Prog. Ser. 255, 27–41.

Smaal, A., Vonk, A., 1997. Seasonal variation in C, N and P budgets and tissue composition of the mussel *Mytilus edulis*. Mar. Ecol. Prog. Ser. 153, 167–179.

Soudant, P., Van Ryckeghem, K., Marty, Y., Moal, J., Samain, J., Sorgeloos, P., 1999. Comparison of the lipid class and fatty acid composition between a reproductive cycle in nature and a standard hatchery conditioning of the Pacific Oyster *Crassostrea gigas*. Comp. Biochem. Physiol., Part B: Biochem. Mol. Biol. 123, 209–222.

Sousa, T., Domingos, T., Poggiale, J., Kooijman, S., 2010. Dynamic energy budget theory restores coherence in biology. Phil. Trans. R. Soc. B 365, 3413.

Sousa, T., Mota, R., Domingos, T., Kooijman, S., 2006. Thermodynamics of organisms in the context of dynamic energy budget theory. Phys. Rev. E 74, 51901.

Steele, K., Daniel, R., 1978. Fractionation of nitrogen isotopes by animals: a further complication to the use of variations in the natural abundance of ^{15}N for tracer studies. J. Agr. Sci. 90, 7–9.

Suzuki, K., Kasai, A., Nakayama, K., Tanaka, M., 2005. Differential isotopic enrichment and half-life among tissues in Japanese temperate bass (*Lateolabrax japonicus*) juveniles: implications for analyzing migration. Can. J. Fish. Aquat. Sci. 62, 671–678.

Sweeting, C., Polunin, N., Jennings, S., 2006. Effects of chemical lipid extraction and arithmetic lipid correction on stable isotope ratios of fish tissues. Rapid Commun. Mass Spectrom. 20, 595–601.

Sweeting, C.J., Barry, J., Barnes, C., Polunin, N., Jennings, S., 2007a. Effects of body size and environment on diet-tissue δ^{15}N fractionation in fishes. J. Exp. Mar. Biol. Ecol. 340, 1–10.

Sweeting, C.J., Barry, J., Polunin, N., Jennings, S., 2007b. Effects of body size and environment on diet-tissue δ^{13}C fractionation in fishes. J. Exp. Mar. Biol. Ecol. 352, 165–176.

Thomas, Y., Mazurié, J., Alunno-Bruscia, M., Bacher, C., Bouget, J.F., Gohin, F., Pouvreau, S., Struski, C., 2011. Modelling spatio-temporal variability of *Mytilus edulis* (l.) growth by forcing a dynamic energy budget model with satellite-derived environmental data. J. Sea Res. 66, 308–317.

Tieszen, L., Boutton, T., Tesdahl, K., Slade, N., 1983. Fractionation and turnover of stable carbon isotopes in animal tissues: implications for δ^{13}C analysis of diet. Oecologia 57, 32–37.

Troost, K., 2010. Causes and effects of a highly successful marine invasion: case-study of the introduced Pacific oyster *Crassostrea gigas* in continental NW European estuaries. J. Sea Res. 64, 145–165.

Troost, T., Wijsman, J., Saraiva, S., Freitas, V., 2010. Modelling shellfish growth with dynamic energy budget models: an application for cockles and mussels in the Oosterschelde (southwest Netherlands). Phil. Trans. R. Soc. B 365, 3567.

Trueman, C., McGill, R., Guyard, P., 2005. The effect of growth rate on tissue-diet isotopic spacing in rapidly growing animals. An experimental study with Atlantic salmon (*Salmo salar*). Rapid Commun. Mass Spectrom. 19, 3239–3247.

Van Haren, R., Kooijman, S., 1993. Application of a dynamic energy budget model to *Mytilus edulis* (L.). Neth. J. Sea Res. 31, 119–133.

Vander Zanden, M.J., Rasmussen, J.B., 2001. Variation in δ^{15}N and δ^{13}C trophic fractionation: implications for aquatic food web studies. Limnol. Oceanogr. 46, 2061–2066.

Vanderklift, M., Ponsard, S., 2003. Sources of variation in consumer-diet δ^{15}N enrichment: a meta-analysis. Oecologia 136, 169–182.

Van der Veer, H., Cardoso, J., Van der Meer, J., 2006. The estimation of DEB parameters for various Northeast Atlantic bivalve species. J. Sea Res. 56, 107–124.

Vizzini, S., Mazzola, A., 2003. Seasonal variations in the stable carbon and nitrogen isotope ratios ($^{13}C/^{12}C$ and $^{13}N/^{14}N$) of primary producers and consumers in a western Mediterranean coastal lagoon. Mar. Biol. 142, 1009–1018.

Voigt, C., Matt, F., Michener, R., Kunz, T., 2003. Low turnover rates of carbon isotopes in tissues of two nectar-feeding bat species. J. Exp. Biol. 206, 1419–1427.

Webb, S., Hedges, R., Simpson, S., 1998. Diet quality influences the δ^{13}C and δ^{15}N of locusts and their biochemical components. J. Exp. Biol. 201, 2903.

Whyte, J., Englar, J., Carswell, B., 1990. Biochemical composition and energy reserves in *Crassostrea gigas* exposed to different levels of nutrition. Aquaculture 90, 157–172.

Wijsman, J., Smaal, A., 2011. Growth of cockles (*Cerastoderma edule*) in the Oosterschelde described by a Dynamic Energy Budget model. J. Sea Res. 66, 372 – 380.

Wilson, R., Chanton, J., Lewis, G., Nowacek, D., 2009. Combining organic matter source and relative trophic position determinations to explore trophic structure. Estuaries and Coasts 32, 999–1010.

Yokoyama, H., Ishihi, Y., Yamamoto, S., 2008. Diet-tissue isotopic fractionation of the Pacific oyster *Crassostrea gigas*. Mar. Ecol. Prog. Ser. 358, 173–179.

Yokoyama, H., Tamaki, A., Harada, K., Shimoda, K., Koyama, K., Ishihi, Y., 2005a. Variability of diet-tissue isotopic fractionation in estuarine macrobenthos. Mar. Ecol. Prog. Ser. 296, 115–128.

Yokoyama, H., Tamaki, A., Koyama, K., Ishihi, Y., Shimoda, K., Harada, K., 2005b. Isotopic evidence for phytoplankton as a major food source for macrobenthos on an intertidal sandflat in Ariake Sound, Japan. Mar. Ecol. Prog. Ser. 304, 101–116.

Zar, J., 1996. Multiple regression and correlation. Biostatistical Analysis. 3rd ed. Upper Saddle River , 353–360.

Abstract

The general aim of this doctorate work was to understand how the trophic environment, *i.e.* amount and diversity of food, and the metabolism influence the dynamics of stable isotopes δ^{13}C and δ^{15}N in the tissues of the Pacific oyster (*Crassostrea gigas*). I combined both experimental (under natural and controlled conditions) and dynamic energy budget modelling (DEB) approaches to decipher the role of oyster metabolism and trophic resource relatively to stable isotopes discrimination.

Trophic resource is frequently characterized thanks to stable isotopic ratios, *i.e.* δ^{13}C and δ^{15}N. Natural stable isotopes are forms of the same element that differ in the number of neutrons in the nucleus. Isotopes with extra neutron are qualified of "heavy isotopes". The δ notation (‰) stands for the difference in the ratio of heavy isotopes over the light ones relative to a standard. The enrichment in heavy isotopes of a predator relative to its prey is classically called the trophic fractionation Δ (*i.e.* $\Delta = \delta_{predator} - \delta_{consumer}$, ‰). At first approximation, Δ has been frequently considered constant across trophic levels, with an average enrichment of ≈ 1 ‰ and ≈ 3.4 ‰ for Δ^{13}C and Δ^{15}N respectively. However, the increasing bulk of results from experimental and modelling approaches shown that Δ depends on numerous environmental (*e.g.* diversity and quality of food source(s)) and physiological (*e.g.* growth) factors.

n the first part of this doctorate work (chapter 2), I carried out an *in situ* survey of oysters growth and isotopic composition (δ^{13}C and δ^{15}N) over one year in two different ecosystems, the Bay of Veys (BDV) and the Brest Harbor (BH). The BDV was characterized by an higher amount of food and an higher diversity of food source(s) compared to BH. I expected that the amount of food was the main factor accounting for the spatial differences in stable isotopic composition of oysters. In BDV, oysters exhibited higher growth and CN ratios for both whole soft body tissues (W_d) and organs (gills, G_i, muscle adductor M_u and remaining tissues R_e). However, the isotopic ratios of the whole soft body tissues (δ_{W_d}) exhibited opposite patterns between the two sites with, on average, a higher $\delta^{13}C_{W_d}$ and a lower $\delta^{15}N_{W_d}$ in BH compared to BDV. The interplay of both growth and temporal variations of the trophic resource

certainly accounted for these spatial differences in δ_{W_d}. The dynamics of stable isotopes in organs were similar, *i.e.* with $\delta_{Mu} > \delta_{Gi} > \delta_{Re}$ regardless of the studied area and season. I thus concluded that the metabolism and the temporal variations of the trophic resource (amount and diversity) had to be considered together to explain the stable isotopes trajectories. However, I could not quantify the impact of metabolism on the dynamics of stable isotopes yet. I thus concluded on the necessity to select an appropriate bioenergetic model *i)* to understand how oysters discriminate stable isotopes of their food sources and *ii)* to consider the variations of Δ values according to both environmental and physiological factors.

The theoretical study I carried out in the chapter 3 allowed me to better understand how both the amount of food consumed and the metabolism impacted the dynamics of $\delta^{13}C_{W_d}$ and $\delta^{15}N_{W_d}$ in the soft tissues of *C. gigas*. I used a dynamic energy budget model (DEB) combined with a dynamic isotope budget model (DIB) (*i.e.* from the DEB theory Kooijman, 2010), calibrated and parametrized thanks to data from literature. Based on physical and chemical rules, the DEB model quantifies the state of the individual under varying food and temperature regimes. It delineates catabolic and anabolic aspects of assimilation, maintenance and growth. It makes explicit use of balances of the chemical elements C, H, O and N, as well as the mixing and fractionation of stable isotopes. The results demonstrate that the higher the feeding level, the lower δ_{W_d} and Δ_{W_d}. The mass effect on δ_{W_d} was not sufficient to explain trophic enrichment classically observed in field. The separation of anabolic and catabolic pathways is key to fractionation. Moreover, the Δ values are dynamically calculated by the IsoDEB model (DEB and DIB models) according to both environmental and metabolism effect.

To test consistency of the model's predictions, I carried out a fractionation experiment under controlled conditions (chapter 4). First, the oysters spat was fed at two different feeding levels (high food, HF; low food, LF) with a single type of food depleted in ^{13}C and ^{15}N, and then starved. The oysters reared at HF level had *i)* an higher growth and C/N ratios and *ii)* lower $\delta^{13}C_{W_d}$ and $\delta^{15}N_{W_d}$ compared to those reared at LF. The same pattern also occurred for *Gi*, *Mu* and *Re*. As observed during the *in situ* monitoring, δ_{Mu} was heavier than δ_{Gi} and δ_{Re} regardless of the feeding level. The differences between $\delta^{13}C_{W_d HF}$ and $\delta^{13}C_{W_d LF}$ were more important compared to the trends simulated by the model (chapter 3). The comparison with literature results led me conclude on a potential effect of the diet isotopic ratios (δ_X) on the Δ value. During the starvation the whole soft body tissues and organs were enriched in heavy isotopes. This enrichment was due to the maintenance of the body. Experimental results also revealed that diet isotopic ratios can exhibited strong temporal variations with consequences on Δ values. The next step was thus to applicate the model under varying conditions of food.

To this end, the set of parameters for the DEB model has been improved by using a wide variety of data *i)* to characterized the full life cycle of *C. gigas* from birth to adult stage (including development acceleration process and metamor-

phosis) and *ii)* to take into account the large physiological plasticity of this species. With a single set of parameters, the model successfully fitted all the data for the different life stages (embryo, juvenile, adult). Based on this set of parameters, the effect of the ingestion rate on the growth and δ_{W_d} was successfully described by the IsoDEB model. During the starvation phase, the model also correctly described the enrichment in heavy isotopes due to the maintenance of the body. However, model simulations were less accurate during strong variations of δ_X for both carbon and nitrogen isotopes. This deviation might link to an inaccurate estimation of the elemental composition of reserve and structure. It might also be that fast changes can only be captured accurately with much more complex models.

According to the results of this doctorate work, both the metabolism and the amount of the trophic resource influence the dynamics of stable isotopes in the soft tissues of the Pacific oyster *C. gigas*. The results also revealed that an accurate quantification of the metabolism (from a modelling point of view) is of primary importance to accurately describe the dynamics of $\delta^{13}C_{W_d}$ and $\delta^{15}N_{W_d}$. The consideration of the (temporal) fluctuations of the environment (food quantity, temperature, diet isotopic ratios) by the IsoDEB model also considerably helped to understand variations of the trophic fractionation. The DEB theory constitutes a promising and innovating ecophysiological tool to understand stable isotope trajectories among living organisms. However, I did not investigated yet the effect of the diversity of the trophic resource on the growth and its consequences on the dynamics of stable isotopes in oyster tissues. The coupling of DEB modelling with *e.g.* mixing model could be the next step.

Résumé

Samenvatting

Acknowledgments

To do!